Master's thesis

NTNU
Norwegian University of Science and Technology
Faculty of Engineering
Department of Energy and Process Engineering

Hiran Putlur Yeshwanth Kumar

Energy Systems For Salmon Process Plants

Master's thesis in Sustainable Energy - Heat Pumping Processes and Systems
Supervisor: Armin Hafner
June 2023

NTNU
Norwegian University of Science and Technology

Hiran Putlur Yeshwanth Kumar

Energy Systems For Salmon Process Plants

Master's thesis in Sustainable Energy - Heat Pumping Processes and Systems
Supervisor: Armin Hafner
June 2023

Norwegian University of Science and Technology
Faculty of Engineering
Department of Energy and Process Engineering

NTNU
Norwegian University of
Science and Technology

Preface

This is the Master Thesis of Hiran Putlur Yeshwanth Kumar written during the final year master's study program in Sustainable Energy – Heat Pumping Processes and Systems at the Department of Energy and Process Engineering at the Norwegian University of Science and Technology (NTNU). The research work was carried out during the academic year 2022-2023.

This thesis work builds upon the project work conducted during the autumn semester of 2022 (Hiran, 2022). While some findings and theory from the project report have been utilized, it is important to note that this thesis expands upon and extends the previous research. The aim is to delve deeper into the subject matter, explore new aspects, and provide additional insights and analysis. It is crucial to emphasize that this thesis work goes beyond the scope of the previous project. It incorporates new system models, simulations, additional data analysis, and further evaluation to enhance the overall understanding of the subject matter.

The motivation behind this thesis stemmed from the critical need to enhance efficiency and sustainability in Norway's salmon processing industry. The complex, energy-intensive nature of the industry's operations, with its myriad of specialized systems, presented an opportunity for impactful research. The potential to inform optimal system design through the development of a simulation tool offered a promising avenue to guide future advancements.

First and foremost, I wish to express my deepest gratitude to my esteemed supervisor, Professor Dr. Armin Hafner, and co-supervisor, Yves Ladam (PTG). Their unwavering guidance, profound expertise, and constructive feedback were instrumental in shaping this thesis. I am truly fortunate to have been under their umbrella. Additionally, I am indebted to Professor Dr. Trygve M. Eikevik, whose insightful advice and encouragement have greatly enhanced my academic journey. Special appreciation is also reserved for my PhD supervisor, Muhammad Umar Khan, whose invaluable assistance with the Dymola and EES simulations was a cornerstone of this work.

On a more personal note, my heartfelt thanks go to my parents, Amudha and Yeshwanth Kumar. Their unending inspiration and unwavering faith in my abilities have been my rock throughout this process. Their teachings and values form the foundation upon which I stand today.

I also want to give a shout-out to the game of basketball, my constant source of hype and stress-relief.

Trondheim, 11th June 2023

Hiran Putlur Yeshwanth Kumar

Abstract

Salmon farming, a major cornerstone of Norway's economy and its second-largest export, necessitates complex, energy-intensive operations. Contemporary salmon processing plants utilize a variety of specialized energy systems, including dehumidification, Refrigerated Sea Water (RSW) systems, ice production units, freezing tunnels, cold storage rooms, and heat recovery units. These systems, each with their unique heating, cooling, and energy consumption profiles, contribute to the intricate daily operations of the plant. Significant refrigeration infrastructure is essential to cater to the demands of these diverse energy systems, ensuring the plant's efficient and effective functioning.

The primary objective of this research is the development of a simulation tool. This tool is intended to assess and compare different system configurations for future salmon processing plants, thereby guiding optimal design choices. In the context of this study, PTG is implementing a comprehensive temperature control system for a facility operated by the Holmøy group in Holmen, Norway. A detailed analysis of this facility, considering factors such as its geographical location and specific operational demands, was conducted. Based on these insights, two distinct refrigeration solutions were proposed. The first solution proposed a single heat pump system to meet all requirements of the SPP. The second solution recommended implementing two separate systems: a two-stage parallel compression R717 refrigeration system (System 1) and an R744 RSW system (System 2). After assessing each solution's pros and cons, the dual-system approach was selected as the optimal choice.

A thorough examination was conducted on both systems, delving into the intricacies of their operation and mechanisms. This involved breaking down the systems into their individual components for a more detailed exploration. With a focus on approximating real-world performance while adhering to time constraints, simplified models of both systems were developed. These models were then brought to life in the simulation environment of Dymola. The models were designed to closely mimic the behaviour of the actual systems. In Dymola, the simulation process was bifurcated into static and dynamic stages. Static simulations provided a robust understanding of system performance under different conditions, using set parameters to analyse system behaviour, efficiency, and viability. This formed the bedrock for the subsequent dynamic simulations. A lot of emphases was put on accurately simulating the seasonal operation of both systems. These simulations provided critical insights and generated the major KPIs for the study by modelling variations in heating and cooling demands, weather conditions, and other elements that influence the systems' performance.

System 1 demonstrated a peak cooling capacity of 890 kW, consuming 939,408 kWh yearly. Its SCOP varied from 3.98 in summer to 3.22 in winter. System 2, adjusted pressure levels between 33 bar and 97 bar to deliver hot water at 70°C, utilising 242,811 kWh annually. The system has the capability to produce approximately 95,771 litres of hot water on a typical

summer day and 57,720 litres on a typical winter day. Its SCOP remained relatively stable, at 3.91 in summer and 3.93 in winter.

After examining KPIs, customized simulations were conducted, focusing on each system's unique application. This enabled a deeper understanding of the physics underpinning each system's performance. Every result set was scrupulously reviewed and discussed, backed by an extensive literature survey, leading to a more insightful analysis.

This simulation tool is poised to significantly aid PTG in optimizing similar systems, fostering informed decisions, and promoting more efficient, sustainable industrial processes.

Keywords: *Salmon processing plants, Temperature management systems, Energy systems, Refrigeration / Heat pumps, R744 heat pumps, R717 parallel compression system, Dynamic simulation, Seasonal operation, Process analysis, Energy analysis.*

Sammendrag

Lakseoppdrett, en viktig hjørnestein i Norges økonomi og dens nest største eksport, krever kompliserte, energikrevende operasjoner. Moderne lakseprosesseringsanlegg bruker en rekke spesialiserte energisystemer, inkludert avfukting, systemer for nedkjølt sjøvann (RSW), isproduksjonsenheter, frysetunneler, kjølelager og varmegjenvinningsenheter. Disse systemene, hver med sine unike oppvarmings-, kjøle- og energiforbruksprofiler, bidrar til den intrikate daglige driften av anlegget. Betydelig kjøleinfrastruktur er avgjørende for å imøtekomme kravene til disse forskjellige energisystemene, for å sikre at anlegget fungerer effektivt.

Hovedmålet med denne forskningen er utviklingen av et simuleringsverktøy. Dette verktøyet er ment å vurdere og sammenligne ulike systemkonfigurasjoner for fremtidige lakseforedlingsanlegg, og dermed veilede optimale designvalg. I forbindelse med denne studien implementerer PTG et omfattende temperaturkontrollsystem for et anlegg som drives av Holmøygruppen i Holmen, Norge. En detaljert analyse av dette anlegget, tatt i betraktning faktorer som dets geografiske plassering og spesifikke operasjonelle krav, ble utført. Basert på denne innsikten ble det foreslått to distinkte kjøleløsninger. Den første løsningen foreslo et enkelt varmepumpesystem for å oppfylle alle kravene til SPP. Den andre løsningen anbefalte å implementere to separate systemer: et to-trinns parallellkompresjon R717 kjølesystem (System 1) og et R744 RSW system (System 2). Etter å ha vurdert fordeler og ulemper for hver løsning, ble tilnærmingen med to system valgt som det optimale valget.

En grundig undersøkelse ble utført på begge systemene, og fordypet seg i vanskelighetene ved deres drift og mekanismer. Dette innebar å bryte ned systemene i deres individuelle komponenter for en mer detaljert utforskning. Med fokus på å tilnærme den virkelige ytelsen og samtidig overholde tidsbegrensninger, ble det utviklet forenklede modeller av begge systemene. Disse modellene ble deretter brakt til live i simuleringsmiljøet til Dymola. Modellene ble designet for å etterligne oppførselen til de faktiske systemene. I Dymola ble simuleringsprosessen delt inn i statiske og dynamiske stadier. Statiske simuleringer ga en robust forståelse av systemytelse under forskjellige forhold, ved å bruke angitte parametere for å analysere systematferd, effektivitet og levedyktighet. Dette dannet grunnfjellet for de påfølgende dynamiske simuleringene. Det ble lagt mye vekt på nøyaktig simulering av sesongdriften til begge systemene. Disse simuleringene ga kritisk innsikt og genererte de viktigste KPIene for studien ved å modellere variasjoner i varme- og kjølebehov, værforhold og andre elementer som påvirker systemenes ytelse.

System 1 viste en topp kjølekapasitet på 890 kW, forbruker 939 408 kWh årlig. Dens SCOP varierte fra 3,98 om sommeren til 3,22 om vinteren. System 2, justerte trykknivåer mellom 33 bar og 97 bar for å levere varmt vann ved 70°C, med 242 811 kWh årlig. Systemet har kapasitet til å produsere omtrent 95 771 liter varmt vann på en typisk sommerdag og 57 720

liter på en typisk vinterdag. Dens SCOP forble relativt stabil, på 3,91 om sommeren og 3,93 om vinteren.

Etter å ha undersøkt KPIer, ble det utført tilpassede simuleringer, med fokus på hvert systems unike applikasjon. Dette muliggjorde en dypere forståelse av fysikken som ligger til grunn for hvert systems ytelse. Hvert resultatsett ble nøye gjennomgått og diskutert, støttet av en omfattende litteraturundersøkelse, noe som førte til en mer innsiktsfull analyse.

Dette simuleringsverktøyet er klar til å hjelpe PTG betydelig med å optimalisere lignende systemer, fremme informerte beslutninger og fremme mer effektive, bærekraftige industrielle prosesser.

Nøkkelord: *Laksebehandlingsanlegg, Temperaturstyringssystemer, Energisystemer, Kjøle-/varmepumper, R744 varmepumper, R717 parallellkompresjonssystem, Dynamisk simulering, Sesongdrift, Prosessanalyse, Energianalyse.*

Table of Contents

List of Figures

List of Tables

Nomenclature

Abbreviations

SPP	Salmon processing plant
RSW	Refrigerated seawater
UK	The United Kingdom
R744	Carbon Dioxide (CO_2) refrigerant
R717	Ammonia (NH_3) refrigerant
R290	Propane refrigerant
CFCs	Chlorofluorocarbons
GWP	Global Warming Potential
ODS	Ozone Depleting Substances
HFCs	Hydrofluorocarbons
HVAC	Heating, ventilation, and air conditioning
HTF	Heat transfer fluid
COP	Co-efficient of performance
IHX	Internal heat exchanger
DHW	Domestic hot water
DX	Direct expansion
HP	High pressure
LP	Low pressure
PTG	Perfect Temperature Group
70HS	70°C Heating System
EES	Engineering equation solver
PI	Proportional–integral–derivative controller
$\dot{W}_{Pu1}$	Shaft power of pump in system 1
$\dot{W}_{Pu2}$	Shaft power of pump in system 2
$\dot{m}_w$	Mass flow rate of hot water produced in the R744 HP

Symbols

Q_o	Evaporator (cooling) capacity (kJ)
Q_c	Condenser (heating) capacity (kJ)
$\dot{W}c$	Work input to compressor (kW)
h	Enthalpy (kJ/kg)
$\dot{m}_r$	Refrigerant mass flow rate (kg/s)
$\dot{Q}_c$	Condenser heat rejection (kW)
$\dot{Q}_o$	Evaporator heat absorption (kW)
COP_{LZ}	COP of modified Lorentz cycle
T_m	Middle temperature in Lorentz cycle (K)
T_o	Evaporator temperature (K)
η_{LZ}	Lorentz efficiency
COP_{HP}	COP of heat pump
$COP_{R717\,RF}$	COP of R717 refrigeration system
η_{HP}	Efficiency of the HP compressor
η_{LP}	Efficiency of the LP compressor
$\dot{Q}_{low}$	Heat transfer in low stage (separator 2) (kW)
$\dot{m}_l$	Mass flow rate of refrigerant in lower stage (kg/s)
$\dot{m}_t$	Mass flow rate of entire charge in R717 system
$\dot{m}_f$	Mass flow rate of the flash gas from separator 1 (kg/s)
$\dot{W}_{LP}$	Shaft work of the LP compressor (kW)
$\dot{W}_{HP}$	Shaft work of the HP compressor (kW)
$\dot{Q}_{GC}$	Heat rejected in the gas cooler (kW)
$\dot{Q}_{IHX}$	Heat transfer inside the IHX (kW)
T_{wo}	Water outlet temperature (°C)
T_{wi}	Water inlet temperature (°C)

DT	Discharge temperature	$\dot{m}_c$	Mass flow rate of CO_2 in the R744 heat pump
ST	Suction temperature	$COP_{R744\ HP}$	COP of the R744 heat pump
70-90HW	Special case simulation of system 2 (4.2.2.3)	NOK	Norwegian Krone (currency)
SCOP	Seasonal COP	Øre	Subunit of NOK

Chapter 1: Introduction

1.1 Salmon Production

The escalating global population is placing significant strain on our current food production methods. The United Nations predicts a 70% increase in food demand by 2050, necessitating innovative measures to meet nutritional needs. The fisheries and aquaculture industries play a vital role in ensuring food accessibility for all, and it is imperative for Norway, a major producer of seafood and the world's leading exporter of salmon, to lead the way in promoting sustainable practices within the industry. (Food and Agriculture Organization of the United Nations, 2018).

Norway holds the distinction of being the largest exporter of salmon globally, and in conjunction with Chile, it dominates nearly 80% of the salmon export market (Romero-Ayala et al., 2021). The chilly and nutrient-rich seas of Norway provide an optimal habitat for the thriving growth of Atlantic Salmon.

Norway's cold and nutrient-rich waters provide an optimal environment for Atlantic Salmon, making it an ideal habitat for their growth. Throughout more than five decades of salmon farming in Norway, significant advancements have been made, progressing from basic net cages to state-of-the-art installations driven by scientific breakthroughs. In their quest to minimize environmental impact, increase productivity, and enhance the welfare of the fish, Norway has actively engaged in a process of overcoming challenges and uncovering innovative solutions. (Norwegian Seafood Council, 2017).

The salmon production cycle is about 3 years and comprises of three cycles (Bravo et al., 2013):

- Smolt rearing in freshwater - aiming to produce salmon eggs that are transported to a hatchery for fertilization and nurturing. After hatching, the fish progress into the fingerling stage, where they receive care until the smoltification phase commences. As the smolt reaches a weight of around 100 to 200 grams, adaptive mechanisms are triggered, facilitating the transition of the fish to the seawater stage.
- Further growing in seawater - with the primary objective being to nurture the fish until they reach an optimal size for harvesting and sale. Seawater temperatures, which vary based on seasonal and geographical factors, exert a significant influence on the development of the fish during this stage.
- Processing in production plants - After the salmon has been harvested, it undergoes a process of calibration and cleaning. Following this, the fish is filleted, and depending on the desired end products, it is either divided into various parts or subjected to additional processing. These additional processes add value to the salmon, and examples include the production of cold- or hot-smoked salmon, among other products.

This project focuses on the refrigeration/cooling systems employed during the second and third stages of the above-mentioned production cycle. The third stage is further divided into substages: (i) Reception of raw material, (ii) Treatment room, (iii) Cooling system, (iv) Packaging, and (v) Storage of end products (Romero-Ayala et al., 2021). Temperature management plays a huge role in substages (ii), (iii), (iv) and (v).

1.2 Inside a Salmon Processing Plant

A very basic layout of the different stages/steps inside a salmon processing plant has been shown in **Figure 1**.

Dedicated fishing vessels transport the fresh catch of salmon to the factory. Once at the factory, the salmon is transferred to seawater cages for further growth. Before euthanasia, a process known as live chilling or precooling takes place, where the salmon is placed in tanks filled with Refrigerated Sea Water (RSW) to maintain their freshness and quality (Brodal et al., 2018) stage (i).

Following the pre-cooling process in the RSW, the salmon proceed to stage (ii) where they are sequentially stunned and killed. In this stage, the fish undergo a series of steps, including the removal of the viscera, assessment of quality, and determination of weight.

Following the classification, washing, and sanitization processes, the fish are subsequently sorted into two categories: whole fish and filleted fish. The whole fish are categorized without detailed structural information, and they undergo a passage through a saline solution before being sorted as either fresh or frozen salmon. Fresh salmon items are carefully packaged and prepared for transfer to the cold stage.

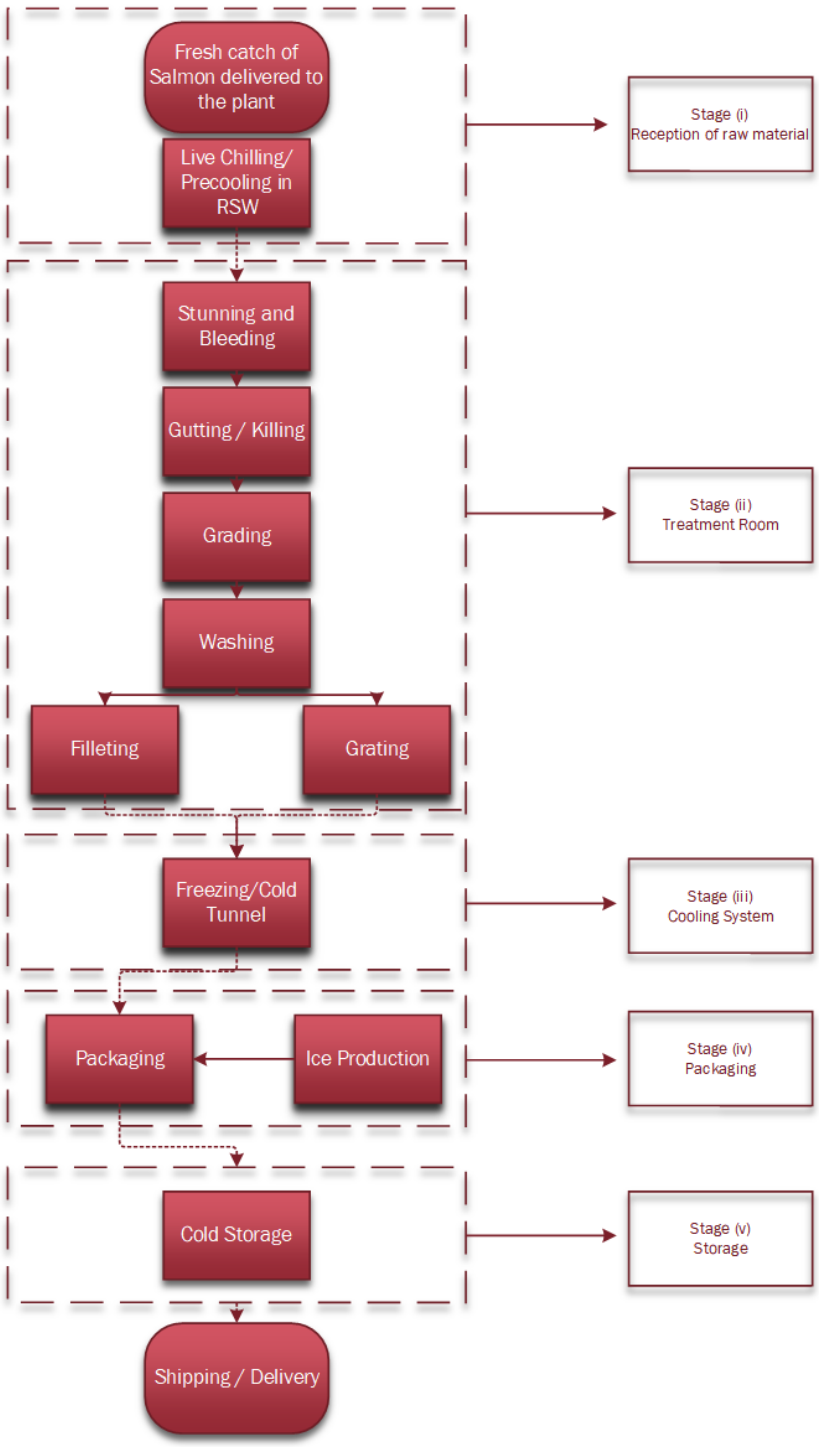

Figure 1: *Salmon Production Plant Process*

Stage (iii) encompasses the cooling system, which comprises tunnels that can be categorized as either static or continuous. These tunnels operate within a temperature range of -25°C to -35°C, depending on their specific type. After undergoing the cooling process, the fish proceeds to stage (iv), where the items are meticulously packaged with appropriate labels and specifications. The packaged products are then transferred to the freezer, which serves as the final sub-stage aimed at maintaining an average temperature of 5 degrees Celsius. The fish remains in the freezer until it is ready for future shipment.

1.3 Aim of the Master Thesis

According to the findings reported by (ENOVA, 2010, 2009, 2008), the average specific energy consumption in investigated fish slaughterhouses ranged from 99 to 181 kWh per tonne. However, scientific literature and reports focusing on energy usage in fish slaughtering stages are relatively scarce. A study conducted by Rosenberg et al., 2007 highlighted that chilling or freezing procedures accounted for a significant portion (69%) of the overall energy usage in fish processing plants. Given this context, optimizing the refrigeration and heating systems in salmon process plants becomes imperative to reduce annual electricity consumption.

This master's thesis aims to analyse the heating and cooling requirements of various energy systems within a specific salmon processing factory in Norway. The primary goal is to design efficient refrigeration systems that can effectively meet these demands. The outcomes of this research will serve as a valuable reference for similar industrial process facilities in the future.

The Holmøy group has undertaken the construction of a cutting-edge salmon slaughterhouse in Sortland, Norway, with a vision to incorporate advanced energy technologies for optimal salmon processing. PTG has been entrusted with the responsibility of providing a comprehensive temperature control system, encompassing Refrigerated Sea Water cooling, Ice Production Systems, Freezing Tunnels, Freezing/Storage Rooms, Heat Pumps, and Heat Recovery Units. After careful consideration of various influencing factors, different solutions will be formulated. The refrigeration systems associated with each solution will undergo thorough evaluation through simulations and extensive research.

The ultimate objective of this thesis is to develop a robust simulation tool capable of assessing and recommending system configurations based on actual load profiles provided by clients. Such a tool will serve as a valuable resource for evaluating and optimizing the performance of refrigeration systems in salmon processing facilities.

To enhance the uniqueness and provide additional information, it would be beneficial to include details about the specific challenges faced in salmon processing facilities, such as the need for precise temperature control to maintain product quality and meet regulatory requirements.

1.3.1 About the chosen salmon processing plant / Lakseslakteri

After careful consideration of various factors, The Holmøy group has decided to construct a state-of-the-art salmon abattoir in Holmen, which will mark their largest single investment to date. The aim is to create a modern fish slaughterhouse that will predominantly operate through the use of robotics and automation.

The architectural firm Snøhetta has been entrusted with the design of this ambitious project (Snøhetta, 2022). One of the primary objectives of the structure is to provide transparency in

the manufacturing process, allowing for a clear view of the operations. Additionally, the project will incorporate well-designed and spacious offices for the staff, featuring large glass surfaces. The overall project comprises three main structures: a salmon slaughterhouse with an administration section, a storage facility, and a tank farm. Outdoor spaces will also be integrated into the project design. The location chosen for the project is an existing sea embankment, and the combined gross area of the three structures will amount to approximately 16,315 m^2 (Holmøy Maritime, 2022; iLaks.no, 2020).

Figure 2: *Illustration of the salmon slaughterhouse (front view) by Snøhetta* (Holmøy Maritime, 2022)

A detailed description of the various energy systems and their demands has been provided in section 3.1.

Chapter 2: Theory and literature review

2.1 Refrigeration and Heat Pumping

Heat naturally flows from regions of high temperature to regions of low temperature, following a path of decreasing temperature. Conversely, the reverse process does not occur spontaneously.

The distinction between a heat pump and a refrigerator lies in their primary purpose. In a refrigeration system, the external fluid passing through the evaporator is cooled, while in a heat pump, the external fluid passing through the condenser is heated. The key difference between a refrigerator and a heat pump lies in their mode of operation, specifically in terms of cooling or heating. If the intended application is cooling, the focus will be on the cooling aspect, denoted as Qo in **Figure 3**, which occurs over the evaporator. In this case, the device will be referred to as a refrigerator, air conditioner, chiller, or similar terms. On the other hand, if the intended application is heating, the emphasis will be on the heating component, denoted as Qc in **Figure 3**, which occurs over the condenser. In this scenario, the device will be known as a heat pump (Çengel and Boles, 2008; Meyer, 2011).

2.1.1 History

During the 1800s, the natural refrigeration industry thrived, and there was a high demand for natural ice, particularly obtained from Norway. Large quantities of ice were harvested and stored in insulated ice huts, often using sawdust as insulation material. Throughout the 1800s, various mechanical refrigeration systems were developed, employing different refrigerants such as sulphur dioxide, methyl chloride, ether, carbon dioxide, and even substances like wine, brandy, and vinegar. However, in 1930, the use of natural fluids started to decline with the introduction of synthetic refrigerants, which offered improved operating conditions. These synthetic fluids gradually replaced the natural ones. Unfortunately, it was later discovered that these artificial refrigerants posed a significant threat to the ozone layer and the environment. This realization prompted efforts to find alternative solutions that are more environmentally friendly. (T. M. Eikevik, 2021a).

The first heat pump, as we recognize it today, was invented by Peter von Rittinger in 1856. His discovery of the heat pump concept came about during his experiments on harnessing the latent heat of water vapour for the evaporation of salt brine.

In the early 1950s, another notable development in the field of heat pumps took place when John Sumner installed a closed-loop ground source heat pump system in his own home. The ground loop of Sumner's system was initially constructed using copper tubing filled with circulating antifreeze. Although Sumner's heat pumps were fully functional and technically advanced for their time, they did not receive substantial support or recognition in the United Kingdom. These early contributions by von Rittinger and Sumner laid the foundation for the development and advancement of heat pump technology, which has since become an

important and widely used method for heating and cooling applications (Automatic Heating, 2022).

2.1.2 Working Principle

Vapour-compression cycle refrigeration is a technique that transfers heat from a relatively cold source to a hot medium by utilizing the mechanics of phase change heat transfer and the features of a refrigerant. The refrigerant is compressed and expanded alternatively as it flows through the system, changing its condition from liquid to vapour. Heat is absorbed and released by the system when the refrigerant changes state, decreasing the temperature of the conditioned room. As shown in **Figure 3**, the compressor, condenser, expansion valve, and evaporator are the basic refrigeration system components (Thermal Engineering, 2019).

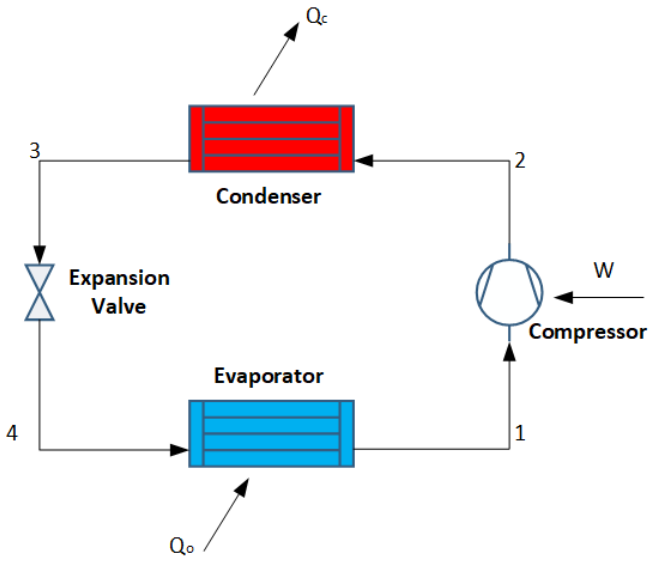

Figure 3: *Principle sketch of a vapour-compression refrigeration cycle*

In a heat pump cycle, the system the cycle undergoes a series of four processes:

Isentropic Compression (1-2): a process in which a refrigerant, such as a circulating fluid, enters a compressor in the form of low-pressure vapour, typically at or slightly below the temperature inside the refrigerator. During this process, the gaseous medium is adiabatically compressed from state 1 to state 2, resulting in a significant increase in both pressure and temperature. The surrounding environment influences the gas, causing its internal energy (temperature) to rise and its pressure to increase. Throughout the compression process, the entropy of the system remains constant. The work required for the compressor is given by:

$$\dot{W}c = \dot{m}_r\,(h_2 - h_1)\ \ (kW) \qquad (2.1)$$

Isobaric heat rejection (2-3): The superheated vapour is forced through the condenser's coils or tubes. During this phase, the refrigerant flows through the condenser, where it condenses, and heat is transferred from the refrigerant to the colder surroundings. The net heat rejected is given by:

$$\dot{Q}_c = \dot{m}_r\,(h_2 - h_3)\ \ (kW) \tag{2.2}$$

Isenthalpic Expansion (3-4): At state 3, the refrigerant enters the expansion valve, where it undergoes a process of expansion to reach the desired pressure in the evaporator. This expansion process is commonly depicted as a throttling process with constant enthalpy, meaning that the enthalpy of the refrigerant remains constant during this phase.

As the refrigerant passes through the expansion valve and experiences a sudden pressure drop, a portion of the liquid refrigerant undergoes rapid evaporation, resembling an explosive-like phenomenon. Typically, around 50% of the liquid refrigerant evapourates in this flash evaporation process. The sudden decrease in pressure causes the refrigerant to vapourize quickly, absorbing heat from its surroundings and resulting in a significant drop in temperature. This cooled and partially vaporized refrigerant is then ready to enter the evaporator for the next stage of the refrigeration cycle.

$$h_3 = h_4\ \ (kJ/kg) \tag{2.3}$$

Isobaric heat absorption (4-1): The partially vaporized refrigerant flows through the coils or tubes of the evaporator unit. Because the chamber is open to flow in and out throughout this phase, there is a constant-pressure heat transfer to the liquid medium from an external source. The refrigerant vaporizes as it goes through the evaporator due to heat transfer from the chilled environment.

$$\dot{Q}_o = \dot{m}_r\,(h_4 - h_1)\ \ (kW) \tag{2.4}$$

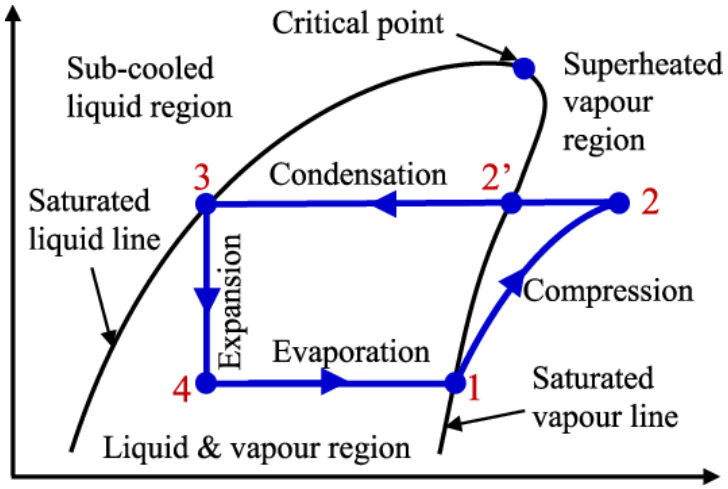

Figure 4: *Principle log p-h diagram for a refrigeration system* (Bolaji, 2020)

2.1.2.1 Co-efficient of Performance (COP)

The thermal efficiency of a refrigeration system or heat pump refers to its ability to effectively convert the energy provided by work into net heat output. From an economic perspective, an ideal refrigeration cycle can extract the maximum amount of heat from the inside of the refrigerator (cold reservoir) while minimizing the mechanical work or electric energy required. The coefficient of performance (COP) is used to measure this ratio, where a higher COP indicates a more efficient refrigerator (Duarte et al., 2017).

In the context of a refrigeration system, the COP is calculated by dividing the heat removed from the refrigerated space (heat absorbed by the evaporator) by the work performed to remove the heat (work done by the compressor).

$$COP_{RF} = \frac{\dot{Q}_O}{\dot{W}_c} \tag{2.5}$$

The COP of a heat pump (**Figure 3**) is determined by the ratio of the heat added to the system (hot reservoir) to the input work. According to the first law of thermodynamics, the COP is calculated by considering both the heat extracted from the cold reservoir and the input work required.

$$\dot{Q}_c = \dot{Q}_o + \dot{W}_c \tag{2.6}$$

$$COP_{HP} = \frac{\dot{Q}_C}{\dot{W}_c} \tag{2.7}$$

2.1.3 Refrigerants

Refrigerants play a significant role in various aspects of society, as they are utilized in systems that serve purposes such as food preservation, ice production, creating comfortable indoor environments, and supporting industrial processes. These substances can exist in either a liquid or gaseous state, and they possess the capability to efficiently absorb heat from the surrounding environment. When combined with components such as compressors and evaporators, refrigerants enable the generation of cooling effects and facilitate air conditioning systems. Notable examples of early refrigerants include ammonia (R-717), carbon dioxide (R-744), ethyl chloride (R-160), isobutane (R-600a), methyl chloride (R-40), methylene chloride (R-30), and sulphur dioxide (R-764) (Dincer and Kanoglu, 2010).

Figure 5: *Examples of CFC Refrigerants such as R22, R32, etc.* (Legacy Air, 2022)

When compared to natural compounds, the emergence of chlorofluorocarbons (CFCs) in the early 1930s was revolutionary. CFCs and similar substances contribute significantly to the loss of the stratospheric ozone layer and the greenhouse effect, all of which are regarded as

major environmental issues. CFCs (**Figure 5**) are greenhouse gases that contribute to incremental global warming of the same scale.

2.1.4 Natural Refrigerants

Organic and inorganic substances known as natural refrigerants have become increasingly popular as alternatives to fluorocarbons in various refrigeration and air conditioning applications. These refrigerants offer several benefits, including low Global Warming Potential (GWP) and a reduced risk of environmental impact. Examples of natural refrigerants include ammonia, carbon dioxide, hydrocarbons, water, and air. Although some natural refrigerants have been used in the market for many years with varying degrees of success, they are not without their challenges. Drawbacks such as corrosion, toxicity, high pressures, flammability, and potentially reduced operational efficiency need to be considered when utilizing natural refrigerants. Despite these limitations, the environmental advantages of natural refrigerants continue to drive their increased adoption in recent years (ASHRAE, 2011).

2.1.4.1 Why Natural Refrigerants?

Evidence began to emerge in the 1970s that CFCs, which were used in common home appliances such as air conditioners and refrigerators, were depleting the Earth's protective ozone layer and increasing the amount of ultraviolet light reaching our planet's surface. The member countries argued for strict regulations on the production and use of ODS such as chlorofluorocarbons (CFCs) and halons, as well as for more international cooperation and consensus building to phase out ODS.

In 1987, The Montreal Protocol was signed, it is a global agreement that aims to safeguard the stratospheric ozone layer by phasing out the production and use of ozone-depleting chemicals (ODS). The Montreal Protocol is creative and effective, and it is the first pact to be ratified by all countries on the planet (United Nations, 1998; U.S.Department of State, 2015).

Several recognizable HFCs and HFC-blend refrigerants were affected by the regulations: R-404A, R-134a, R-410A and R-407C, which were used to replace R-22. On October 15, 2016, Montreal Protocol Parties accepted the Kigali Amendment to scale down global production and consumption of hydrofluorocarbons (HFCs) (Danfoss, 2018).

Secondary coolants were examined for use in indirect refrigeration systems in addition to natural refrigerants. In addition to typical secondary coolants like glycols and salt brines, new coolants have arrived on the market, with CO_2 as a secondary coolant showing particularly promising results (ASHRAE, 2011). Because of the inclusion of a secondary working fluid, these solutions trade off the environmental benefits of lower refrigerant charge for decreased system running efficiency. Another challenge that numerous natural refrigerants have is the need to progress the development of system components that can achieve required energy and performance savings at a low cost.

2.1.4.2 Ammonia (R717)

Ammonia emerges as the primary natural refrigerant, renowned for its extensive historical usage in food and beverage production, as well as its growing presence in various applications such as HVAC chillers, thermal storage systems, process cooling, air conditioning, district cooling, supermarkets, and convenience stores. Importantly, it is worth noting that ammonia carries no implications for global warming and ozone layer depletion, boasting a remarkable track record with zero Ozone Depletion Potential (ODP) and Global Warming Potential (GWP). Additionally, owing to its lower molar mass, ammonia exhibits higher particle velocities compared to other refrigerants, allowing for the utilization of smaller pipe diameters, which presents an engineering advantage (Hafner, 2019).

Nevertheless, it is crucial to be aware of the challenges associated with ammonia usage. While it features self-alarming properties even at lower concentrations (5 ppm), it does pose a potential risk at higher concentrations (above 300 ppm), which could have lethal effects. However, it is worth mentioning that this risk is partially mitigated by the distinct pungent odour of ammonia, serving as a human alert system. To ensure safety, proper precautions must be taken, including the installation of ammonia refrigeration systems in dedicated rooms, comprehensive training for personnel, and the provision of suitable safety equipment comparable to those used for handling flammable substances (ASHRAE, 2011). Notably, in specific applications such as utilizing waste heat in district cooling and combined cooling, heating, and power (CCHP) systems, the practicality and economic advantages of employing absorption chillers with an ammonia/water blend have been recognized.

Table 1: *Characteristics of R744 and R717* (Trygve M Eikevik, 2021a)

Refrigerants	T_{NBP}	T_{crit}	P_{crit}	$T_{c\text{-}23bar}$	GWP
R717	-33.1	132.3	113.5	55/76	0
R744	78.4	31.1	73.8	-14.8	1

2.1.4.3 Carbon Dioxide (R744)

Throughout the late 1800s, carbon dioxide has been extensively employed as a working fluid in refrigeration systems. However, its utilization in maritime applications was discontinued in the 1950s due to technical difficulties and the emergence of synthetic working fluids with lower operating pressures. The rediscovery of carbon dioxide as a refrigerant transpired in the 1980s when Prof. Gustav Lorentzen and colleagues at NTNU and SINTEF developed automotive air conditioning systems and CO_2 heat pumps for water heating (Lorentzen, 1994). Presently, carbon dioxide has achieved widespread adoption across various refrigeration systems, ranging from low-temperature freezers to high-temperature heat pumps. Moreover, it has become increasingly popular as a secondary refrigerant, offering significant efficiency enhancements over conventional water, glycol, or brine systems.

One distinguishing characteristic of carbon dioxide is its pressure/temperature behaviour, which sets it apart from other refrigerants. The pressures encountered in carbon dioxide systems are roughly ten times higher than those in ammonia or R-404A systems. This high pressure correlates with an elevated gas density, enabling a more substantial refrigerating effect from a given compressor. Additionally, carbon dioxide exhibits relatively small reductions in saturation temperature for a given pressure drop, facilitating greater mass flow in evaporators and suction pipes without compromising efficiency. This feature is particularly pronounced at low temperatures (-30°C to -50°C), elucidating the remarkable effectiveness of carbon dioxide systems under such conditions. The unique fluid properties of carbon dioxide, including its high density and low critical point, make it exceptionally well-suited for cooling highly dense heat loads (Lorentzen, 1995).

Furthermore, carbon dioxide exhibits a low critical temperature. Notably, the COP experiences a greater reduction when the condensing temperature hovers around 28°C. To operate at higher heat rejection temperatures, carbon dioxide systems employ a transcritical process, wherein the pressure exceeds the critical pressure. In this process, heat is absorbed at a constant temperature but rejected at variable temperatures. When the pressure surpasses the critical point (7.3773 MPa), carbon dioxide cannot condense, necessitating heat rejection through chilling the highly dense gas and resulting in a temperature glide effect. This particular feature has proven immensely beneficial in water-heating heat pumps across a range of applications, encompassing both residential and industrial settings (Hafner and Eikevik, 2016).

Table 2: *Thermal and physical properties of R717 and R744 at saturation temperature 0°C* (Trygve M Eikevik, 2021a)

Properties	**Unit**	**R717**	**R744**
Molecular Weight	g/mol	17	44
Heat of evaporation	kJ/kg	1261.7	232
Thermal conductivity, liquid	W/mK	0.5455	0.111
Thermal conductivity, gas	W/mk	0.0260	0.0131
Specific volume, liquid	dm^3/kg	1.566	0.850
Specific volume, gas	dm^3/kg	289.39	32.63
Kinematic viscosity, liquid	m^2/s	0.2760	0.1423
Kinematic viscosity, gas	m^2/s	2.7672	0.3883
Ignition Temperature	°C	630	NA

2.1.5 Heat transfer fluid

In various heat transfer applications, a heat transfer fluid (HTF) plays a crucial role as an intermediate fluid responsible for transferring heat from a heat source to one or more cold streams. By utilizing an HTF, a single heater can efficiently heat multiple cold streams. The HTF, a circulating fluid, carries heat from the heat source (heater) to the cold streams through

heat exchangers, subsequently returning to the heat source for recirculation. The selection of the appropriate HTF depends on factors such as the specific industrial application, the required temperature range for safe operation, and the longevity of the HTF (Sahasranaman, 2005). While manufacturers and process engineers have dedicated their efforts to HTF system design and operation, previous research in the field has primarily focused on individual components rather than the holistic system.

This project encompasses an investigation into water-to-water pumps, which play a pivotal role in pumping the HTF to a heating system and extracting energy from this system in a time-efficient manner. Heat pumps, regardless of whether they utilize air, water, or the earth as the energy recovery source, enable the utilization of thermal renewable energy (Ouadha et al., 2008). The study aims to explore the various aspects related to water-to-water pumps and their integration within HTF systems, contributing to the efficient utilization of thermal renewable energy resources.

When choosing a heat transfer fluid, various factors must be considered (Singh, 1985):

Temperature limitations	Energy conservation/power generation
Heat transfer coefficient	Hazards and limitations of construction
Operating pressure	Cost of fluid

2.1.5.1 Water as a heat transfer fluid

Water is commonly employed as a heat transfer fluid primarily because of its affordability, high heat capacity, and efficient transport properties. However, its practical temperature range is limited due to the potential for freezing below 0°C and boiling at extreme temperatures, depending on the system pressure. It is worth noting that water is compatible with copper, which is an excellent material for heat transmission in fluid paths.

In temperature control devices, water is extensively utilized for operating temperatures up to 90°C. However, when temperatures exceed this threshold, the operator must make a choice between water and thermal oil for the heat transfer process. Water possesses several advantages as a heat transfer fluid, as supported by (REGLOPLAS, 2022; Schobeiri, 2022):

- High Specific Heat: Water exhibits a specific heat approximately double that of thermal oil. This characteristic enables water to convey a greater amount of thermal energy as a heat transfer fluid. Additionally, water has a higher heat transfer coefficient, at least double that of thermal oil. This implies that water efficiently transfers thermal energy from the walls to the heat transfer fluid.
- Low Viscosity: Water maintains a low viscosity that remains relatively constant across its application range. This property facilitates smooth flow and efficient circulation of the heat transfer fluid.

- Low Expansion Coefficient: Water possesses a very low expansion coefficient. This attribute proves advantageous when utilizing systems that involve significant volumes of heat transfer fluid. The low expansion coefficient helps minimize the impact of thermal expansion and contraction, ensuring system stability.
- No Coking: Water does not undergo coking, a process of carbonaceous deposit formation. This characteristic allows for a larger specific heating capacity, resulting in the design of smaller and more cost-effective heat transfer units.

Overall, the unique properties of water make it a favourable choice as a heat transfer fluid, offering high thermal capacity, efficient heat transfer, low viscosity, low expansion coefficient, and avoidance of coking-related issues.

2.2 Energy systems in salmon process plants

Energy consumption in salmon process plants is a critical aspect that directly impacts operational costs and environmental sustainability. Research by (Ates et al., 2017) provides an overview of energy consumption patterns in such facilities. The study highlights that the majority of energy is utilized for refrigeration, freezing, and heating processes, accounting for a significant portion of the overall energy demand. Understanding the energy consumption patterns is crucial for identifying potential areas of improvement and implementing energy-efficient strategies.

2.2.1 Primary energy sources and environmental impacts

Traditional energy sources, such as electricity and fossil fuels, are generally used by salmon processing factories. Electricity is widely used to power various pieces of equipment and machinery, whilst fossil fuels such as natural gas and diesel are used for heating. These energy sources, however, have environmental consequences. (Colt et al., 2008) conducted research on the environmental consequences of various energy sources utilized in salmon processing factories. The study underlines the importance of shifting to cleaner and renewable energy sources to minimize greenhouse gas emissions and prevent climate change.

2.2.2 Potential for energy efficiency improvements

Improving energy efficiency is a priority in salmon processing plants to minimize energy usage and operational expenses. To improve energy efficiency in these facilities, many tactics and technologies have been examined. (Gennitsaris et al., 2023) investigate the possibilities for improving energy efficiency through strategies such as equipment upgrades, process optimization, and energy management systems. The findings reveal enormous prospects for energy savings that may be realized by deploying efficient technology and practices. Furthermore, the use of energy recovery equipment, such as heat exchangers, has demonstrated potential in minimizing energy waste and boosting overall system efficiency.

2.3 Temperature management systems

Temperature control is critical in salmon processing operations for ensuring product quality and safety. Temperature control and maintenance are critical at various phases of processing, storage, and transportation to avoid bacterial development, enzymatic activity, and quality deterioration. According to (González-Fandos et al., 2005), temperature control is critical in guaranteeing the microbiological safety and freshness of salmon products throughout the supply chain.

2.3.1 Key challenges and requirements for temperature control

Temperature regulation in salmon processing plants involves several issues that must be overcome to ensure maximum product quality and safety. One of the most difficult difficulties is keeping temperatures constant throughout the processing and storage rooms. Ambient temperature, air circulation, and machine performance can all have an impact on product quality. (Georges et al., 2014; Zhang et al., 2019) identify temperature management issues, including thermal losses, temperature stratification, and unequal cooling rates.

Specific prerequisites must be met to overcome these obstacles. Proper insulation is essential for minimizing heat transmission and maintaining temperature stability. (Larsen Ringvall and Larsen Ringvall NTNU, 2020) investigates insulating materials and procedures suited for processing factories. The study highlights the importance of selecting insulation with low thermal conductivity, adequate thickness, and proper installation methods to achieve effective temperature management.

Refrigeration systems are another important aspect of temperature control. Nistad and Pettersen, 2020 conducted research on the various refrigeration methods used in fish processing facilities, such as direct expansion (DX) systems, cascade systems, and carbon dioxide (CO_2) transcritical systems. The study assesses their energy efficiency, cooling capacity, and environmental effect, offering information for selecting appropriate refrigeration systems for best temperature management.

2.4 CO_2 Heat Pump

2.4.1 Theoretical reference for transcritical cycles

In the context of transcritical cycles, the selection of appropriate reference cycles is essential for analysing and evaluating the performance of systems operating with carbon dioxide as the working fluid. While the reversed Carnot cycle serves as the theoretical reference cycle for conventional heat pump cycles with nearly constant temperature heat transfer, different reference cycles are more suitable for transcritical CO_2 cycles.

The modified Lorentz Cycle and Ideal Lorentzen Cycle are considered the appropriate reference cycles for transcritical CO_2 systems. These reference cycles are specifically designed to account for the unique characteristics and operating conditions of carbon dioxide as a working fluid.

By utilizing the modified Lorentz Cycle and Ideal Lorentzen Cycle as reference cycles, researchers and engineers can effectively analyze and compare the thermodynamic properties and efficiency of transcritical CO_2 cycles. These reference cycles provide a theoretical framework for understanding the performance limits and potential improvements of transcritical CO_2 systems, enabling the optimization and design of such systems for various applications (Haiozan and Ritter, 1994; Lorentzen, 1994; Stene, 2005a).

2.4.1.1 Modified Lorentz Cycle

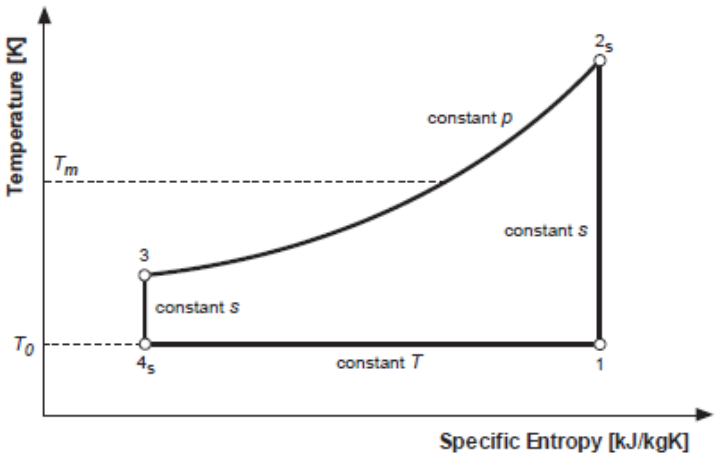

Figure 6: *Modified Lorentz Cycle in a T-s diagram*

1 – 2s: Isentropic compression

2s – 3: Isobaric heat rejection at gliding temperature

3 – 4s Isentropic expansion

4s – 1: Isothermal heat absorption

COP of the modified Lorentz cycle is given by:

$$COP_{LZ} = \frac{T_m}{T_m - T_o} \tag{2.8}$$

Lorentz efficiency is utilized instead of Carnot efficiency in transcritical CO_2 heat pumps. It is given by (HP subscript is for heat pump while LZ subscript is for ideal Lorentz cycle):

$$\eta_{LZ} = \frac{COP_{HP}}{COP_{LZ}} \tag{2.9}$$

2.4.1.2 Ideal Lorentzen Cycle

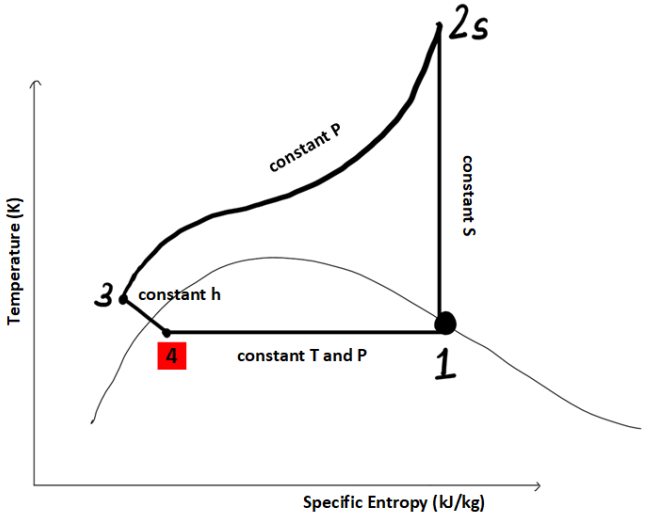

Figure 7: *Ideal Lorentzen Cycle in a T-s diagram*

1 – 2s: Isentropic compression to supercritical pressure

2s – 3: Isobaric heat rejection at gliding temperature

3 – 4: Isenthalpic expansion

4 – 1: Isothermal heat absorption

When conducting a comparison between an actual transcritical CO_2 heat pump cycle and an ideal Lorentzen cycle, it is important to note that the ideal cycle assumes a temperature approach of zero at the output of the gas cooler. However, a significant challenge arises when determining the ideal cycle's high-side pressure, as it directly impacts the CO_2 output temperature from the gas cooler, the heating capacity, and the COP of a real transcritical CO_2 heat pump cycle (Stene, 2005a).

2.4.1.3 Lorentzen Cycle – CO_2 Heat Pump Cycle

The Lorentzen cycle is the true cycle for transcritical CO_2 heat pumps. Simply put, it is a non-ideal variation of the Ideal Lorentzen Cycle mentioned above.

1 – 2: irreversible non-isentropic compression

2 – 3: supercritical non-isobaric heat rejection at gliding temperature

3 – 4: non-isenthalpic expansion

4 – 1': non-isobaric and non-isothermal heat absorption

1' – 1: Suction gas superheating

2.4.2 Transcritical CO_2 Heat Pump

In a typical heat pump cycle, heat is released through subcritical condensation at nearly constant pressure and temperature. However, in a subcritical CO_2 cycle, the practical upper limit for the condensation temperature is approximately 28°C due to the low critical temperature of CO_2. For household heating applications like space heating and domestic hot water, which require temperature levels above this limit, a transcritical cycle is employed (see **Figure 10**). Unlike the subcritical cycle, in a transcritical CO_2 heat pump system, heat rejection occurs at nearly constant pressure but with varying temperatures. This heat rejection process takes place in a gas cooler (Hafner and Eikevik, 2016).

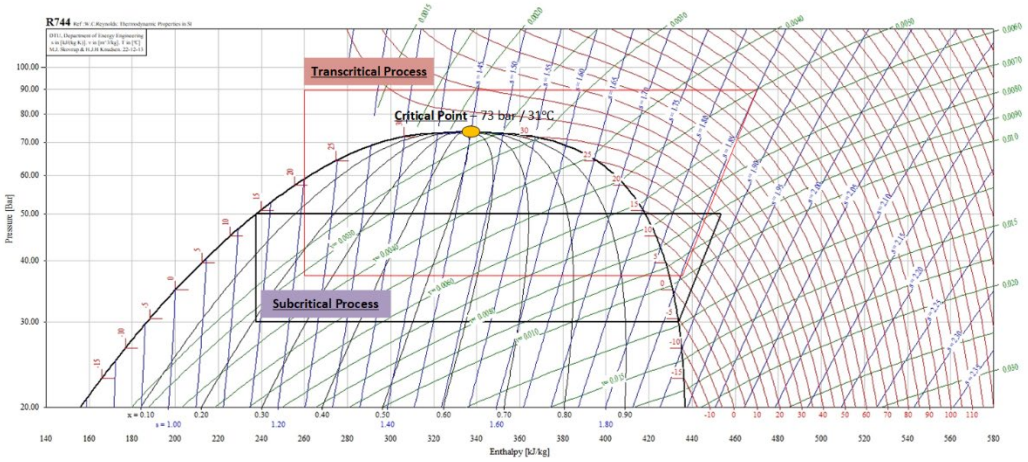

Figure 8: *Subcritical vs Transcritical process in a log p-h diagram*

The COP for a heat pump can be calculated using equation 2.7. It is well-established that the temperature at which heat rejection occurs plays a significant role in determining the efficiency of the system. In a typical heat pump cycle, this temperature corresponds to the constant temperature in the condenser (T. M. Eikevik, 2021b). Additionally, it is important to note that to achieve a high COP, the fluid to be heated by the heat pump should have the lowest possible temperature level (Stene, 1999).

In cases where the temperature glide of the secondary fluid is low, traditional heat pumps tend to have a higher COP compared to CO_2 heat pumps. This is because the condenser temperature can be maintained at a lower level than the average gas cooler temperature while still delivering the same amount of heat.

The heating capacity and COP of CO_2 heat pumps are primarily influenced by the temperature glide in the gas cooler and the operating pressure. Increasing the amount of refrigerant cooled in the gas cooler leads to an increase in heating capacity. However, the gas cooler design needs careful consideration due to CO_2's high working temperature and temperature glide during supercritical cooling.

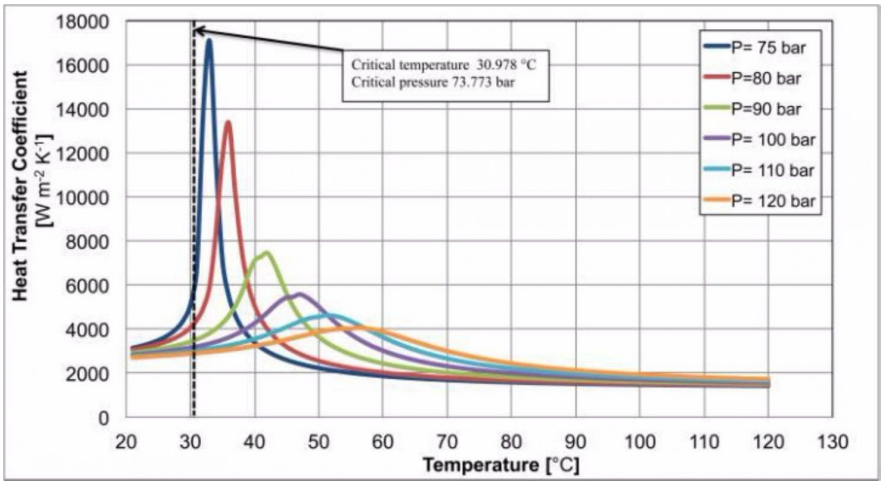

Figure 9: *CO_2 heat transfer coefficient at supercritical gas cooler operating pressures* (UNILAB, 2019)

In **Figure 9**, the relationship between specific heat and temperature is shown for different supercritical pressures. It can be observed that as the pressure increases, the fluctuation in specific heat decreases, eventually reaching a point where the specific heat becomes nearly constant at very high pressures. These fluctuations in specific heat are a distinct characteristic of CO_2 and differentiate the gas cooling process from the conventional condensation process. These unique characteristics should be taken into account when modelling gas coolers in CO_2 systems.

While CO_2 heat pumps offer several advantages, they are not without disadvantages. One significant drawback of a transcritical CO_2 cycle is the reduced COP caused by significant energy loss through the expansion valve. This energy loss has a negative impact on the overall efficiency of the system.

2.4.2.1 Improvement of COP – using an Internal heat exchanger (IHX)

To improve the COP of a CO_2 transcritical cycle in both the heating and refrigeration cycles, various strategies can be explored, with many of them focused on achieving a certain level of subcooling at the gas cooler outlet. Several methods can be employed to increase the COP, including two-stage compression, utilization of an absorption chiller, and replacing the conventional throttle valve with expansion devices such as injectors, vortex tubes, and expanders. One popular approach is the incorporation of an IHX as shown in **Figure 10**.

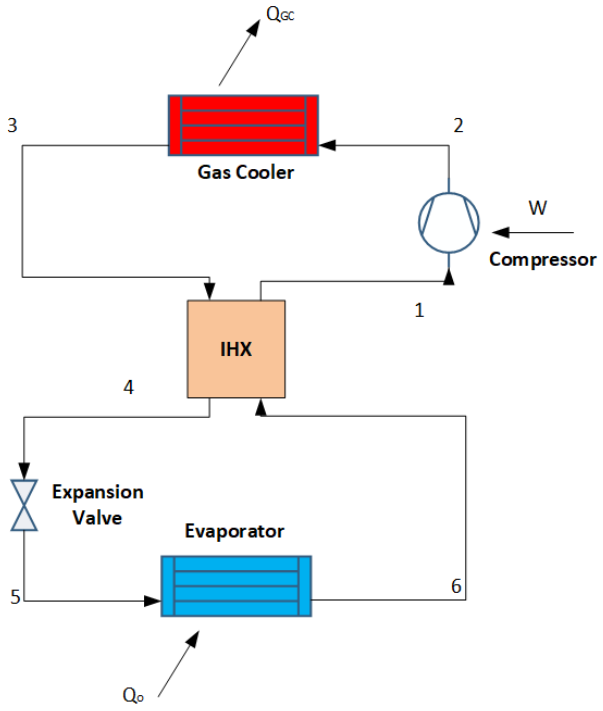

Figure 10: *Transcritical $_{CO2}$ heat pump with an IHX*

The IHX utilizes the refrigerant at the outlet of the evaporator for subcooling at the outlet of the gas cooler. This results in a pressure decrease in the system and helps enhance the system's overall performance. By utilizing the heat from the superheated refrigerant to subcool the liquid refrigerant, the IHX improves the system's efficiency and reduces the energy loss in the cycle (Feng et al., 2020).

In a study conducted by (Chen and Gu, 2005), an air-to-air CO_2 heat pump with an IHX was investigated, and it was found that the system achieved the highest COP values under low-temperature operating conditions. The inclusion of the IHX in the system played a significant role in improving its performance.

Another study by (Cho et al., 2007) focused on the impact of IHX length on the cooling capabilities of a CO_2 cycle. The IHX in this study was a double-tube heat exchanger with a length ranging from 0 to 3 meters. It was observed that increasing the length of the IHX led to a notable improvement in COP, with a 7 to 9% increase compared to the system without an IHX.

Furthermore, it was found that when the discharge pressure of the CO_2 heat pump system reached its optimal value, the COP of the system with an IHX was higher than that of the system without an IHX. This suggests that the presence of an IHX contributes positively to the system's overall COP. Additionally, a longer IHX length was found to be advantageous for achieving a higher COP, primarily due to the resulting higher gas cooler outlet temperature.

These findings highlight the significance of incorporating an IHX in CO_2 heat pump systems and optimizing its length to maximize the system's COP, particularly under low-temperature operating conditions. The IHX serves as a key component for enhancing the cooling capabilities and overall efficiency of CO_2 heat pump systems.

2.4.2.2 Other enhancements

Other upgrades are feasible to increase the energy efficiency and performance of transcritical R717 systems; different enhancements have been investigated. These are some examples:

- Parallel Compression: Parallel compression entails compressing the gas discharged from the system's low-pressure side and injecting it into the system's high-pressure side. This strategy reduces compression work while increasing overall system efficiency.
- Optimization of Gas Cooler Design: The design of the gas cooler, which is in charge of rejecting heat from the CO_2 refrigerant, can have a considerable influence on system performance.
- Heat recovery: Transcritical R717 systems allow for waste heat from the system to be recovered and used for other reasons like room heating or water heating.

2.4.3 Gas Coolers

In R744 heat pump systems, gas coolers serve as the final heat exchangers where the supercritical carbon dioxide (CO_2) refrigerant releases heat to the hot water supply. The working principle involves the transfer of heat from the CO_2 refrigerant to the water through direct or indirect contact. This heat transfer process allows for efficient heat recovery and hot water generation.

Advantages of gas coolers in R744 heat pumps:

- Hot Water on Demand: The R744 heat pump's gas coolers enable the generation of hot water on demand, providing a dependable and efficient solution for residential, commercial, and industrial applications. The recovered heat from the CO_2 refrigerant can be utilized for space heating, home hot water delivery, or other industrial activities, eliminating the need for separate hot water systems.
- High Energy Efficiency: Because carbon dioxide has favourable thermodynamic characteristics, R744 heat pumps with gas coolers have high energy efficiency. The supercritical CO_2 cycle facilitates heat transfer and energy recovery.
- Environmental Friendliness: R744 (CO_2) is a natural refrigerant with a low global warming potential, which contributes to environmental sustainability. The usage of R744 in heat pumps corresponds to the increased demand for environmentally friendly heating and cooling solutions. Gas coolers allow CO_2 to be used as a working fluid, reducing the system's environmental effect.

2.4.3.1 Challenges and enhancements

Heat Transfer Enhancement: Due to the unique features of CO_2, gas coolers in R744 heat pumps confront heat transfer problems. Heat transfer techniques have been improved by adopting modern heat exchanger designs and improving flow patterns.

For maximum performance, effective integration and control of gas coolers in R744 heat pumps are critical. Considerations for system design, such as scale and layout, are critical in maximizing heat recovery and hot water output. To improve system performance, advanced control techniques such as variable speed drives and adaptive algorithms have been investigated.

Recent improvements in R744 heat pump gas coolers include the use of new heat exchanger designs, such as microchannel and printed circuit heat exchangers, to increase heat transfer efficiency. Furthermore, the advancement of smart control algorithms and predictive control techniques has demonstrated the potential for further improving system performance and hot water delivery.

2.4.4 Industrial hot water production

The use of CO_2 heat pumps for domestic hot water (DHW) production is gaining popularity due to the sustainability and environmental potential of CO_2 (R744). It aligns with the goals of a future circular economy by utilizing this environmentally friendly refrigerant. In the building sector, low GWP (Global Warming Potential) type A1 refrigerants are highly recommended in future decarbonization policies, and CO_2 stands out as one of the most effective options (Bamigbetan et al., 2017).

CO_2 is particularly suitable for heat pump water heaters with transcritical cycles, thanks to its low critical point, which occurs at a critical temperature of 31°C. The utilization of transcritical cycles allows CO_2 heat pumps to achieve high COP values for heating water, even from very low inlet water temperatures. This is due to the efficient heat transfer that occurs at the hot sink, where sensible energy is transferred both on the water side and the refrigerant side of the heat exchanger, leading to increased overall efficiency (Illán-Gómez et al., 2021).

A study by (Hu et al., 2014) investigated an air source transcritical CO_2 heat pump water heater under various operating conditions. Their findings indicate that increasing the input water temperature or reducing the inlet water flow rate can result in higher hot water temperatures. This demonstrates the flexibility and potential for optimization in CO_2 heat pump water heaters to meet specific requirements for DHW production.

Overall, the use of CO_2 heat pumps with transcritical cycles offers significant advantages for heating water, especially for DHW applications. It aligns with the demand for low GWP refrigerants and provides high COP values, making it an attractive and sustainable choice for future decarbonization efforts in the building sector.

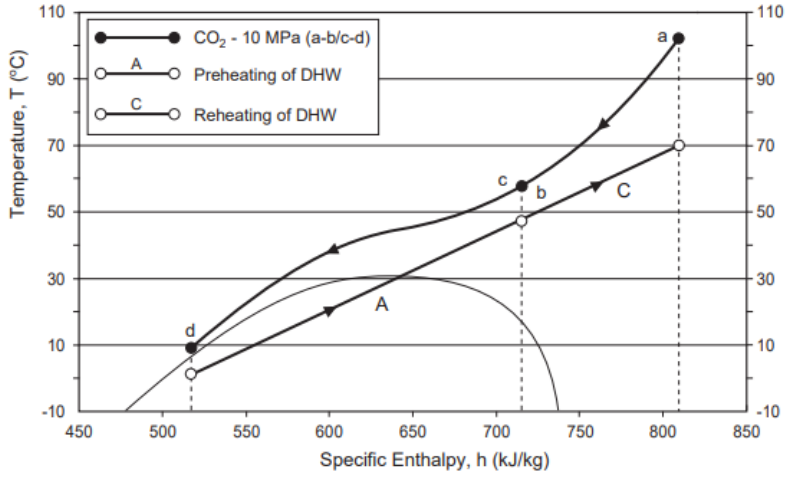

Figure 11: *T-s diagram of the heat rejection from CO_2 heat pump gas cooler for heating tap water* (Stene, 2005b)

CO_2 heat pumps offer superior performance metrics for hot water production due to several reasons outlined by (Hafner and Eikevik, 2016):

- High water temperature: CO_2 heat pumps have the capability to heat tap water to temperatures ranging from 60-90°C (140-194°F). This is achieved through the use of high CO_2 gas cooler intake temperatures and the temperature glide during heat rejection, as depicted in **Figure 11**. The elevated temperatures attained eliminate the need for a separate disinfection cycle, providing hot water suitable for various applications.
- Improved temperature adaptation: CO_2 heat pumps benefit from enhanced temperature adaptation between the refrigerant and water sides of the counterflow gas cooler. This results in lower average refrigerant temperatures during heat rejection, leading to improved efficiency and performance of the system. The effective heat transfer between the refrigerant and water sides enables efficient heat exchange and maximizes the utilization of thermal energy.
- Reduced pressure ratio operations: CO_2 heat pump compressors operate at lower pressure ratios compared to traditional systems. This allows the compressor to achieve high levels of performance and efficiency while minimizing energy consumption. By operating at lower pressure ratios, the compressor can work more efficiently and deliver the desired heating capacity with reduced energy requirements.

2.4.4.1 Basic operation of CO_2 heat pump to produce DHW

Figure 12 illustrates the operation of a basic hot water heating system using a CO_2 heat pump. The system is described as follows:

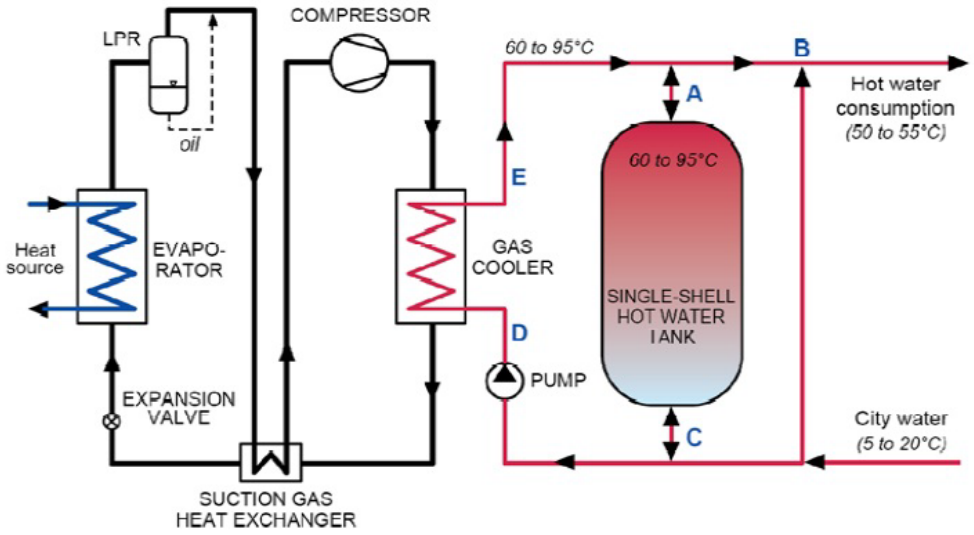

Figure 12: *Diagram of heat pump water heating with a single DHW tank* (University of Strathclyde, 2010)

Hot water extraction – Hot water ranging from 60 to 95°C is extracted from the top of the storage tank at point A. This water is mixed with cold water at point B, which has a temperature of 50 to 55°C. The mixing of hot and cold water allows for the desired outlet temperature to be achieved.

Water replenishment – To replenish the water that is withdrawn, city water enters the tank from the bottom at point C. It is important to note that a well-designed diffuser is installed at the lower water entrance port to prevent the mixing of stratified water and the introduction of a jet of cold water into the tank. This ensures that the temperature stratification in the tank is maintained.

Water circulation – When the water temperature in the tank drops below a certain limit, a pump is activated to circulate water between points D and E. The pump's speed, controlled by its revolutions per minute (rpm), determines the flow rate of the water circulating through the gas cooler.

Temperature control – Adjustments to the flow rate of the water pump are made to achieve the desired temperature in the storage tank. By optimizing the pressure and modifying the water mass flow rate, the system aims to achieve the highest possible COP, which indicates the system's efficiency in converting energy input into heat output.

This basic hot water heating system using a CO_2 heat pump allows for the extraction of hot water from the storage tank while maintaining temperature stratification. When the water temperature decreases, the system activates water circulation through the gas cooler to heat the water and maintain the desired temperature. The control of pump speed and water flow rate optimization contribute to achieving optimal system performance and efficiency (Hafner and Eikevik, 2016).

2.5 Industrial Ammonia Refrigeration System

The fundamental operation of an ammonia refrigeration system is similar to that of other refrigeration systems. However, ammonia refrigeration systems are often designed and installed as flooded systems. In addition, there are two-stage systems that use ammonia as the refrigerant. This section will go over flooded systems as well as two-stage systems that employ ammonia as a refrigerant.

2.5.1 Flooded evaporator system

In a refrigeration system utilizing a flooded evaporator, the key component is the low-pressure receiver, which distinguishes it from a direct expansion evaporator. The receiver, located after the expansion valve, serves as a separator for gaseous and liquid refrigerant, ensuring that only 100% liquid refrigerant is supplied to the evaporator. Additionally, a pump is connected before the evaporator to provide the necessary driving power for the refrigerant.

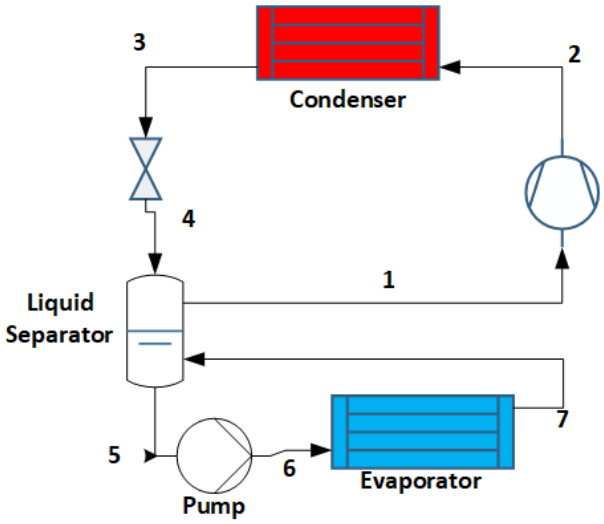

Figure 13: *Flooded refrigeration system*

When heat is transferred from the secondary side, the refrigerant from the receiver enters the evaporator and undergoes evaporation. Due to the pressure rise from the receiver to the evaporator, the refrigerant at the evaporator intake is slightly sub-cooled. The two-phase refrigerant mixture then reaches the receiver, where the liquid and gas phases are separated. The remaining liquid is recirculated through the evaporator while the gas enters the compressor. Following the fundamental compression cycle, the gas is compressed in the compressor and condensed in the condenser (SWEP, 2019).

The use of flooded evaporators mitigates the potential problem of inadequate refrigerant distribution within the evaporator. Unlike direct expansion (DX) systems with a two-phase mixture, a flooded evaporator operates with 100% liquid refrigerant, ensuring a better dispersion of the liquid stream throughout the channels. Since the receiver separates the refrigerant vapour before sending it to the compressor, there is no need for superheating in a flooded evaporator. This is in contrast to DX evaporators, where a significant portion (10-

30%) of the total heat surface area may be used for superheating. Consequently, a higher fraction of the total heat surface area in a flooded evaporator is dedicated to evaporation (Eckert et al., 2022).

One advantage of a flooded evaporator is the reduced pressure lift between the evaporator and condenser sides due to the higher evaporation temperature. This results in a lower compressor workload. The circulation number plays a critical role in flooded systems. Since evaporation is an inefficient process, the two-phase mixture needs to pass through the receiver-evaporator circuit multiple times to ensure complete evaporation. By optimizing the circulation number, the performance of the flooded system can be enhanced.

2.5.2 Two-stage expansion with parallel compression system

Two-stage systems offer significant advantages when there is a need to overcome large temperature rises and associated pressure variations. In such cases, a two-stage expansion is employed to effectively manage the refrigerant. The flash gas resulting from the first expansion stage is typically extracted by the high-pressure (HP) compressor, which reduces the need for suction gas cooling in the HP stage.

In **Figure 14**, the refrigerant from separator 1 is directed to separator 2. Depending on the specific requirements, the refrigerant in separator 2 can either be completely evaporated or only the flash gas is removed by the low-pressure (LP) compressor. Both the HP and LP compressors then raise the pressure of their respective flash gases to match the required condenser pressure on the high side of the system.

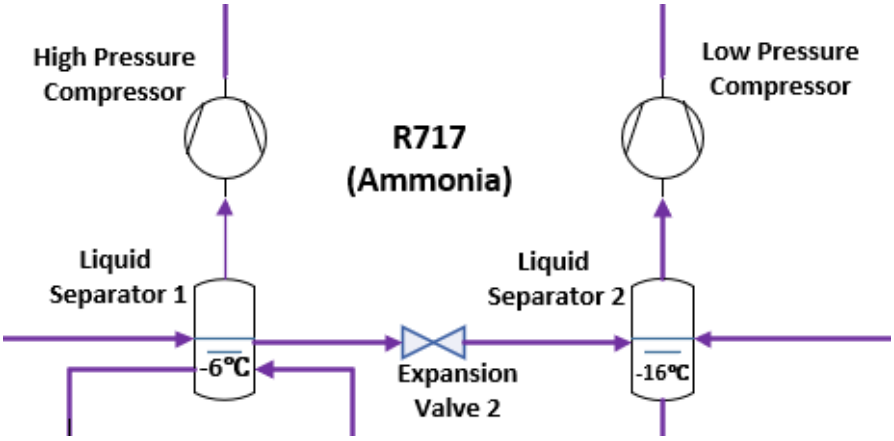

Figure 14: *Two-stage expansion with parallel compression*

In addition to the two-stage expansion process, parallel compression is often employed in refrigeration systems to further enhance performance and efficiency. Parallel compression involves compressing the refrigerant from both stages of expansion simultaneously, utilizing separate compressors for each stage.

By implementing parallel compression in a two-stage system, several benefits can be achieved. Firstly, it allows for better utilization of the compressor capacities and capabilities.

The compressors can be specifically designed and optimized for their respective stages, considering the different pressure ratios and operating conditions. This results in improved overall system performance and higher efficiency.

Moreover, parallel compression helps to mitigate the temperature and pressure drop issues that can occur during the expansion process. The combined compression of the refrigerant from both stages helps to maintain higher suction pressures, minimizing the potential for temperature drops and ensuring more efficient heat transfer in the evaporator. This is particularly advantageous in situations where the evaporator operates at low temperatures or in applications with large heat load variations.

These features make the combination of two-stage expansion and parallel compression in refrigeration systems a preferred choice for applications where significant temperature rises and pressure variations need to be overcome while maintaining optimal system operation.

2.5.3 Cascade Systems

Varying goods require different freezing temperatures; hence refrigeration equipment must be Different goods have varying freezing temperature requirements, which necessitates refrigeration equipment capable of reaching these low temperatures efficiently and affordably. Traditional single-stage vapour compression refrigeration systems face challenges in achieving such low temperatures effectively. To address this, the cascade refrigeration system was developed.

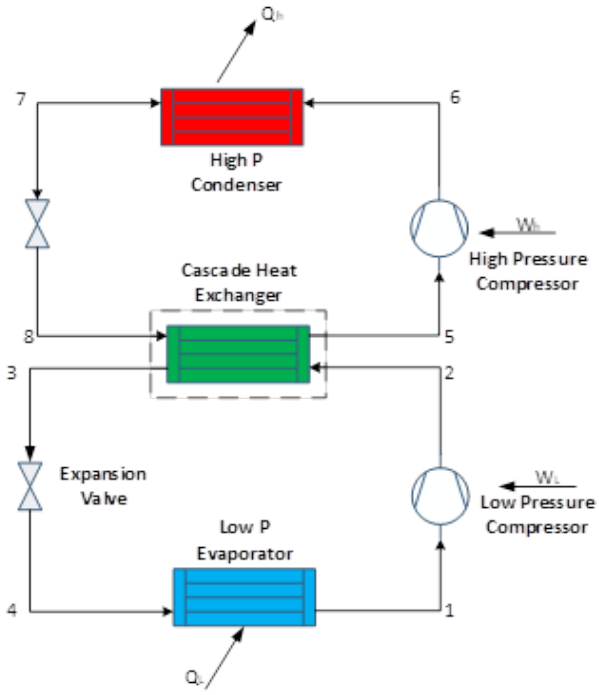

Figure 15: Illustration of a Cascade Refrigeration System

By combining two typical single-stage vapour compression refrigeration systems, the cascade system enables efficient refrigeration even in the presence of significant temperature

fluctuations. In simple terms, the cascade refrigeration system employs two different refrigerants with distinct boiling points, each operating in its independent freezing cycle. These refrigerants are connected through a heat exchanger, with one refrigerant condensing the other at the desired evaporator temperature (Coker, 2015).

In low-temperature applications like rapid freezing and frozen food storage, the required evaporating temperature of the refrigeration system typically ranges from -40°C to -55°C. Consequently, single-stage vapour compression refrigeration systems are insufficient, and two-stage or cascade refrigeration systems are employed. While two-stage systems utilize the same refrigerant on both the high and low-pressure sides, cascade systems utilize separate refrigerants in their high and low-temperature circuits. The use of natural refrigerants in both two-stage and cascade refrigeration systems helps meet environmental requirements (S. et al., 2006).

Research by Mumanachit et al., 2012 found that a two-stage cascade system exhibits higher efficiency below the COP optimum point and is more cost-effective at temperatures below -46.2°C.

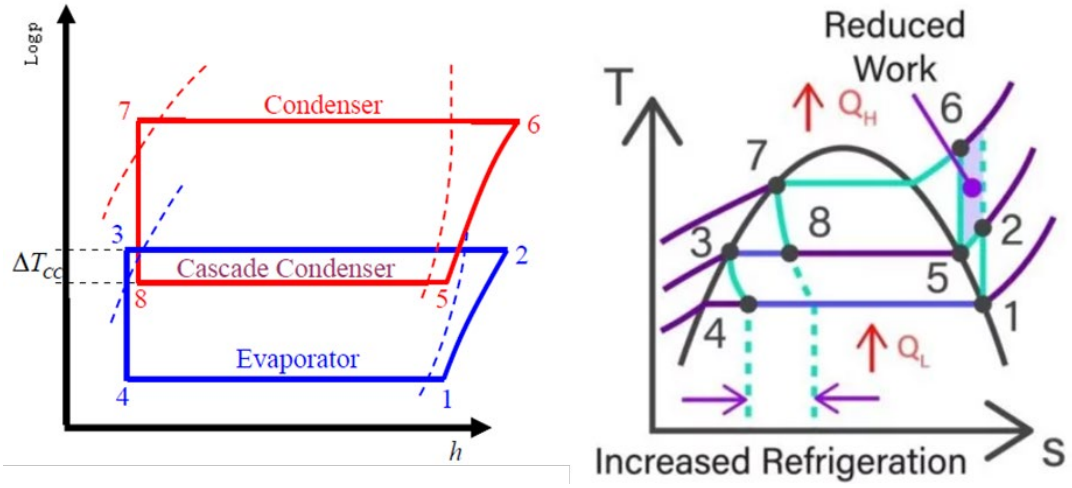

Figure 16: *log p-h diagram (left) and T-S diagram (right) of a cascade refrigeration system* (HVACR GUY, 2017; Ouadha et al., 2007)

Furthermore, Hoşöz, 2005 presented the advantages of a cascade system compared to a traditional two-stage refrigeration system in terms of a given refrigeration capacity:

- Lower evaporating temperature
- Lower compressor discharge temperature
- Lower ratio of discharge to suction pressures.
- Higher compressor volumetric efficiency

2.5.3.1 R717/R744 Cascade System

The NH3/CO_2 cascade refrigeration system has emerged as an alternative for low-temperature operations. This configuration involves carbon dioxide (CO_2) in a low-

temperature vapour compression circuit connected to an ammonia (NH3) vapour compression refrigeration system through an indirect cascade heat exchanger. By separating the refrigerants, each can operate within its suitable pressure/temperature range. The NH3/CO_2 cascade system combines the advantages of high vapour density for CO_2 at low temperatures with the desirable properties of ammonia at higher temperatures (Fleming, 2003).

In a thermodynamic study, (Getu and Bansal, 2008) compared the NH3/CO_2 cascade refrigeration system to cascade systems with high-temperature circuits using other working fluids. Their findings demonstrated that combining NH3/CO_2 can achieve a COP while reducing refrigerant quality. MEHDIZADEH, 2021 compared this cascade setup with a dual-stage NH3 system at a specific operating temperature and identified several advantages and disadvantages:

Advantages:

- The CO_2 low-stage circuit requires a compressor size approximately 97% smaller than the ammonia low-stage circuit due to CO_2's smaller vapour volume at low temperatures.
- The compression ratio (CR) in the CO_2 low-stage circuit is about 45% lower than in the ammonia low-stage circuit.
- The COP for the CO_2 low-stage circuit is significantly higher compared to an ammonia 2-stage system.
- The CO_2 circuit has a much lower suction vapour volume than an ammonia circuit, resulting in cost savings on pipe widths and insulation thickness.
- CO_2 compressors are smaller and require fewer compressors than NH3 compressors for equivalent capacity and operating conditions, despite being approximately 80% more expensive due to food-grade synthetic lubricating oil.
- The CO_2/NH3 cascade system reduces ammonia charge through the integration of modern technology compressors and efficient heat exchangers, offering a favourable price-performance ratio in terms of both capital and operating costs.

However, there are certain disadvantages to consider:

- In overfeed refrigeration systems with liquid, the CO_2 liquid pump capacity requires a pump size 2.5 to 3.5 times larger than the NH3 pump for equivalent operating settings. Consequently, the liquid liner sizes for CO_2 pumps' suction and discharge will be larger than those for ammonia.
- The design pressure of CO_2 pressure vessels and heat exchangers is higher than that of booster ammonia pressure vessels and heat exchangers.
- During vacuum conditions, the CO_2 refrigerant should not be charged after the evacuation is complete. Charging liquid CO_2 when the system pressure is below -5.5

bar will result in the formation of dry ice internally at the charging port. Therefore, the pressure must be raised above 5.5 bar before charging liquid CO_2.

Ouadha et al., 2007 compared cascade cycles utilizing R744 (CO_2) in the low stage with R717 (ammonia) or R290 (propane) in the high stage to two-stage cycles using R717 or R290. Their conclusion highlighted that, for a given refrigeration capacity, evaporator and condenser temperature, and cascade-condenser temperature, the compressor of R744 in the cascade cycle is more compact than those of R290 and R717 in the two-stage cycles. However, it also exhibits lower exergy efficiency for both R744/R290 and R744/R717 blends.

The NH3/CO_2 cascade refrigeration system offers promising advantages for low-temperature applications, but careful consideration of the system's characteristics and operational requirements is necessary to optimize its performance and overcome certain challenges.

Table 3: *Performance comparison of Cascade System with R717 Two-stage cycle* (Ouadha et al., 2007)

Properties	**Cascade System**		**Two-stage cycle**
	R717/R744	**R290/744**	**R717**
m_h (kg/s)	0.1614	0.6384	0.1695
m_l (kg/s)	0.5573		0.1221
v_l (m^3/kg)	0.0320		1.2475
W_h (kW)	60.57	62.64	39.24
W_l (kW)	27.34		37.20
V_h (m^3/h)	295.71	353.65	176.57
V_l (m^3/h)	64.29		535.93

2.6 Refrigerated Sea Water (RSW) System

Refrigerated Sea Water (RSW) systems play a crucial role in enhancing the quality and freshness of food products in various food production settings, whether on land or at sea. These systems provide a controlled and consistent environment for the stored fish, minimizing temperature fluctuations and preventing spoilage. By rapidly chilling the fish close to the freezing point of seawater, RSW systems effectively slow down the natural deterioration processes, such as enzymatic reactions and microbial growth, prolonging the shelf life of the catch.

RSW systems are particularly advantageous for the long-distance transportation of seafood products. The precise temperature control and uniform chilling provided by these systems ensure that the catch remains fresh and meets stringent quality standards throughout the entire

journey. This is especially important for seafood exports, as maintaining the product's freshness and quality is essential for market competitiveness and customer satisfaction. Furthermore, RSW systems contribute to sustainable fishing practices. By reducing the reliance on excessive ice usage, these systems help conserve resources and minimize waste. The use of cold sea water as a chilling medium is environmentally friendly and reduces the overall carbon footprint of the fishing industry.

Overall, refrigerated sea water systems play a vital role in the seafood industry, enabling efficient preservation, quality maintenance, and extended shelf life of the catch, while also promoting sustainability in fishing operations (Kæling, 2019; Torp, 2012).

2.6.1 Working of a RSW system

The operation of a Refrigerated Sea Water (RSW) system involves the maintenance of the water and fish in the storage tank at a temperature close to -1°C. Heat rejection is achieved by utilizing cold seawater with a temperature of approximately 12°C (Bodys et al., 2018).

Figure 17 illustrates the functioning of the system, where pumps are employed to circulate the seawater through the tanks and the cooling system. To ensure effective cooling, the refrigeration mechanism cools the seawater before it enters the tanks, primarily through the bottom. The distribution of the chilled seawater throughout the tanks is achieved through the use of perforated plates or similar devices, which facilitate its uniform distribution across the entire cross-section of the tanks.

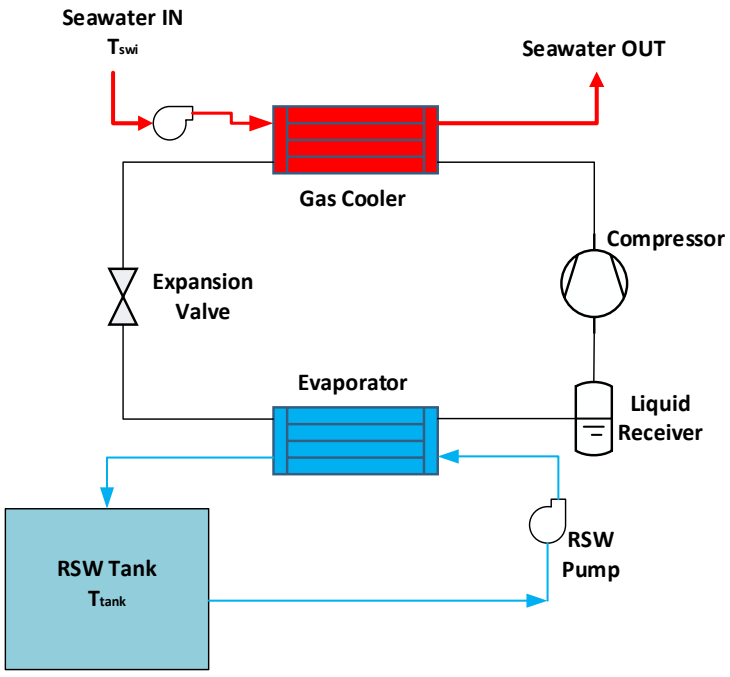

Figure 17: *Refrigeration Unit along with flow diagram of the RSW tank*

As the chilled seawater flows upward through the tanks, it passes through the layers of fish, maintaining them in a semi-floating suspension and promoting their chilling. The water then moves through suction screens located at the top of the tanks before returning to the cooling

unit of the system. Here, it undergoes further cooling, completing the circulation process (Heinen & Hopman, 2017). In order to maintain the circulating water in optimal condition, a small amount of feedwater can be introduced, while any "dirty" water is drained out.

This operational principle ensures that the fish are consistently maintained at the desired temperature, preserving their quality and freshness throughout the storage process in the RSW system.

2.6.2 RSW system with CO_2 Refrigeration System

Refrigerated seawater (RSW) cooling systems utilizing CO_2 have emerged as a promising and eco-friendly technology, particularly in cold regions. The fishing industry has embraced these new advancements in an effort to adopt more environmentally friendly practices. Commercial adoption of CO_2-based RSW systems gained momentum due to various factors outlined in sections 2.1.4.3 and 2.4.2. In 2010, Kuldeteknisk AS successfully deployed the world's first commercial CO_2-based RSW system on the vessel Bragutt MS (PTG AS, 2017).

Hafner et al., 2019 found that CO_2-based RSW units outperform HCFC-22 systems in cold areas, specifically at condensing temperatures below 21°C. However, when operating in warm seawater, the efficiency and cooling capacity of CO_2-based RSW units significantly decrease compared to other technologies, likely due to the low critical temperature of CO_2 (Kim et al., 2004).

Figure 18: *RSW system based on CO_2 developed by Kuldeteknisk AS* (Kuldeteknisk AS, 2011)

Brodal et al., 2018 conducted a study on a transient model of an RSW system using CO_2 refrigeration to assess overall performance and the impact of various parameters. The study yielded several conclusions, including:

- CO_2-based systems in warm areas need to operate close to or above the critical pressure, and their performance is highly dependent on sea temperature.
- In warm regions like Southern Europe, the evaporator pressure must be carefully adjusted to avoid exceeding the compressor's requirements.
- The study considered the effect of precooling the water in the RSW tank, but it showed a reduction in COP. The average COP difference with or without precooling for cooling procedures from 20°C to 0°C was less than 7%. Therefore, precooling does not have a significant impact on COP and yields almost identical results in cold regions.
- Many studies tend to underestimate CO_2 as a refrigerant option due to the smaller temperature approaches observed for the gas cooler.

These findings highlight the importance of optimizing CO_2-based RSW systems for different operating conditions and emphasize the need for further research and development to fully exploit CO_2 as a viable refrigerant option in RSW applications.

2.7 Food Freezing

Freezing plays a vital role in preserving the quality and extending the shelf life of food products. However, freezing operations in the food industry tend to be energy-intensive and often lack significant improvements in energy efficiency. To better understand freezing processes, the industry employs two temperature classifications: frozen food and deep-frozen food.

Frozen food refers to products that are maintained at a constant temperature of -10℃ or lower. The freezing of these items typically involves a gradual reduction in temperature to achieve the desired frozen state. On the other hand, deep-frozen food is characterized by a product's temperature rapidly dropping to -18 degrees Celsius and remaining at that temperature for an extended period. The freezing of deep-frozen food involves various processes that facilitate quick and abrupt freezing, subjecting the products to temperatures ranging from -30℃ to -196℃ (Schudel et al., 2021).

The energy-intensive nature of freezing operations presents an opportunity for innovation and improved efficiency. Implementing advanced freezing technologies, such as cryogenic freezing methods that utilize liquid nitrogen or carbon dioxide, can enhance the freezing process by rapidly reducing the product's temperature. These technologies enable efficient freezing while preserving the quality attributes of the food, such as texture, flavour, and nutritional value. Additionally, advancements in insulation materials and equipment design can help reduce energy losses during freezing operations.

Efforts to optimize freezing processes also involve considerations of packaging materials and practices. Proper packaging can protect the product from dehydration and freezer burn, maintaining its quality over an extended period. Furthermore, innovative freezing techniques

like individual quick freezing (IQF) allow for the freezing of individual food items separately, preventing them from clumping together and enabling easier portioning and serving.

As the food industry continues to prioritize sustainability and energy efficiency, ongoing research and development efforts focus on improving freezing technologies, exploring alternative refrigerants, and optimizing operational practices to reduce energy consumption and enhance the overall freezing process. These advancements aim to minimize the environmental impact of freezing operations while meeting the increasing demand for high-quality frozen food products.

Bogh-Sorensen, 2006 classified the equipment needed for the deep-freezing process into four major classes based on the heat transmission medium:

- Direct Contact (Horizontal and Vertical plate freezers) (**Figure 19**)
- Tunnel blast freezers based on air or other cooling media.
- Immersion freezers are based on liquid evaporation.
- Cryogenic freezers based on rapid heat absorption by cryogens such as liquid nitrogen or liquid carbon dioxide (Trygve M Eikevik, 2021b) (**Figure 19**)

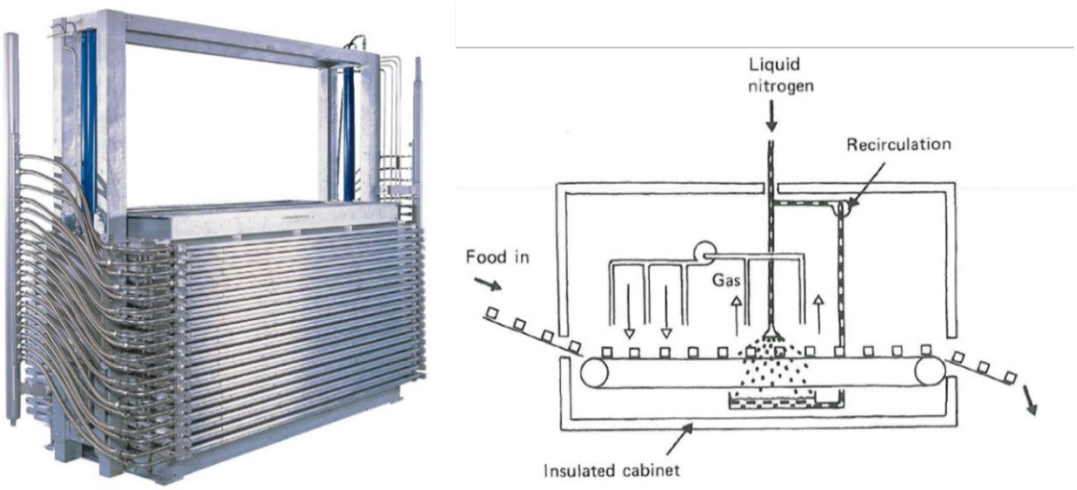

Figure 19: *Horizontal plate freezer (left) and Liquid nitrogen freezer (right)* (Fellow, 2010; Teknotherm, 2022)

2.7.1 Fish Freezing

Fish processing businesses deal with a diverse range of fish species and products, each with varying freezing requirements in terms of time, packaging, and size. This necessitates the use of adaptable freezing equipment that can accommodate different needs. Choosing the appropriate freezers can be challenging, considering factors such as product quantities, seasonal fluctuations, and the potential introduction of new products. As a result, generic equipment that requires significant labour and comes at higher costs is often employed. The refrigeration load varies significantly due to differences in products, freezing times, and quantities. Many facilities utilize large screw compressors with sliding valve regulation for

capacity control, leading to substantial energy consumption during partial loads. To improve energy efficiency, the implementation of enhanced systems like frequency control is recommended (Judith A. Evans, 2009).

Air freezing is the predominant method used in fish freezing due to its affordability, sanitation, and equipment compatibility. Air systems can be specifically designed as blast-freezing tunnels or spirals, or they can be as simple as a fan circulating chilled air within an enclosed space through an evaporator. In air systems, the rate of heat transfer to the product surfaces is relatively moderate. The major advantage of air systems lies in their adaptability, particularly when freezing items with irregular shapes or single products (Trygve M Eikevik, 2021b).

Among the various freezing methods, air-blast freezing is widely employed in fish processing plants due to the diverse range of products that require freezing. There is a multitude of air-blast freezer types and configurations available, ranging from general-purpose equipment to highly specialized systems designed for specific products. These freezers offer efficient and reliable freezing capabilities, ensuring the preservation of fish quality while meeting the specific freezing requirements of different products.

2.7.1.1 Tunnel Freezer

Tunnel freezers (**Figure 20**) are highly versatile freezing units that can accommodate a wide range of fish products, whether they are packaged or unpacked, and come in various sizes and geometries. The freezer operates by circulating air that is cooled through the evaporator and then directed onto the product at high speeds using fans, typically between 3 and 6 m/s. The air temperature in the tunnel freezer is maintained at around -25°C to -40°C or even lower, ensuring rapid and efficient freezing of the fish (Badri et al., 2021).

To ensure uniform freezing, the products should be positioned on racks with appropriate shelf space to allow for consistent airflow over the items. Individual product items or goods packaged in cardboard are placed in the forced air stream within the tunnel. Freezing periods can extend over several hours due to the thickness of the products or the bulk freezing of fish. In tunnel freezers, the packing and the air barrier between the fish and the lid significantly reduce heat transfer. Freezing primarily occurs from the bottom of the boxes due to the tight stacking on shelves. Typical batch freezing in tunnel freezers can take around 18-20 hours, and when considering the loading and unloading periods, the total freezing time can exceed 24 hours.

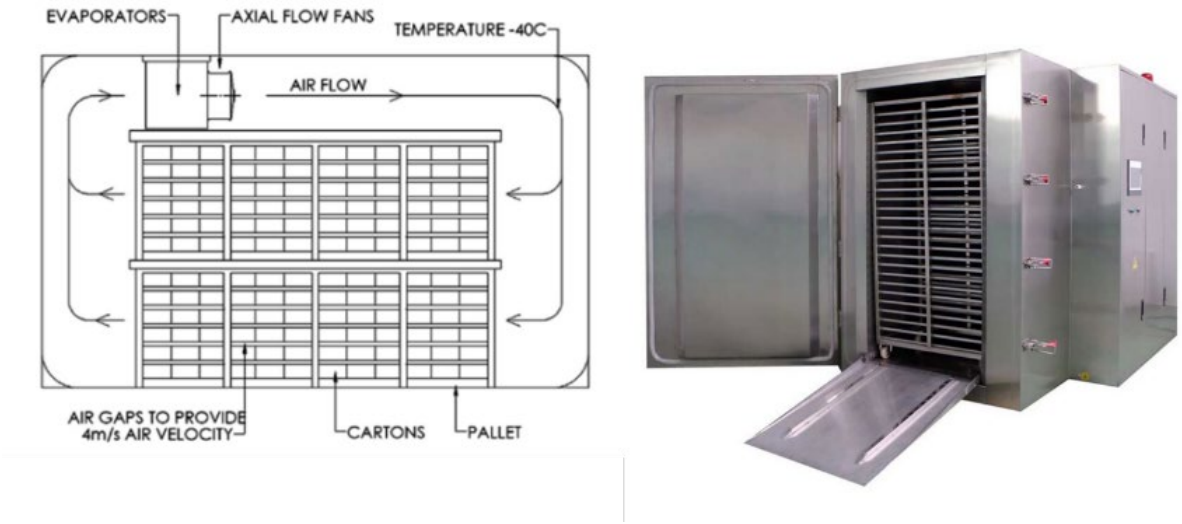

Figure 20: *Schematic of a tunnel freezer (left) and Blast Freezer unit (right)* (Dempsey and Bansal, 2012; SFT, 2022)

Computer simulations are often employed to optimize airflow patterns and freezing times, ensuring uniform freezing throughout the freezer. Measures such as the use of fan diffusers, controlling fan speed, and adjusting freezing time can help reduce energy consumption in tunnel freezers (Dempsey and Bansal, 2012).

Tunnel freezers' adaptability to different product sizes and geometries, along with their ability to provide rapid and uniform freezing, make them a popular choice in the fish processing industry.

2.7.1.2 Continuous Freezers

In fish processing operations, it is crucial to maintain a continuous and uninterrupted flow of processing and freezing to meet production targets. This requirement often leads to the use of continuous air-blast freezers, which are designed to freeze products while they are in motion on a conveyor belt system (Figure 21). The key to efficient freezing in these systems is to maintain low temperatures and ensure swift air movement above or vertically onto the products (Shaikh and Prabhu, 2007).

The multi-belt air-blast freezer is a popular type of continuous freezer that offers advantages in freezing larger and shapeless fish fillets. The length of the shell-freezing belt determines the minimum required length of the freezer and the amount of floor space it occupies. To achieve optimal freezing results, continuous freezers with vertical air flow, which provide superior control over air distribution around the products, are preferred. However, it's important to note that freezers with vertical air flow tend to be more expensive (Judith A. Evans, 2009).

Figure 21: Continuous belt air freezer – complete unit (Bid-On-Equipment, 2016)

Continuous freezers provide an efficient and continuous freezing process, ensuring high productivity in fish processing facilities. The use of conveyor belt systems allows for seamless integration into the production line, reducing interruptions and maximizing efficiency. The control over air temperature and flow in these freezers helps achieve rapid freezing and uniform product quality. The versatility of continuous freezers makes them suitable for various fish processing applications, including freezing large fillets or other irregularly shaped fish products.

2.8 Cold Storage

A cold storage facility (**Figure 22**) is a dedicated structure designed to store perishable food items using artificial refrigeration techniques. It plays a crucial role in the cold chain, which involves maintaining the desired temperature conditions to preserve the quality and safety of food from the manufacturing stage to consumption (Yang et al., 2022). All chilled and frozen products go through a cold storage facility at least once during their journey. Chilled storage areas typically maintain temperatures between -1 and 12°C, while frozen storage areas keep temperatures below -18°C. The cold storage market encompasses a wide range of facilities, from small 10-20 m3 storage units to large warehouses spanning hundreds of thousands of cubic meters. Regardless of their size, all cold storage facilities aim to preserve products at the appropriate temperature while minimizing quality degradation.

Temperature management is a critical aspect of food safety in chilled storage rooms, as temperature fluctuations can pose risks to food safety and shelf life. On the other hand, frozen storage rooms, as long as the temperature remains below -10°C, are generally considered safe in terms of foodborne microbial growth. However, it's important to note that food quality changes can still occur in frozen storage due to factors such as moisture migration and texture changes. Most frozen storage facilities operate within the temperature range of -18 to -22°C, keeping the majority of frozen food above its glass transition temperature. The glass

transition temperature is the point at which further water freezing is restricted, and for most foods, it is below -30°C (J. et al., 2018).

Cold storage facilities are equipped with specialized refrigeration systems, insulation materials, and temperature monitoring systems to maintain the desired temperature conditions. They are designed to provide an optimal environment for food preservation, preventing spoilage, and extending the shelf life of perishable products. Additionally, cold storage facilities play a crucial role in the distribution and supply chain management of temperature-sensitive food items, allowing for efficient storage and distribution to meet consumer demand.

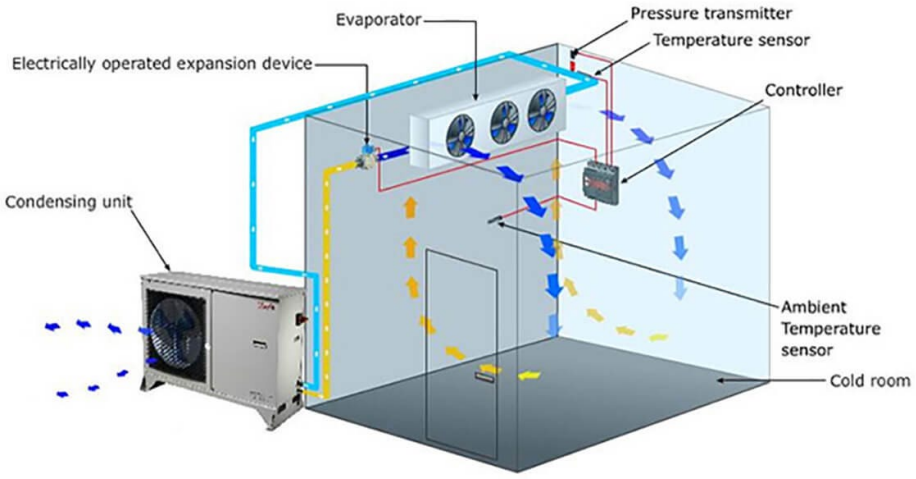

Figure 22: *Example of a cold room maintained by the refrigeration system* (Danfoss, 2013)

2.9 Ventilation / Dehumidification System

Norway presents exceptional opportunities for expanding its fisheries industry due to its ideal climates for at-sea fish farming. However, seizing these opportunities requires the improvement of current indoor butchery, filleting, and processing techniques, as well as the introduction of new, sustainable practices. To address these challenges, businesses in Norway have embraced the concept of indoor fish farming, constructing state-of-the-art facilities equipped with cutting-edge technologies that prioritize temperature control and environmental sustainability (OECD, 2021).

2.9.1 Operation of the system

Processing (slaughtering, cutting, filleting – section 1.2) of fish places stricter requirements on hygiene, the temperature must be low and dry conditions must be maintained, bacteria need moisture to survive and multiply if the ambient air is kept below 50%, relative humidity in most bacteria will not reproduce.

In Norway, F-Tech has emerged as a prominent manufacturer specializing in humidifying and dehumidifying devices for the fish processing industry (F-Tech, 2020). Their long-standing presence and expertise in the field have made them a trusted name within the Norwegian processing sector. For a better understanding of advanced dehumidification systems, let us delve into the operational principles of one such system developed by F-Tech.

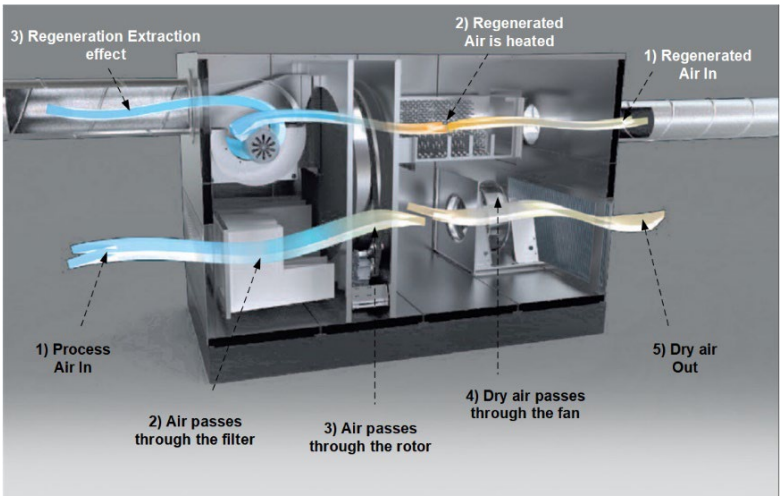

Figure 23: *Working of the dehumidification system* (F-Tech, 2021)

The heart of the dehumidification system lies in its adsorption dehumidifier. This system efficiently removes water from the process air by utilizing a specially designed adsorption rotor coated with silica gel. As the air passes through the rotor, the silica gel absorbs water molecules, effectively reducing the moisture content. The water removed from the process air is then carried away from the dehumidifier using regeneration air. The adsorption rotor is divided into two zones: the dry zone and the regeneration zone. The moist air flows through the dry zone, exiting the rotor as dry air, while a small portion of the process air is used for regeneration in specific sectors of the rotor. When the rotor becomes saturated with moisture, it undergoes a rotation to the regeneration zone. Here, the rotor is dried using heated air at temperatures ranging from 100 to 140°C. Subsequently, fresh air flows through the rotor in the opposite direction, effectively driving out the moisture absorbed by the silica gel. The expelled moisture is then safely directed away from the production area through a well-designed duct system. This process readies the rotor to begin absorbing new water molecules once again (F-Tech, 2021; Kezza, 2022).

Chapter 3: Systems and Methods

A newly established salmon processing plant located in Holmen, Sortland, Norway has been selected as the focal point for investigating the energy systems employed in onshore salmon processing. This state-of-the-art slaughterhouse is scheduled to commence operations in the first quarter of 2024. PTG has been entrusted with the task of designing and implementing the comprehensive temperature control system, catering to the customer's specific heating and cooling requirements. PTG has collaborated with the NTNU to conduct extensive research and development activities. This partnership aims to deliver a cutting-edge temperature control system that maximizes energy efficiency and meets the demanding needs of the salmon processing industry. The outcome of this collaborative effort will contribute to advancing the understanding and implementation of sustainable energy solutions in the field of onshore salmon processing.

3.1 Energy systems inside the salmon processing plant / Lakseslakteri

The salmon processing plant operates around the clock, with three distinct phases: the washing phase, production phase 2, and production phase 3 (section 1.2). Each phase requires specific heating and cooling demands, which can vary depending on the season, whether it is summer or winter. The systems contribute to the overall processing and preservation of the salmon while adhering to strict temperature and humidity controls to meet the required standards for food safety and quality. The three different phases:

- Washing phase (12:00 – 6:00) - systems such as water heating, ventilation and dehumidification, cleaning and disinfection, and waste management are essential to ensure a hygienic environment for salmon processing.
- Production phase 2 (7:00 – 14:00) - systems for chilling and cooling the salmon, filleting, and cutting equipment, packaging and labelling, as well as conveyor systems play a crucial role in efficiently processing and preparing the salmon for distribution.
- Production phase 3 (15:00 – 23:00) - systems for freezing the salmon, storage and inventory management, quality control and inspection equipment, and an energy management and control system are utilized to maintain the desired product quality, prolong shelf life, and ensure efficient operations.

The major systems employed for carrying the different stages mentioned in section 1.2 can be classified based on the stages of production - Table 4

Table 4: *Classification of different systems based on the stages of salmon processing.*

Stage (i) – Reception of raw material	Stage (ii) – Treatment Room	Stage (iii) – Cooling system	Stage (iv) – Packaging	Stage (v) – Storage
CO_2 based RSW system (section 2.6)	Dehumidification (2.9) Ventilation (2.9) Fan Coils Warm water (2.4.4)	Freezing Tunnel (section 2.7)	Ice Production	Cold Storage (section 2.7, 2.8)

Within the SPP facility, specific areas/rooms, namely the killing, grading, filleting, pallet warehouse, support room, and office, have specific needs for dehumidification, ventilation, and fan coil services. While the treatment room holds particular significance in this project, it is crucial to also consider the office and support system room. To effectively address the heating and cooling demands of the systems outlined in **Table 4**, two separate heat pump systems have been meticulously designed and simulated. These systems have undergone thorough modelling processes to ensure their suitability and efficiency within the facility.

3.1.1 Winter – Daily load profile

Located near the Arctic Circle at approximately 68° N, Sortland is subjected to a prolonged winter season that spans from mid-October to the end of March. With daily temperatures consistently dipping below freezing, averaging around 0.7°C (Wikipedia, 2022), the region experiences a harsh climate during these months. The formidable winter conditions pose a substantial heating demand, necessitating efficient and reliable heating systems to maintain comfortable and conducive indoor environments. In contrast, the cooling demand remains relatively subdued in Sortland, as the temperatures tend to remain cool throughout the year. Considering the unique climatic challenges of the region, it becomes imperative to design and implement effective heating solutions while ensuring optimal energy utilization.

3.1.1.1 Heating demand

The killing/gutting and grading rooms have the greatest dehumidification and ventilation system demand of 4477kW per day (peak load - 242kW). This is one of the main reasons for operating the gas cooler at such a high pressure.

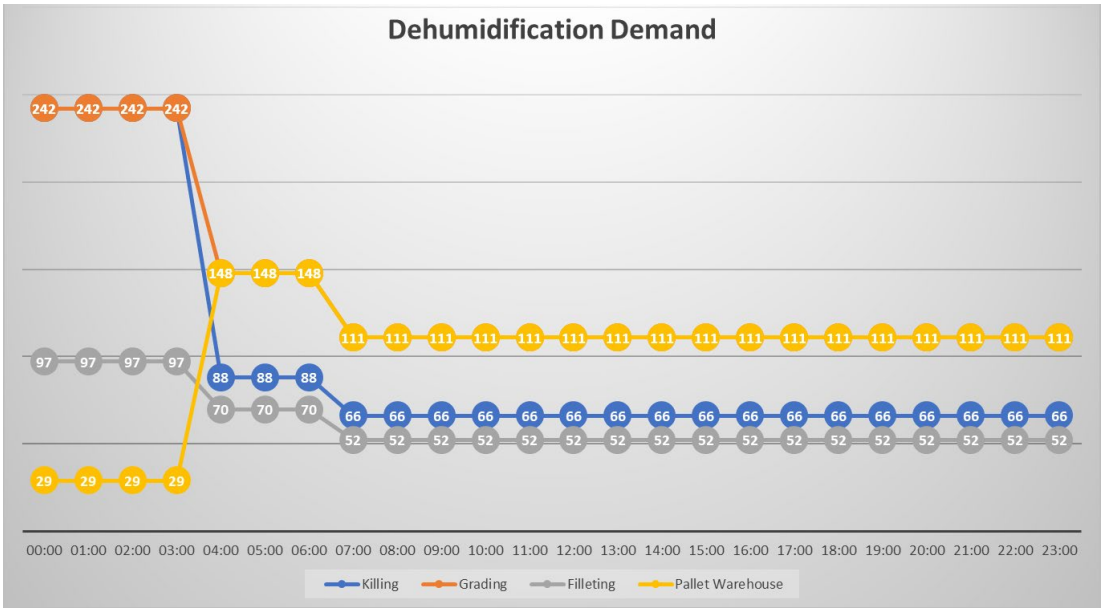

Figure 24: *Dehumidification – daily heating demand during winter*

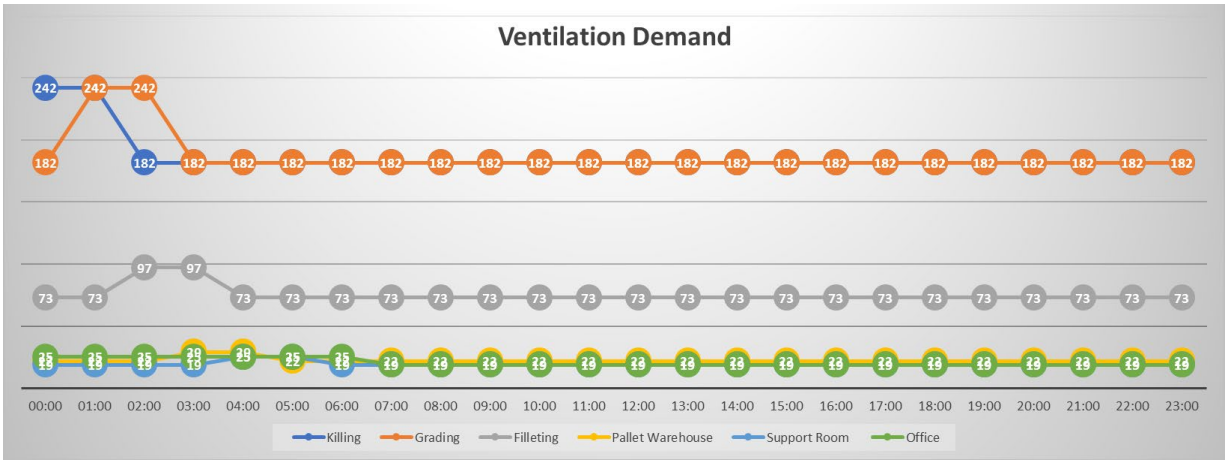

Figure 25: *Ventilation – daily heating demand during winter*

The need for hot water is consistent throughout the day. The floor heating is in great demand, consuming around 3600kW per day at a maximum load of 150kW. While the snow-melting equipment operates every other hour, it consumes a total of 480kW at a maximum load of 40kW.

3.1.1.2 Cooling demand

The fan coils and dehumidification system has no cooling need (runs in ventilation mode only). The biggest cooling requirement is during the product production steps shown in **Table 4**

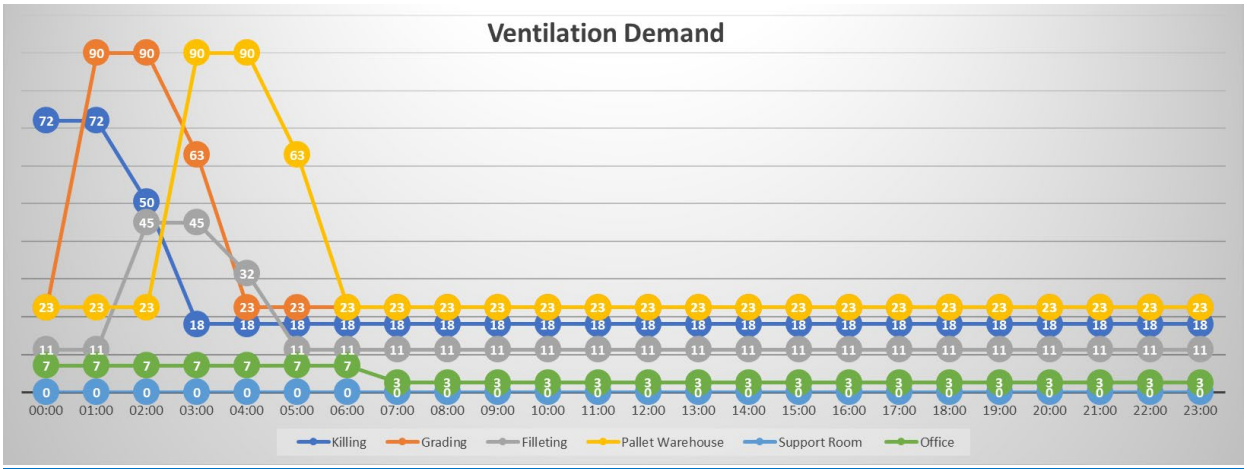

Figure 26: *Ventilation – daily cooling demand during winter*

Table 5: *Product refrigeration daily demand during the winter*

Operation	Max Load (kWh)	Daily Average (kWh)	Total per day (kWh)
RSW Slaying	435	154	2162
RSW Fillet	40	12	210
Ice Production	392	392	9408
Cold Storage	41	9	210
Freezing Tunnel 1	75	43	1031
Freezing Tunnel 2	75	43	1031
Freezer Storage	14	14	326

The demand from the refrigeration side of the system is quite as evident from **Table 5**. The refrigeration system will be sized according to the maximum but will operate at part load most of the time.

3.1.2 Summer – Daily load profile

During the summer months in Sortland, the temperatures are comparatively lower compared to cities in southern Norway. With an average temperature of 8.85°C between April and August, Sortland experiences milder summer conditions (Wikipedia, 2022). Among these months, July stands out as the warmest, with a daily mean temperature of 13.1°C. It is important to note that despite the warmer climate, the heating demand from the refrigeration system in various systems remains relatively high, while the cooling demand is more prominent during the winter period. This seasonal variation in temperature patterns has significant implications for designing and optimizing heating and cooling systems.

3.1.2.1 Heating demand

There is no requirement for dehumidification until 4 am (just before the start of production phase 2), thus the load on the refrigeration system is low during that time.

The fan coils generate no demand, and the hot water is exclusively utilized for floor heating (the snow melting unit is not operated).

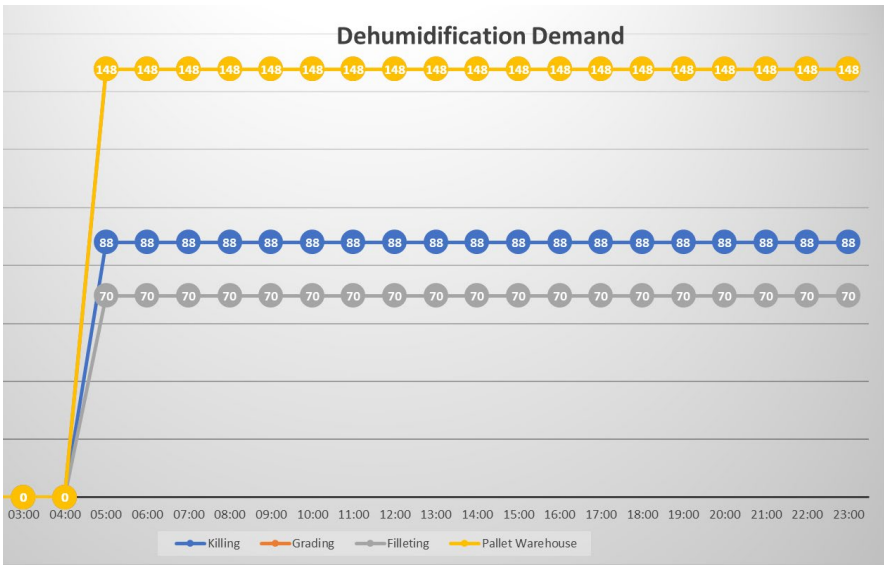

Figure 27: *Dehumidification – daily heating demand during summer*

The ventilation requirement is rather steady throughout the day, with peaks in the early washing phase.

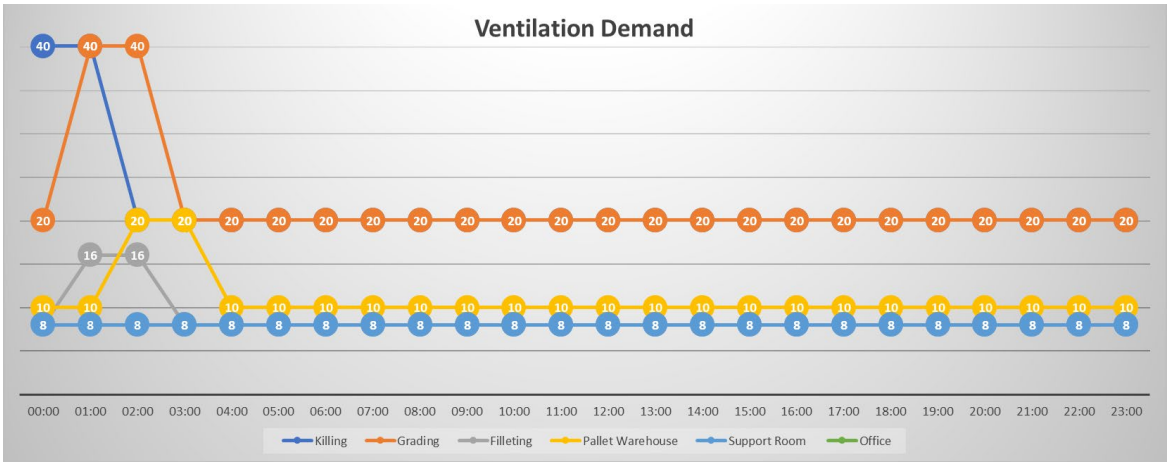

Figure 28: *Ventilation – daily heating demand during summer*

As previously stated, the floor heating uses hot water throughout the day. There is a continual need for 12.5kWh, bringing the total daily consumption to 300kWh.

3.1.2.2 Cooling demand

When compared to wintertime needs, cooling demand is significant (section 3.1.1.2). The dehumidifier is running, but there is no need during the washing process.

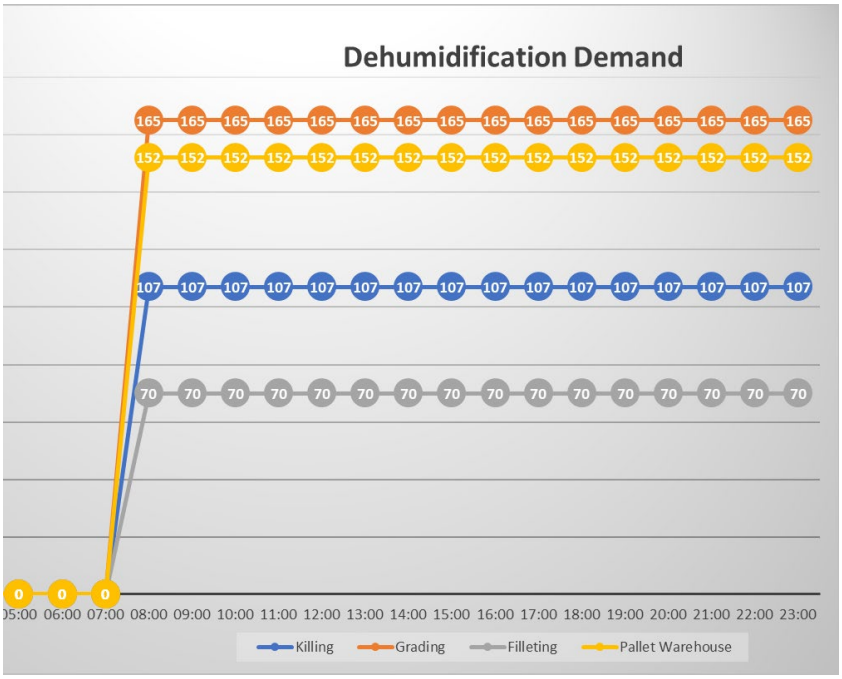

Figure 29: *Dehumidification – daily cooling demand during summer*

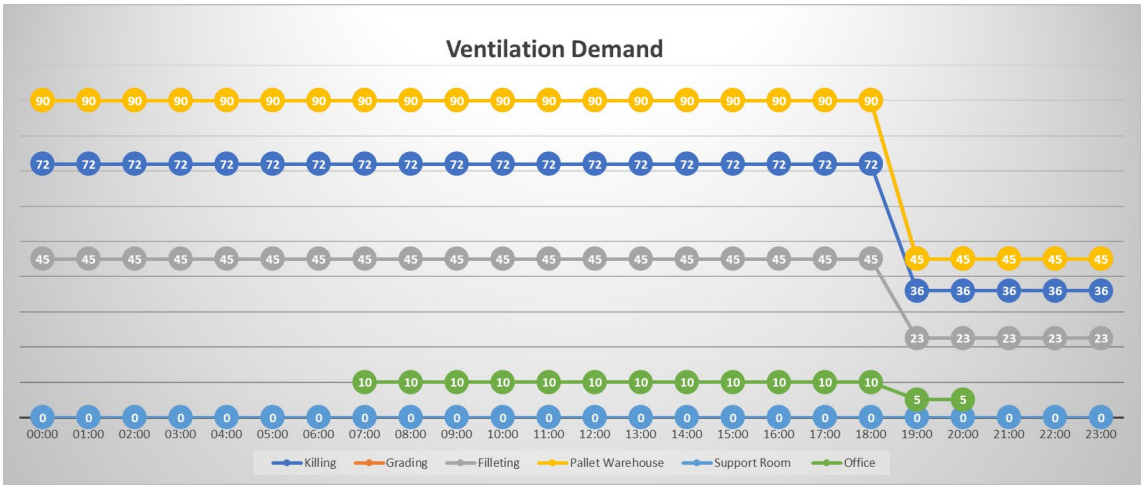

Figure 30: *Ventilation – daily cooling demand during summer*

The fan coils are operational during the summer. The demand is constant across the different rooms.

Table 6: *Product refrigeration daily demand during the summer*

Operation	Max Load (kWh)	Daily Average (kWh)	Total per day (kWh)
RSW Slaying	435	285	3703
RSW Fillet	40	15	249
Ice Production	392	392	9408
Cold Storage	41	9	212
Freezing Tunnel 1	75	43	1031
Freezing Tunnel 2	75	43	1031
Freezer Storage	14	14	326

The product refrigeration demands are likewise comparable to the summer demands (**Table 6**). During the washing phase, the RSW is not required for killing, but it is in considerable need during the manufacturing phase 2.

3.2 The Heat Pump / Refrigeration System Solutions

After a thorough analysis of SPP's requirements outlined in sections 3.1.1 and 3.1.2, the project engineers and research department at PTG were tasked with developing suitable solutions. Following extensive investigation and careful consideration of various factors, two solutions were devised to meet the heating demands of the different systems specified in **Table 4**.

To cater to the heating requirements, a dedicated heat system was designed to distribute the circulating fluid at specific temperatures tailored to the needs of each system. Water was selected as the Heat Transfer Fluid (HTF), as discussed in section 2.1.5.1.

Table 7: *Water supply and return temperature for the different energy systems in the SPP*

Energy systems connected to the Heat System	**Water supply temperature (°C)**	**Water return temperature (°C)**
Dehumidification and Ventilation	70	45
Fan Coils	70	45
Floor Heating	35	20

Consequently, the developed heat pump system was designed to elevate the temperature of the water. In this configuration, the heat pump receives water at 20°C and returns it at 70°C. Given the temperature increase, the gas cooler operates at relatively high pressure, exceeding 80 bar, as outlined in section 2.4.4. As a result, the heating system receives water at 70°C, hereafter referred to as 70HS.

To reduce the strain on the heat pump, a search for heat pump sources was conducted. It was discovered that the vacuum pumps used for the packaging of processed salmon during stage (iv) generate a significant amount of heat loss. This heat energy, measuring 180 kWh and with a temperature of 60°C, can be harnessed. To utilize this heat, it will be directed to a heat recovery system, which will subsequently transfer it to the 70HS system, thereby enhancing the overall efficiency and sustainability of the heat pump system.

3.2.1 Solution 1 – Two stage parallel compression R717 refrigeration system

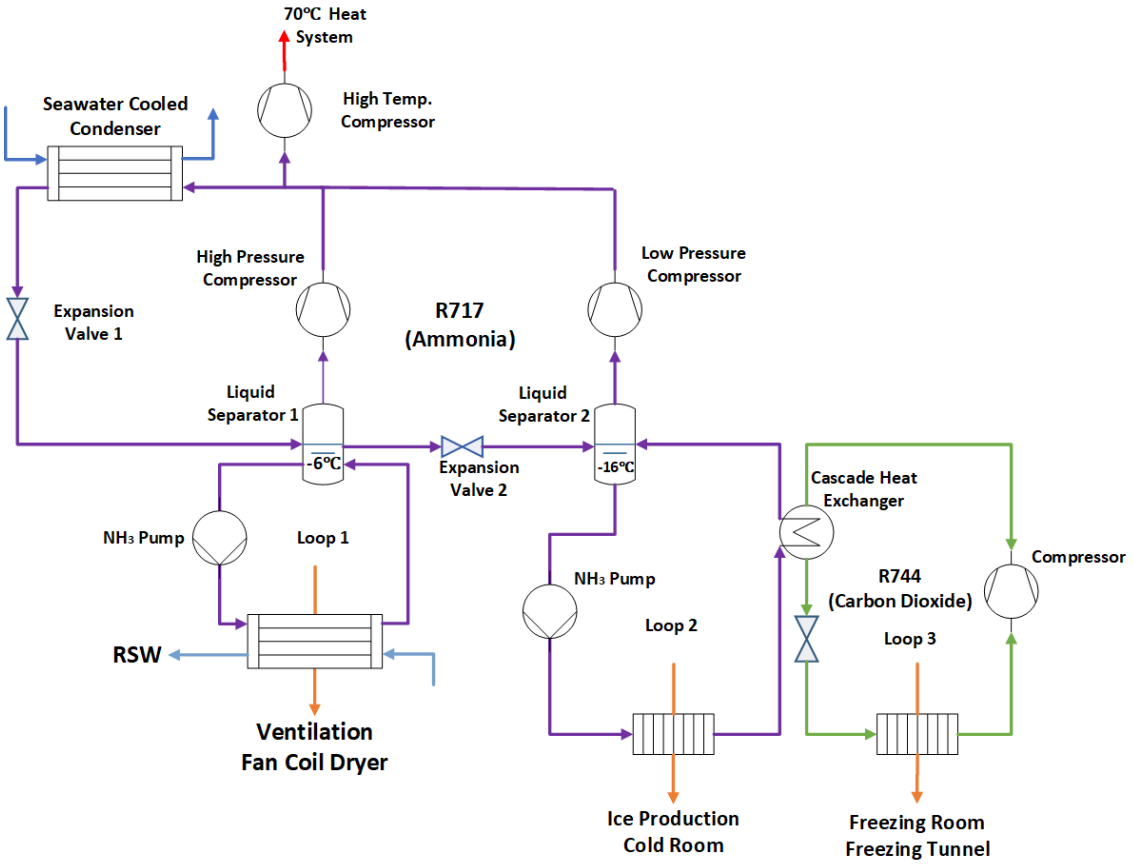

Figure 31: *Two-stage refrigeration system (R717) cascaded with R744 system and integrated with the 70°C-heating system (solution 1)*

To cater to the diverse system requirements of the SPP, an innovative two-stage flooded parallel compression refrigeration system (section 2.5.1) utilizing R717 as the primary refrigerant has been devised. R717 was selected due to its advantageous characteristics, including (section 2.1.4.2) excellent thermodynamic properties, environmental friendliness, and wide availability. Given the SPP's proximity to the shoreline, leveraging the cooling potential of seawater for the condenser aligns with sustainability objectives and ensures efficient operation (Su et al., 2020). While the system assumes a seawater temperature of 12°C, it should be noted that actual seawater temperatures typically range from 4°C to 12°C.

The refrigeration process commences by circulating the full R717 charge through the condenser, followed by regulation through expansion valve 1. To maintain the refrigerant in its liquid phase, liquid separator 1 operates at a temperature of -6°C. Subsequently, the liquid refrigerant enters loop 1, where it cools the incoming seawater (stage (i)) from 14°C to 0°C. Additionally, loop 1 indirectly caters to the cooling requirements of the ventilation system and fan coils. After absorbing heat from these systems, the refrigerant, now in a mixed phase, returns to the receiver. Separator 1 always contains a minimum of 50% liquid refrigerant, while the gaseous phase (flash gas) is directed to the high-pressure compressor, which elevates the refrigerant pressure to match the condenser pressure.

Separator 2 utilizes a portion of the refrigerant from separator 1 to meet additional refrigeration needs. Opening expansion valve 2 results in a drop in refrigerant temperature. To maintain the refrigerant in its liquid phase, liquid separator 2 is designed to operate at -16°C. The liquid refrigerant from separator 2 enters loop 2, where it is employed for ice production and cooling in the designated cool room (**Table 4**). While delivering the necessary refrigeration effects in loop 3, the refrigerant accumulates heat as it cascades with the R744 system. Loops 2 and 3 constitute a cascade refrigeration system (section 2.5.3). The cascade heat exchanger serves as an additional evaporator for loop 2 and a condenser for the R744 refrigeration system in loop 3.

Loop 3 represents a standalone R744 refrigeration system that is integrated with R717 loop 2 to fulfil the cooling requirements of the freezing chamber and freezing tunnel. The amount of the R717 charge is determined based on the cooling demands of these specific systems.

Regarding separator 2, the low-pressure (LP) compressor eliminates the flash gas, while retaining the liquid phase. Due to the higher-pressure lift to the condenser pressure, the LP compressor has a larger pressure ratio compared to the high-pressure (HP) compressor. The overall mass/charge of R717 is allocated appropriately, considering the liquid refrigerant required in separators 1 and 2 to meet their respective refrigeration demands, as well as the charge needed to fulfil the heating requirements of the 70 HS system. The flash gas from both the HP and LP compressors is mixed before a portion of it is extracted by the high-temperature (HT) compressor to supply the 70HS, while the remaining R717 refrigerant proceeds to the condenser, which is cooled by seawater.

To enhance efficiency and minimize waste, the HP and LP compressors are equipped with oil-cooling mechanisms, allowing for the recovery of excess heat through a dedicated heat recovery system. While the system's capacity is designed to meet maximum demand, it is configured to operate on part load to accommodate daily variations in requirements and operator discretion, ensuring optimal performance and energy efficiency.

3.2.2 Solution 2 – Two stage parallel compression R717 refrigeration system + R744 RSW system

In the industry, it is common to explore multiple solutions for a given task. In line with this practice, an alternative approach has been devised for the project at hand. This approach involves the use of two distinct systems, each tailored to meet specific requirements. The first system is designed to address the heating demands of the RSW (refrigerated seawater) and 70HS (70°C heat system), while the second system is dedicated to handling the cooling requirements of the remaining systems.

By employing this two-system approach, a more efficient and targeted solution can be achieved. It allows for a focused allocation of resources, ensuring that each system receives the appropriate heating or cooling support. This approach considers the specific needs and characteristics of the RSW and 70HS, which require dedicated attention due to their unique

heating demands. Simultaneously, it enables the remaining systems to be efficiently cooled, optimizing their performance and overall system effectiveness.

Implementing this alternative method offers a comprehensive and balanced approach to addressing the heating and cooling requirements of the various systems within the project.

3.2.2.1 System 1 – R717 Refrigeration system

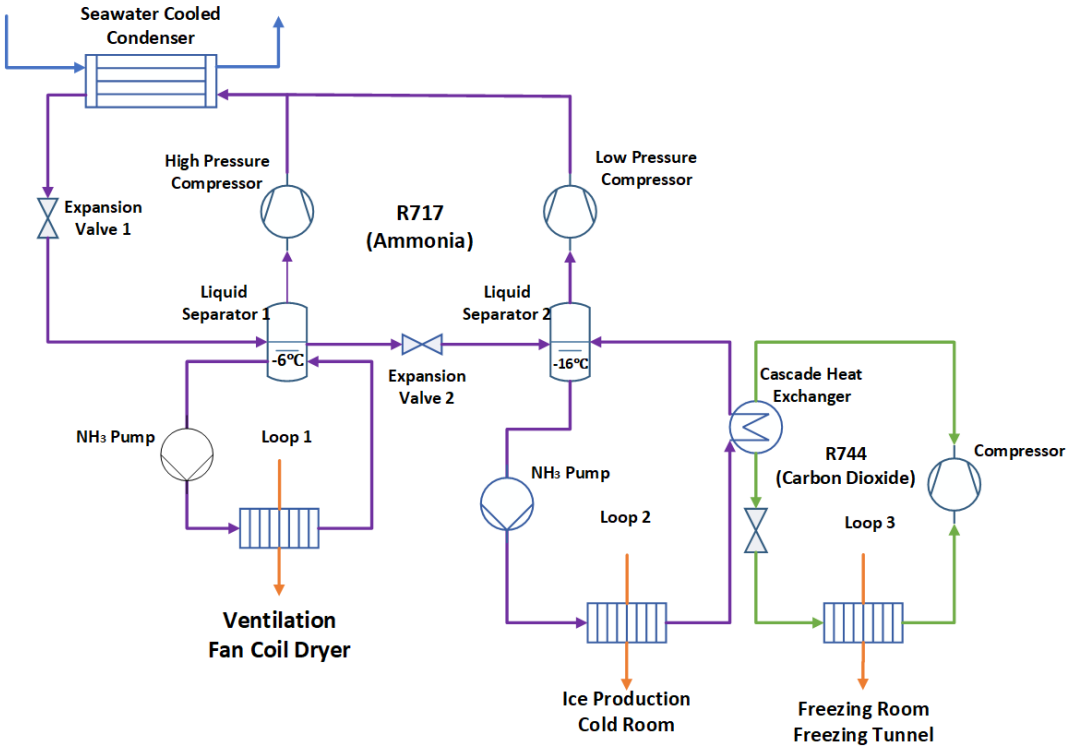

***Figure 32**: Two-stage refrigeration system (R717) cascaded with R744 system (solution 2)*

In solution 2, the R717 system operates similarly to the system in solution 1 (as described in section 3.2.1). However, there are some notable differences. Firstly, the R717 system is no longer connected to the 70HS system, as shown in **Figure 35**. This leads to the following changes:

- Total R717 charge reduction: The entire R717 charge will be utilized solely to meet the cooling requirements of the various systems. Consequently, the total amount of R717 refrigerant needed will be reduced compared to solution 1, where it was also used for heating purposes.
- Lower condenser pressure: With the disconnection of the R717 system from the 70HS system, the pressure in the condenser (high side) will be lower. This reduction in pressure will also result in decreased pressure ratios for both HP and LP compressors. As a consequence, the workload on the compressors will be reduced, potentially leading to improved efficiency and performance.
- Change in loop 1: In solution 2, loop 1 will no longer fulfil the requirements of the RSW system. This modification eliminates the need for loop 1's pump to handle the

RSW demands. As a result, the pumping effort required for loop 1 will be reduced, contributing to improved overall system efficiency.

These modifications in solution 2 aim to optimize the R717 system's performance by focusing its capacity solely on cooling demands and reducing the workload on the compressors.

3.2.2.2 System 2 – R744 transcritical RSW system

In response to the relatively high demand for RSW, a separate system has been developed to specifically address this requirement, while also alleviating the load on the R717 system. The decision to implement this approach was driven by the advantageous characteristics of R744 (carbon dioxide) as a refrigerant and its greater capacity to generate hot water, as discussed in detail in section 2.4.4. The utilization of R744 offers several benefits, including its low environmental impact, non-toxicity, and excellent thermodynamic properties.

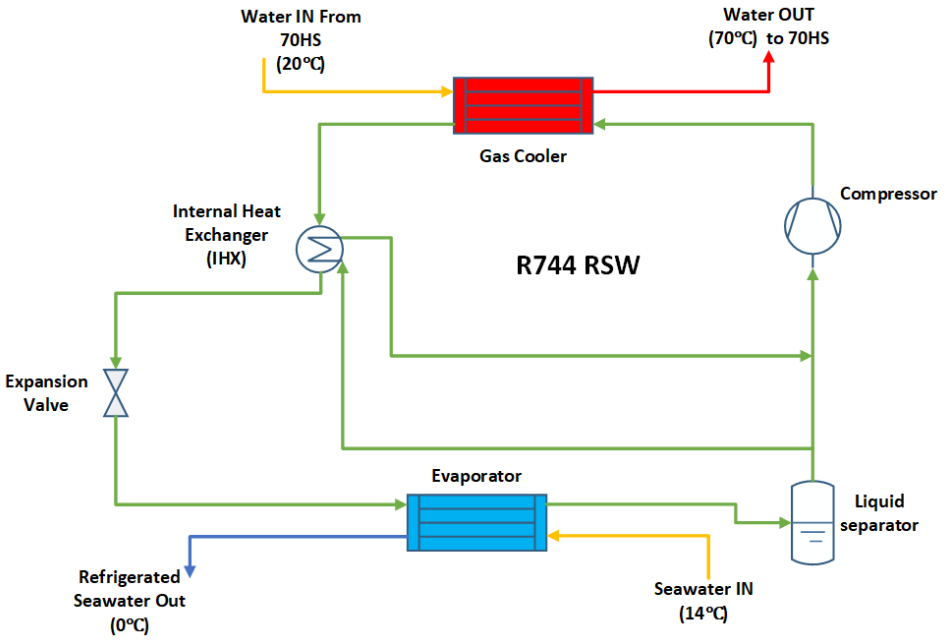

Figure 33: *Transcritical CO_2 (R744) system integrated with the 70HS.*

The R744 water-to-water transcritical RSW system operates in a dual-benefit configuration, employing the principles of heat pumping to provide both cooling and heating effects. On the evaporator side, seawater enters the system at an initial temperature of 14°C and undergoes a cooling process, reaching a final temperature of 0°C. The resulting RSW is then utilized for various operations in stage (i), catering to the specific cooling requirements of different systems.

However, the R744 system's primary objective extends beyond cooling alone. It plays a crucial role in providing the necessary heat energy to the returning water from the 70HS system, which is vital for maintaining optimal water temperature in the heating system. This is achieved through the gas cooler, carefully designed to raise the temperature of the

returning water from 20℃ to the desired level of 70℃. The heat transfer process in the gas cooler involves heat exchange between the supercritical carbon dioxide (R744) and the water, enabling efficient heat transfer and achieving the desired heating effect.

The operation of the R744 transcritical RSW system in transcritical mode is specifically chosen to optimize its performance. Transcritical operation refers to the utilization of carbon dioxide above its critical point, where the refrigerant transitions between the gas and liquid phases. This mode of operation ensures that the system takes full advantage of the thermodynamic properties of carbon dioxide, allowing for efficient heat transfer and temperature control.

3.3 Simulations and calculations – software and systems

In order to thoroughly investigate and evaluate the chosen option, extensive software simulations and calculations were conducted. Upon careful consideration and consultation with PTG, it was determined that option 2 presented the most viable solution. Subsequently, additional research efforts were initiated to delve deeper into the system's performance.

To facilitate the modelling and simulation process, the software tool Dymola was employed. To ensure the accuracy and reliability of the simulation results, the findings obtained from theoretical calculations using the Engineering Equation Solver (EES) were employed to validate the Dymola models. By comparing the results obtained from both approaches, any discrepancies or inconsistencies could be identified and addressed, ensuring the robustness of the simulation outcomes.

- Engineering Equation Solver (EES) - EES is renowned for its capability to solve complex nonlinear equation systems, making it an invaluable asset for addressing thermodynamic and heat transport problems. Engineers may model and evaluate complicated thermodynamic processes using EES's functions and equations. Its capacity to handle complicated equations with several variables and parameters is a significant benefit. It can solve these equations quickly and offer numerical answers for various system factors including temperatures, pressures, and heat transfer rates.
- Dymola - can handle complicated systems, and with support for the Modelica modelling language, it offers a full environment for constructing detailed models of such systems. Virtual models of refrigeration and heat pumping systems may be created by combining components such as compressors, condensers, evaporators, expansion valves, and heat exchangers. These components can be chosen from pre-existing libraries or constructed from scratch to meet unique needs. TLK-Thermo GmbH's component and refrigerant libraries, including TIL 3.12.1 and TIL Media 3.12.1, are available from Dymola and give a large choice of preconfigured components and refrigerants to pick from. Dymola allows users to define the system's operating circumstances, boundary conditions, and control techniques after the system model has been built.

3.4 Static simulations

In the early design and assessment of refrigeration and heat pumping systems, static simulations are critical. Various characteristics, including demands, pressure levels, and equipment specifications, are established during this phase depending on the system's requirements. The purpose is to look at the compatibility of various system components such as heat exchangers, compressors, and other components.

The simulation models were created utilizing static input parameters by exploiting information and insights gathered from the literature and previous PTG projects. The simulations provide a thorough evaluation of the system's performance under various operating situations. By entering fixed parameters, the system's behaviour, efficiency, and feasibility may be evaluated before incorporating dynamic factors that simulate real-life events. Static simulations serve as a foundation for later dynamic simulations, in which time-changing inputs and conditions may be incorporated to simulate real-world operation and assess system performance under varying loads and environmental circumstances.

It is possible to redefine the system design, optimize control techniques, and analyse the system's responsiveness to dynamic changes by first doing static simulations and then shifting to dynamic simulations. This iterative method allows for a thorough assessment of the refrigeration and heat pumping systems, assuring their dependability, efficiency, and efficacy in fulfilling the required goals.

3.4.1 System 1

3.4.1.1 EES

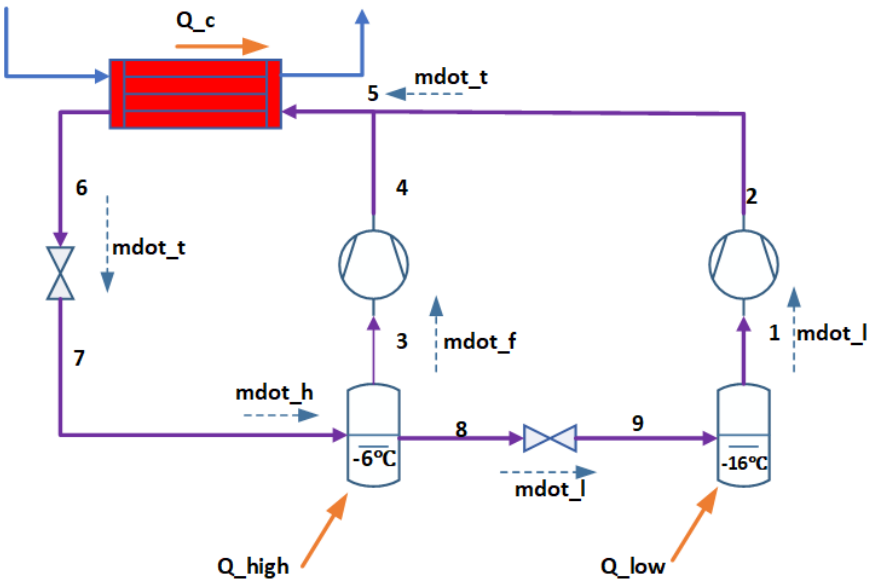

Figure 34: *Simplified sketch of the R717 system used for EES calculations.*

The saturation temperature of the refrigerant contained inside these components was used to determine the pressure levels for separators 1 and 2 in the refrigeration system. After

thorough consideration, it was concluded that a condensing temperature of 25°C provided the best operating conditions for the system. Seawater was fed into the system at an input temperature of 12°C in accordance with this temperature setting.

Table 8: *Pressure levels of the R717 system*

Components	Operating pressure (bar)
Condenser (high side)	10.03
Liquid separator 1 (stage 1)	3.412
Liquid separator 2 (stage 2)	2.263

The system seeks to achieve the desired refrigeration performance while taking the thermal characteristics of the refrigerant into account by selecting a condensing temperature of 25°C. This temperature setting promotes efficient heat transport and effective heat removal from the system, which contributes to its overall efficacy and dependability.

In addition, a seawater input temperature of 12°C is chosen to provide an adequate heat sink for the system. The system can successfully transfer heat and maintain appropriate operating conditions by using relatively cold seawater.

Table 9: *Description of the abbreviations used in EES for modelling the R717 refrigeration system.*

Abbreviations	Description
Q_high (kW)	Maximum cooling load on separator 1
Q_low (kW)	Maximum cooling load on separator 2
mdot_t (kg/s)	Total mass flow rate of R717
mdot_h (kg/s)	Mass flow rate of R717 entering separator 1
mdot_f (kg/s)	Mass flow rate of flash gas from separator 1 entering HP compressor
mdot_l (kg/s)	Mass flow rate of R717 entering separator 2 and taken off in LP compressor

Figure 32 was segmented and numerical IDs were issued to improve clarity to assist the modelling process within EES. The abbreviations corresponding to the different components can be found in **Table 9** as mentioned previously. Numerous equations, as presented by (T. M. Eikevik, 2021c, 2021b), were utilized to calculate diverse parameters such as enthalpy, refrigerant mass flow rate, and more:

- To determine real (non-isentropic) enthalpy after the compression process for both LP and HP compressors

$$\eta_{HP} = \frac{h_{4s} - h_3}{h_4 - h_3} \tag{3.1}$$

$$\eta_{LP} = \frac{h_{2s} - h_1}{h_2 - h_1} \tag{3.2}$$

- In separator 2, it is assumed that the full mdot_l is saturated and removed by the LP compressor. Energy balance for separator 2:

$$\dot{Q}_{low} = \dot{m}_l * (h_1 - h_9) \tag{3.3}$$

- Energy balance for separator 2 and to find the total mass flow rate of the system:

$$(\dot{m}_t * h_7) + \dot{Q}_{high} = (\dot{m}_l * h_8) + ((\dot{m}_t - \dot{m}_t) * h_3) \tag{3.4}$$

- To find the mass flow rate of the flash generated from separator 1:

$$\dot{m}_t = \dot{m}_l + \dot{m}_f \tag{3.5}$$

- To find the enthalpy of refrigerant entering the condenser:

$$h_5 = \frac{((\dot{m}_l * h_2) + (\dot{m}_f * h_4))}{\dot{m}_t} \tag{3.6}$$

- To find the heat rejected in the seawater-cooled condenser:

$$\dot{Q}_c = \dot{m}_t * (h_5 - h_6) \tag{3.7}$$

- To find the COP of the system:

$$COP_{R717\ RF} = \frac{(\dot{Q}_{low} + \dot{Q}_{high})}{(\dot{W}_{LP} + \dot{W}_{HP} + \dot{W}_{Pu1})} \tag{3.8}$$

3.4.1.2 Dymola

To simplify the simulation model, the R717 system was replicated in Dymola, as depicted in **Figure 35**. The inclusion of loops 1, 2, and 3 (**Figure 32**) was omitted to maintain simplicity, as there is insufficient data available for parameters such as pump work and heat exchanger performance in these loops. Appendix A outlines the rough step-by-step designing of the simulation model and provides a comprehensive understanding of how the model was developed. While the loops do play a role in the overall system, the primary focus of the refrigeration system is to deliver and maintain the appropriate refrigerant volume according to the cooling demand. To account for this, the cooling loads of loops 1 and 2 were aggregated and provided as input to separators 1 and 2, respectively. It is important to note that the current model does not include the R744 system for freezing demands. A comprehensive understanding of the model's components (section 3.2.2.1) is necessary, and **Table 10** outlines the functions of each PI controller:

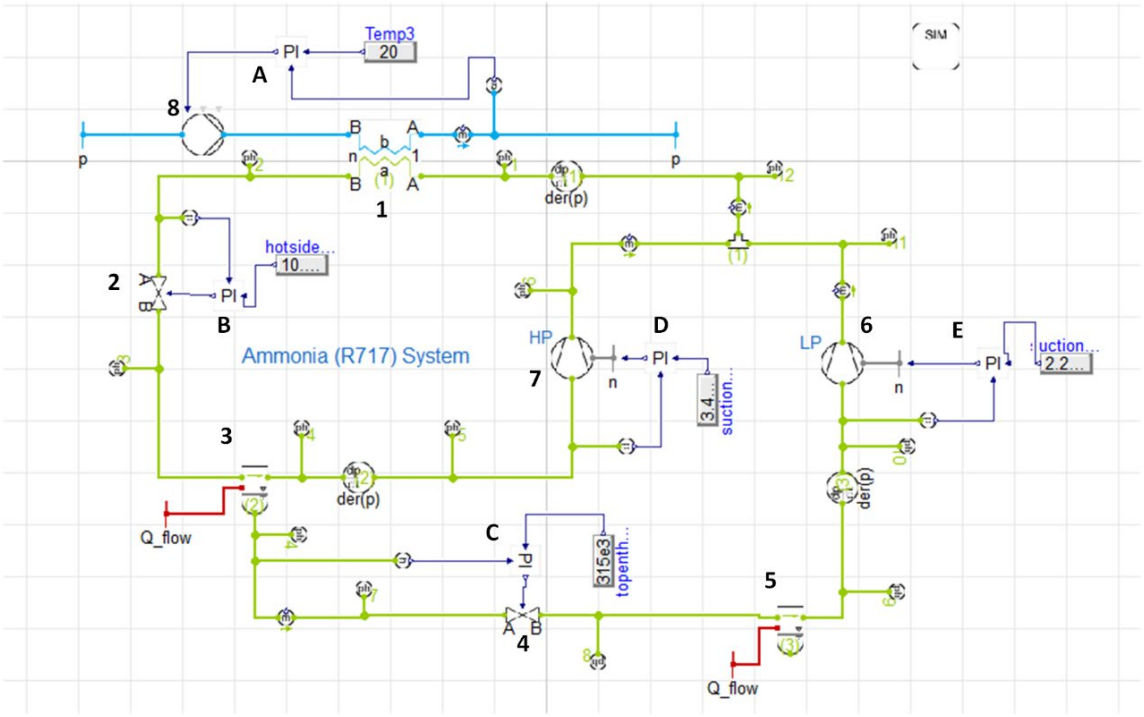

Figure 35: *Simulation model of the R717 refrigeration system (w/o loop 1,2&3) system in Dymola*

- Condenser (1) – counterflow plate heat exchanger design to facilitate efficient heat transfer and condensation of the refrigerant.
- Expansion Valve (2 & 4) – Essential valves responsible for throttling and regulating the high side pressure of the system. They control the flow of liquid refrigerant into separator 2.
- Liquid separator (3 & 5) – Comprises two distinct liquid separators, namely separator 1 and separator 2. The heat port functionality has been activated, allowing for the input of maximum Q values to ensure the effective separation of liquid refrigerant.
- Compressor (6 & 7) – Incorporates compressors characterized by their efficiency-based performance. A conservative efficiency of 70% has been assumed for these compressors.
- Pump (8) - Pumps based on efficiency to pump seawater into the condenser, assuming a 70% efficiency. The pressure difference (dp) was fixed at 0.1 bar.

Table 10: *Functions of the PI controllers employed in the simulation model shown in* ***Figure 35***

PI Controller	Function
A	Controls the mass flow rate of the incoming seawater based on the desired exit temperature of 20°C
B	Controls the area of the expansion valve based on the desired high side pressure (10.03 bar)
C	Controls the area of the valve based on the desired enthalpy of the liquid refrigerant moving towards separator 2
D and E	Controls the speed of the rotation of the shaft of the respective compressors based on the desired suction pressure (3.4 and 2.2 bar)

3.4.1 System 2

3.4.1.1 EES

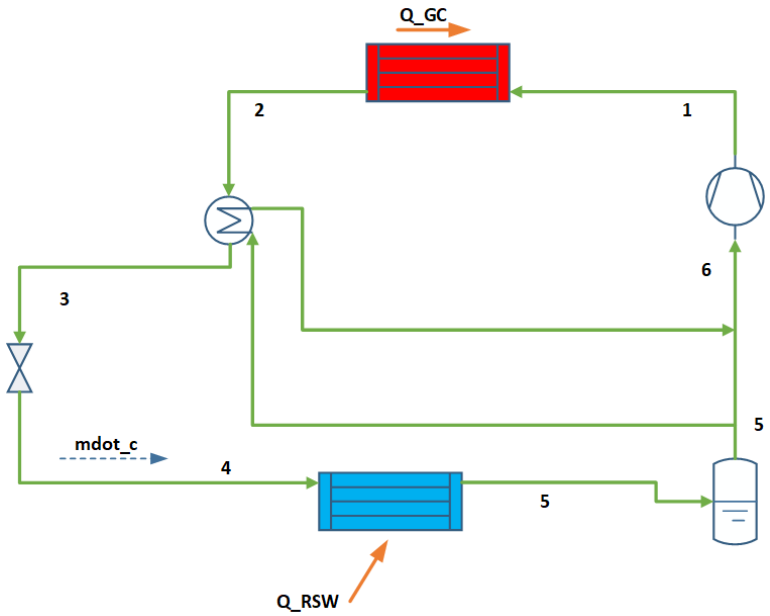

Figure 36: *Simplified sketch of the R744 system used for EES calculations.*

The determination of high and low side pressures played a crucial role in the accurate simulation of the system. Considering the desired outcome of cooling the incoming water to 0°C on the evaporator side, the evaporating temperature of R744, based on relevant literature, was set to -2°C. Correspondingly, at this temperature, the saturation pressure of R744 amounts to 33 bar, providing the necessary conditions for efficient heat exchange.

Table 11: *Pressure levels of the transcritical R744 system*

Components	Operating pressure (bar)	R744 entry temperature (°C)
Gas cooler (high side)	90	90
Evaporator (low stage)	33	-2

To fulfil the requirement of supplying water at a temperature of 70°C to the 70HS, the pressure on the gas cooler end was set at 90 bar. According to literature sources, it is recommended to maintain a temperature differential of at least 20°C in the gas cooler to optimize heat transmission. Consequently, the R744 entering the gas cooler exhibits a temperature of 90°C, contributing to the achievement of desired operational parameters.

- To determine the amount of heat rejected in the gas cooler:

$$\dot{Q}_{GC} = \dot{m}_c * (h_1 - h_2) = \dot{m}_w * c_{pw}(T_{wo} - T_{wi}) \quad (3.9)$$

- To determine the amount of heat transfer in the IHX:

$$\dot{Q}_{IHX} = \dot{m}_c * (h_2 - h_3) = \dot{m}_c * (h_6 - h_5) \quad (3.10)$$

- To determine the mass flow rate of the refrigerant in the system:

$$\dot{Q}_{RSW} = \dot{m}_c * (h_5 - h_4) \tag{3.11}$$

- To find the COP of the system:

$$COP_{R744\ HP} = \frac{\dot{Q}_{GC}}{(\dot{W}_c + \dot{W}_{Pu2})} \tag{3.12}$$

3.4.1.2 Dymola

The complete R744 RSW system, as depicted in **Figure 37**, was successfully modelled in Dymola. Appendix A outlines the rough step-by-step designing of the simulation model. Extensive literature (Hafner and Eikevik, 2016) was consulted to dimension the gas cooler, ensuring a temperature differential of 5°C between the CO_2 gas cooler output temperature and the incoming water temperature from the 70HS. Given that the water intake temperature is 20°C (as discussed in Section 3.2), the target CO_2 outflow temperature was set at 25°C. However, due to technical limitations, a simple tube was employed instead of a conventional evaporator (heat exchanger). The heat input to the tube was provided by Q_{RSW}.

It is crucial to have a comprehensive understanding of the model's key components, as detailed in Section 3.2.2.2. **Table 12** outlines the specific functions performed by each of the PI controllers:

- Gas Cooler (1) – A counterflow plate heat exchanger designed for efficient heat transfer from the CO_2 at its gliding temperature to the incoming water from the 70HS.
- Internal/Suction Line Heat Exchanger (2) – A counterflow heat exchanger is employed to superheat the refrigerant and reduce the compressor's workload.

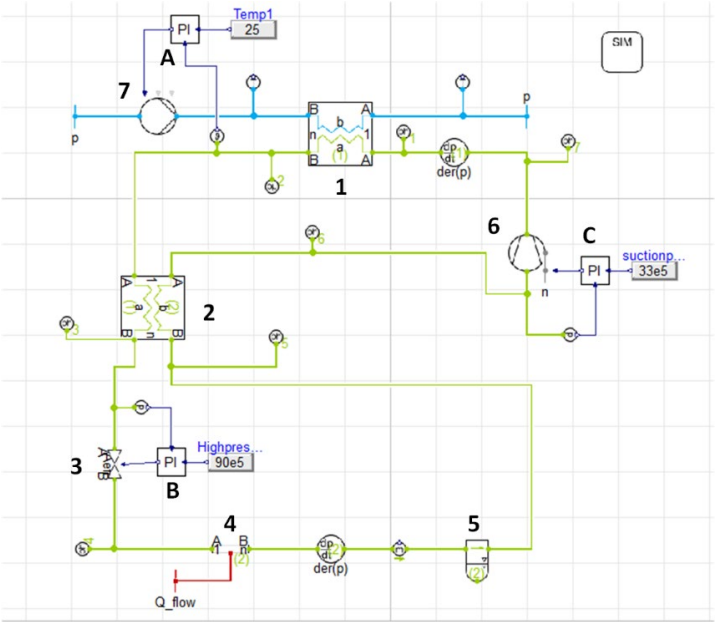

Figure 37: *Simulation model of the transcritical R744 RSW system in Dymola*

- Expansion Valve (3) – Responsible for throttling the refrigerant and regulating the high side pressure.
- Simple Tube (4) – This component serves as the evaporator, where the heat capacity is provided as an input.
- Liquid Separator (5) – Ensures that only gaseous refrigerant reaches the compressor's suction line. In R744 systems, the liquid refrigerant entering the suction line can cause damage to the equipment, such as the Internal Heat Exchanger (IHX) and compressor.
- Compressor (6) – Efficiency-based compressor was utilized, assuming an efficiency of 70%.
- Pump (7) – Pumps based on efficiency to pump cold water into the gas cooler, assuming a 70% efficiency. The pressure difference (dp) was fixed at 0.1 bar.

Table 12: *Functions of the PI controllers employed in the simulation model shown in* ***Figure 37****.*

PI Controller	Function
A	Controls the mass flow rate of the incoming water from the 70HS based on the desired CO_2 outlet temperature (25°C)
B	Controls the area of the expansion valve based on the desired high side pressure (90 bar)
C	Controls the speed of the rotation of the shaft of the compressor based on the desired suction pressure (33 bar)

3.5 Dynamic simulations

Following the conclusion of static simulations, the findings were carefully examined and used to set up parameters for dynamic simulations. Dynamic simulations were critical for reflecting seasonal fluctuations in daily load demand, such as those seen in summer and winter (**Figure 38**, **Figure 39**). The simulations were conducted for a duration of one day (24 hrs/86400s).

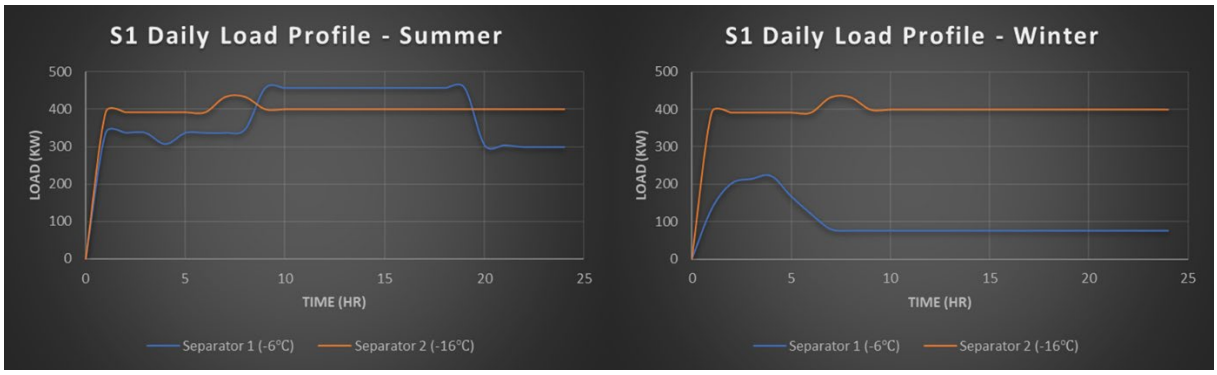

Figure 38: *The summer and winter daily load profile for System 1*

Figure 38 displays the operational schedule of System 1, which maintains a continuous run-time from 1 am to 12 midnight across both seasons. This uninterrupted operation is vital for meeting the various food and building energy requirements.

The simulations provided important information such as the system's transient behaviour, energy consumption patterns, and performance indicators under various load demands. These simulations help identify possible areas for improvement, optimize control systems, and analyse energy-saving options. Simulating the system for a full day allows for a comprehensive analysis of its performance over diurnal variations in load and ambient conditions. Its useful insights into system responsiveness, energy consumption patterns, and optimization potential, allow for informed decision-making and the construction of efficient and sustainable refrigeration systems tailored to the demands of salmon processing plants.

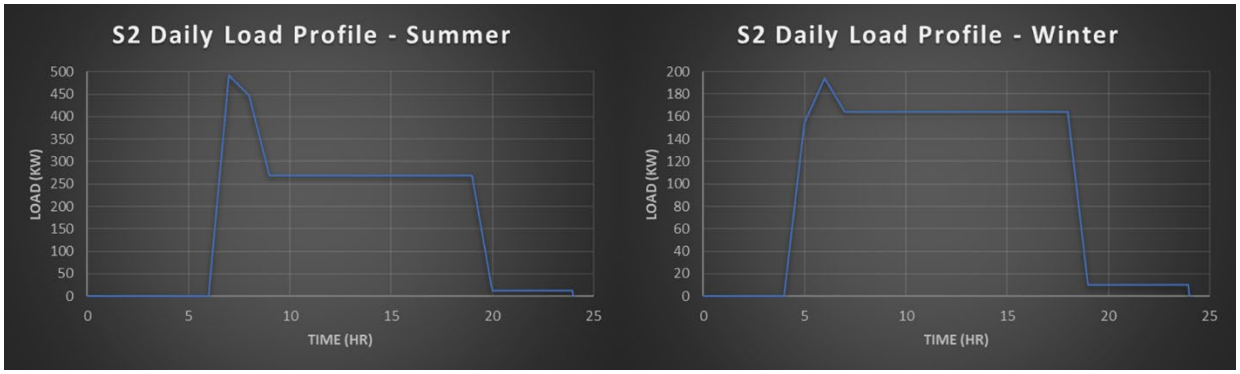

Figure 39: *The summer and winter daily load profile for System 2*

Figure 39 shows system 2's operational pattern, with an on-and-off cycle. The system begins operating at 7 am every day during the summer season, and at 5 am daily during the winter season. In both seasons, the system operates continuously until 12 am (midnight).

The models developed for this study are capable of producing findings based on a wide variety of input parameters as long as they fall within the system's operational conditions. Several critical parameters were dynamically adjusted during the simulations to study the systems' performance and assess the key performance indicators of interest to narrow the area of the study:

- The high side pressure was changed while the load remained constant. The data was analysed and compared to determine the relationship between pressure and COP, condenser/gas cooler output, discharge temperature, compressor frequency, etc. This investigation was particularly relevant because, despite the system's design for maximum load, it frequently operates under part-load conditions for most of the year.
- After determining the ideal pressure, transient simulations for both summer and winter were performed. This simulation assisted in determining the power usage throughout the day, in addition to the primary system performance metrics.

In addition to the common simulations conducted for both System 1 and System 2, specific additional simulations were performed to address the unique characteristics and use cases of each system.

3.5.1 System 1

After determining the optimal pressure range for the refrigeration system, further dynamic simulations were conducted to investigate the behaviour of the system:

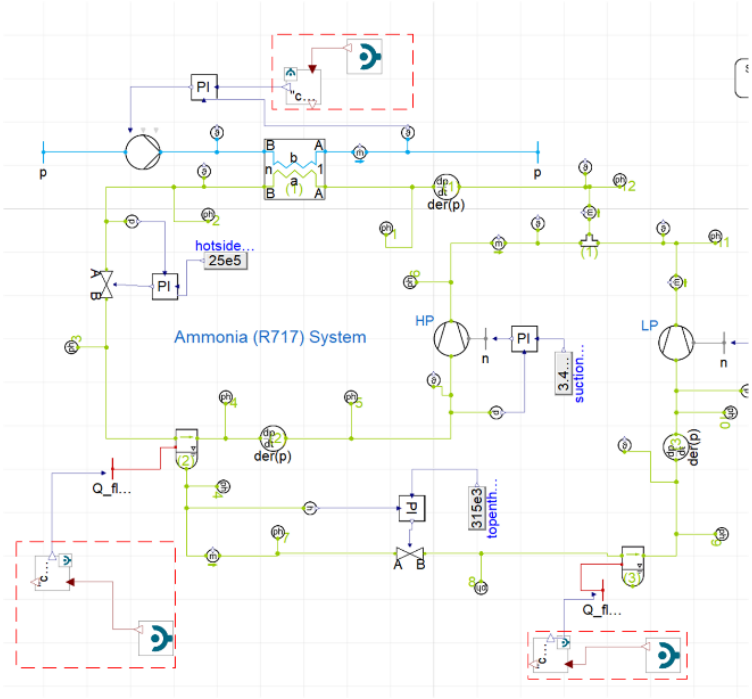

Figure 40: *Pump flow rate varied during summer simulation in system 1.*

- Circulation Pump Flow Rate Analysis: summer load evaluation - This investigation focuses on the influence of the circulation pump's flow rate during the high cooling demands, specifically in the summer season. The flow rate of the pump, responsible for distributing the refrigerant throughout the system, is modified within its operating parameters. By doing so, we can scrutinize the correlation between the pump's flow rate and the system's power consumption. This provides a clearer perspective on the pump's role in managing system efficiency and performance during periods of peak cooling demand.

3.5.2 System 2

The performance metrics of System 2 such as the COP and power usage are constantly monitored and assessed in all the cases.

- Dynamic discharge pressure – There were four load cases, representing the average and peak load of each season. The data was analysed and compared to determine the relationship between pressure and COP, condenser & gas cooler output, discharge temperature, and compressor frequency.

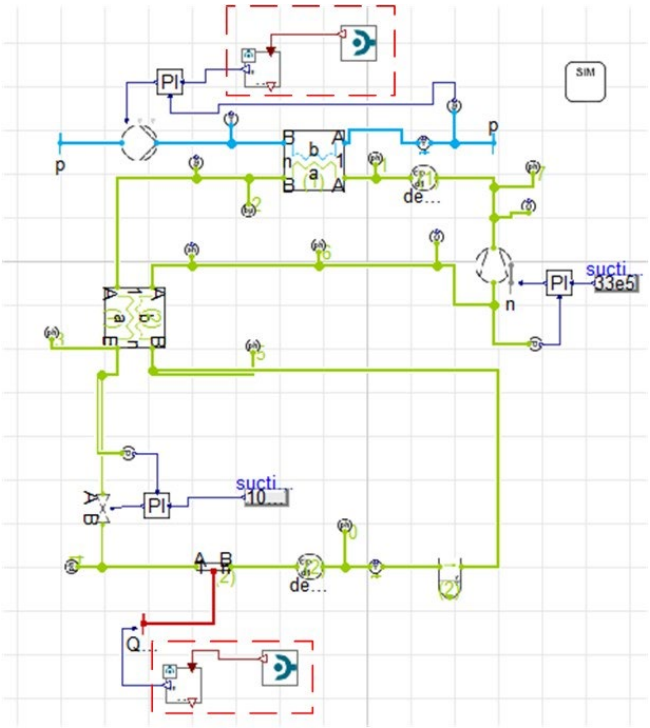

Figure 41: *Dynamic simulations involving the variation of both load (bottom) and water temperature (top) simultaneously.*

- Dynamic increase of required water temperature – The system's ability to deliver hot water at greater temperatures was evaluated during the winter simulation. The system's performance was evaluated by gradually increasing the needed temperature from 70°C to 90°C.

3.5.3 Calculation of daily total - determining the area under the curve

The dynamic simulations performed for both systems yield diverse data, leading to a variety of graphs. To calculate the daily totals of parameters such as hot water production or energy consumption, the area under the curve acquired from simulations must be calculated. Since Dymola does not allow a direct calculation for the total over simulated time, alternative methods using Microsoft Excel and MATLAB were employed.

In Excel, the trendline feature was utilized to analyse the data. As the curve is not a regular shape, it cannot be fitted with a trendline automatically. Instead, the graphs were segmented into different sections, treating each section as an individual curve. A polynomial trendline of order 2 was applied to each segment, resulting in an equation of the curve in the form of y(x).

To provide a clearer illustration of the methodology employed, a specific example has been presented. **Figure 42** illustrates the calculation of the total energy consumed in a day during the summer, as mentioned in **Table 19**.

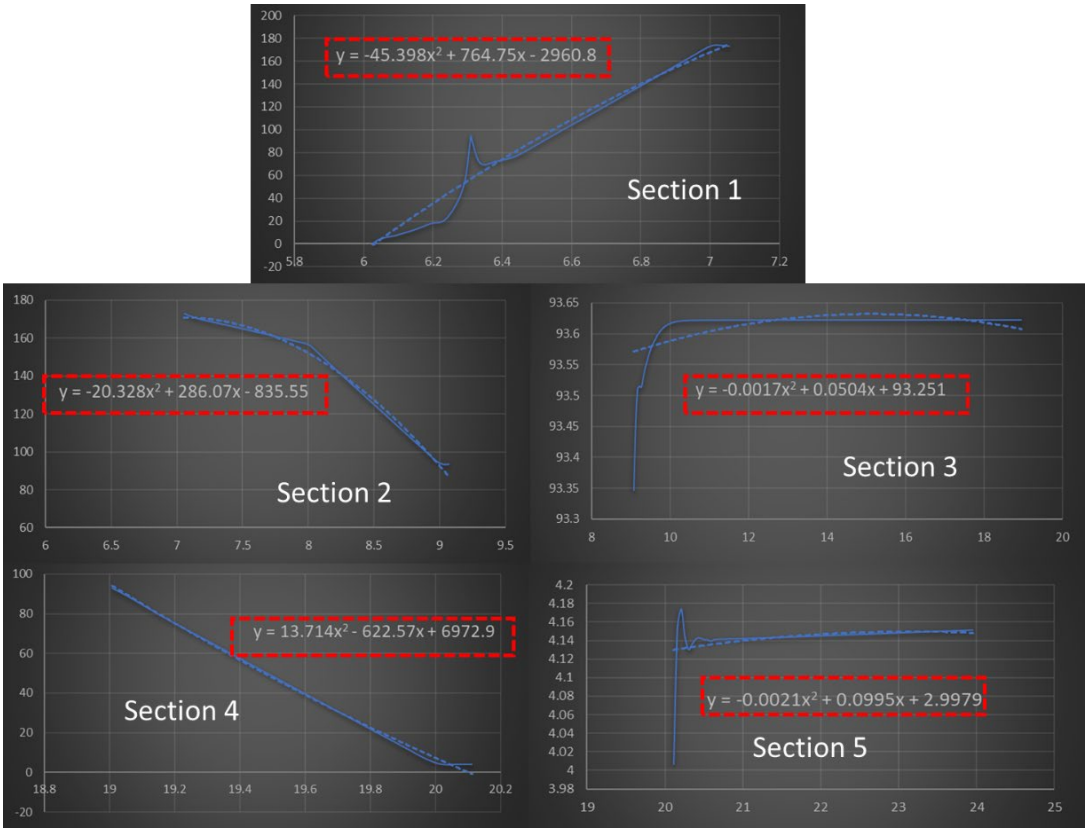

Figure 42: *Segmented trendline analysis of shaft power vs. time during summer (Figure 60) system 2*

The next step involved using MATLAB to code the equation and perform integration, along with other necessary calculations. The area under each section curve was calculated by integrating the equation and determining the difference between its endpoints. The individual regions were then added together to produce the final value under the original curve.

This method has been shown to yield a high level of accuracy, often ranging between 90% and 95%. Given the lack of alternatives that can match this degree of precision, it was deemed the most suitable approach for calculating the desired values.

3.6 Electricity consumption analysis

It is crucial to closely examine both the system's annual electricity consumption. The importance of such an analysis is twofold. Firstly, while the technical efficiency of a system is undoubtedly significant, the ultimate concern for end-users or investors often lies in the practical economic implications. They are interested in understanding the potential annual expenditure or cost savings associated with the systems. Thus, a detailed analysis of the annual electricity consumption becomes paramount. Secondly, from an environmental perspective, the efficient use of electricity in processing plants is an essential aspect of sustainable industrial operations. Therefore, evaluating the electricity consumption of these systems over the course of a year provides insight into both their economic feasibility and their environmental impact.

As mentioned above, the simulations have been conducted for two distinct seasons, which necessitates certain assumptions for extrapolating the results to a full year. Given the factory's location in northern Norway, it experiences approximately 5 months of summer and 7 months of winter. This seasonal distribution directly influences energy consumption due to the changes in temperature and operational adjustments necessary during different periods of the year.

In terms of electricity costs, energy-intensive industries in Norway are charged an electricity price of 49.7 Øre/kWh (Statistisk Sentralbyrå, 2023). This figure includes the cost of electricity and grid rent, while taxes are excluded. Given that salmon processing factories fall under the purview of energy-intensive industries, this price has been used as a basis for our analysis (EU Commission, 2021).

The operational schedule of the processing plant is another crucial factor in determining energy consumption. For the year 2023, the total number of working days in Norway is 251 (Norway Days, 2023). However, maintenance shutdown periods, which typically amount to 2-3 weeks annually, reduce the number of operational days. Distributing this downtime evenly, the plant is estimated to operate for 230 days a year. In accordance with our seasonal assumption, we allocate 96 operational days to the summer and 134 days to the winter. This distribution considers the longer duration of the winter season in northern Norway, providing a more accurate representation of the seasonal electricity consumption.

It should be noted that while our analysis is based on a series of assumptions and averages, the actual electricity consumption of the systems could fluctuate due to a variety of factors. Therefore, our results should be interpreted as indicative rather than absolute values.

Table 13: *Key parameters for annual electricity consumption analysis in salmon processing plants*

Parameters	Values
Electricity price for energy-intensive industries in Norway (Øre/kWh)	49.7
SPP operational days per year (days)	230
Operational summer days in a year (days)	96
Operational winter days in a year(days)	134

The energy cost for each system during the summer and winter seasons can be calculated using the following equation:

$$EC = \frac{E_{day} * OD * e}{100} \tag{3.13}$$

Where (EC) represents the total energy cost for an entire season in NOK, (E_{day}) signifies the daily energy consumption in kWh and (e) denotes the electricity price in Øre/kWh.

Chapter 4: Results

In this chapter, the results obtained from the simulation of the models using Dymola and comparing them with the results obtained from EES (only static simulations were compared as dynamic modelling is not possible) are presented. The simulations were conducted under certain assumptions, including the constant efficiency of the compressors and pumps. The Dymola models were simulated for a full day of operation to capture the system's performance over an extended period. By analysing the results, we can gain insights into the accuracy and effectiveness of the Dymola models in predicting the behaviour of refrigeration systems.

4.1 System 1

4.1.1 Static simulations

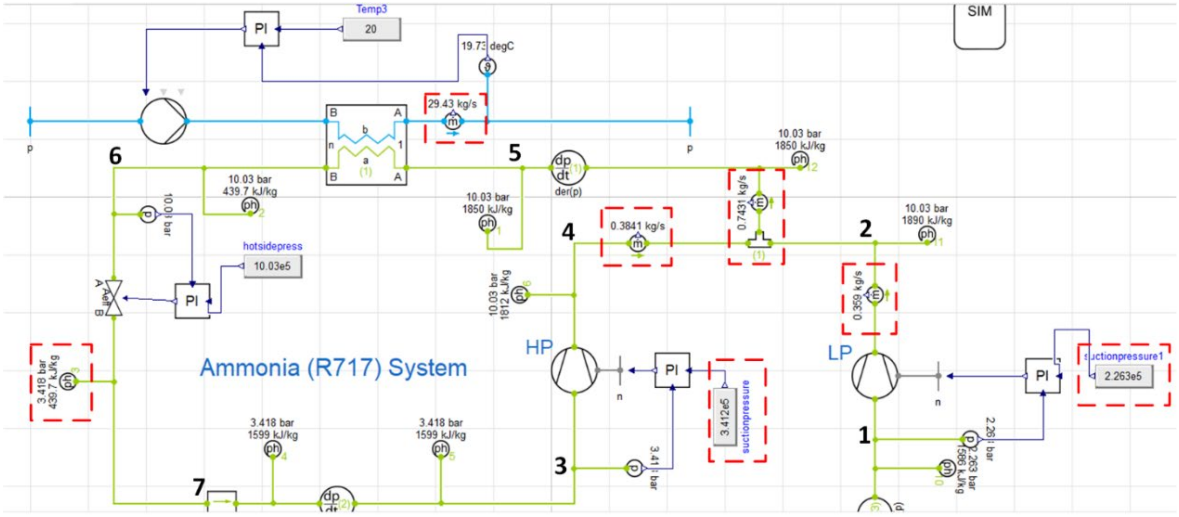

Figure 43: *Upper half of the simulation model of the R717 refrigeration system*

The essential system inputs included cooling loads imposed on the two liquid separators. Adjustments were made to the PI controllers to achieve output values as close to theoretical estimations as possible. The high side pressure achieved a value of 10.03 bar. In the condenser, the high-temperature refrigerant is subjected to a constant temperature condensation (subcritical), further subcooling it to reach state point 6 from state point 5 with an enthalpy value of 439.7 kJ/kg. Given the substantial heat rejection, the seawater's mass flow rate, passing through the condenser at 29.43 kg/s, must mirror this intensity. With this mass flow rate, the seawater absorbs an impressive total of 1048 kW from the refrigerant.

Upon reaching state point 7, the refrigerant undergoes throttling and expansion. As this process is isenthalpic, the enthalpy remains constant at state points 6 and 7. The refrigerant is then introduced into separator 1, where it is divided into a liquid component, flowing to separator 2, and a flash gas component, extracted by the HP compressor. At state point 3, the HP compressor's suction pressure is noted to be 3.418 bar, while the flash gas's enthalpy

entering the compressor stands at 1599 kJ/kg. The HP compressor's (pressure ratio 2.96) shaft rotation is regulated based on the suction pressure via the PI controller.

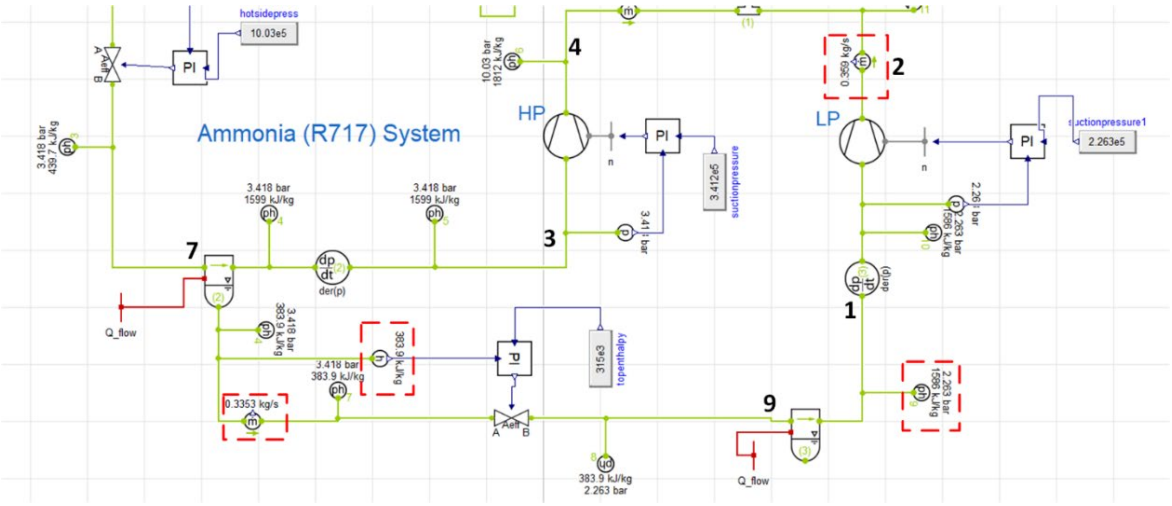

Figure 44: *Lower half of the simulation model of the R717 refrigeration system*

The flash gas, entering the compressor at 0.38 kg/s, is elevated to state 4 with an enthalpy of 1812 kJ/kg. From state point 7 to 3, the working fluid undergoes constant temperature evaporation at -6°C. The fluid from separator 2 is routed to state point 8 at a mass flow rate of 0.34 kg/s and an enthalpy of 383.9 kJ/kg. Following this, the fluid is throttled to achieve further cooling, reaching state point 9 at -16°C. The PI controller regulates the expansion valve's area based on the desired enthalpy at state point 8. The fluid is fully evaporated from separator 2 and extracted by the LP compressor. The LP compressor's suction pressure is 2.26 bar, and the flash gas's enthalpy entering the compressor is 1586 kJ/kg. The LP compressor's pressure ratio is 4.47. The PI controller regulates the shaft rotation based on the suction pressure. The superheated fluid exits the compressor at a rate of 0.36 kg/s, achieving state 2 with an enthalpy of 1890 kJ/kg.

Fluid from state points 2 and 4 converges at a fluid junction and exits at state 5 with a combined mass flow rate of 0.74 kg/s. When a fluid with higher and lower enthalpy (from state points 2 and 4) is mixed, the resulting enthalpy is 1850 kJ/kg. The HP compressor receives a work input of 81.81 kW, while the LP compressor is supplied with 109.14 kW. Therefore, the system's total work input is recorded as 190.95 kW.

4.1.2 EES - static simulations validation

A comparative analysis of the static simulation models in both Dymola and EES is presented in **Table 14**. The majority of the system parameters align within a 10% margin. However, an anomaly was identified in the mass flow rate of the refrigerant entering Separator 2, which deviates significantly from the EES values. This discrepancy subsequently impacts the workload on the LP compressor and, consequentially, the COP, leading to substantial inaccuracy. This issue has been discussed in section 5.1

Table 14: *Comparative assessment of the R717 system's static simulations: Dymola vs. EES.*

Parameters (units)	EES	Dymola	Difference (%)
P_h (bar)	10.03	10.03	-
P_m (bar)	3.412	3.418	-
P_l (bar)	2.263	2.26	-
h_2 (kJ/kg)	1746	1890	8.25
h_4 (kJ/kg)	1669	1812	8.57
h_5 (kJ/kg)	1703	1850	8.63
$\dot{m}_t$ (kg/s)	0.786	0.743	-5.47
$\dot{m}_l$ (kg/s)	0.341	0.359	5.28
$\dot{m}_f$ (kg/s)	0.445	0.3841	-13.69
$\dot{Q}_C$ (kW)	1089	1048	-3.76
$\dot{W}_{LP}$ (kW)	103.32	81.81	-20.82
$\dot{W}_{HP}$ (kW)	95.23	109.14	14.61
COP	4.48	4.66	4.02

The disparity, particularly in the flash gas mass flow rate, could be the reason for the previously mentioned discrepancy in the work input to the LP compressor and, subsequently, the COP. The differences observed between the two simulations could be due to different assumptions, and calculation methods employed in EES and Dymola.

4.1.3 Dynamic simulations

4.1.3.1 Identification of optimal high-side pressure for maximizing COP across seasonal variations

This section explores an analysis centred around the dynamic discharge pressure under varying load scenarios. As illustrated in **Table 15**, the maximum and average loads for separator 2 during both seasons display a minimal difference of just 30kW, while the values for separator 1 vary significantly between the seasons.

Table 15: *Operational scenarios for analysis - Maximum and average load conditions*

Season	Separator 1 max (kW)		Separator 2 (kW)	
	Max	Average	Max	Average
Summer	457	337	433	400
Winter	223	120	433	400

The primary objective of this analysis is to identify the high side pressure at which the system achieves its highest COP. This optimal high-side pressure will then be utilized for the subsequent seasonal simulations. Consequently, a single simulation was conducted wherein the load on separator 2 was set to 400 kW and the load on separator 1 was set to 350 kW. These load values approximately represent the average daily load on the separators, encompassing both seasons.

In the static simulations, the condenser-side water pump was unconstrained, consuming as much energy as required to attain an outlet seawater temperature of 20°C. However, in actual operation, controlling the outlet seawater temperature is not of primary importance, as the seawater is eventually discharged back into the sea. Despite this, it is crucial to consider the environmental impact of the discharged seawater. Excessively hot seawater can adversely affect the surrounding aquatic life, posing potential ecological concerns in the factory's vicinity. As such, a balance was sought to mitigate this issue. The water pump's energy consumption was capped, limiting it to a maximum of 0.25 kW.

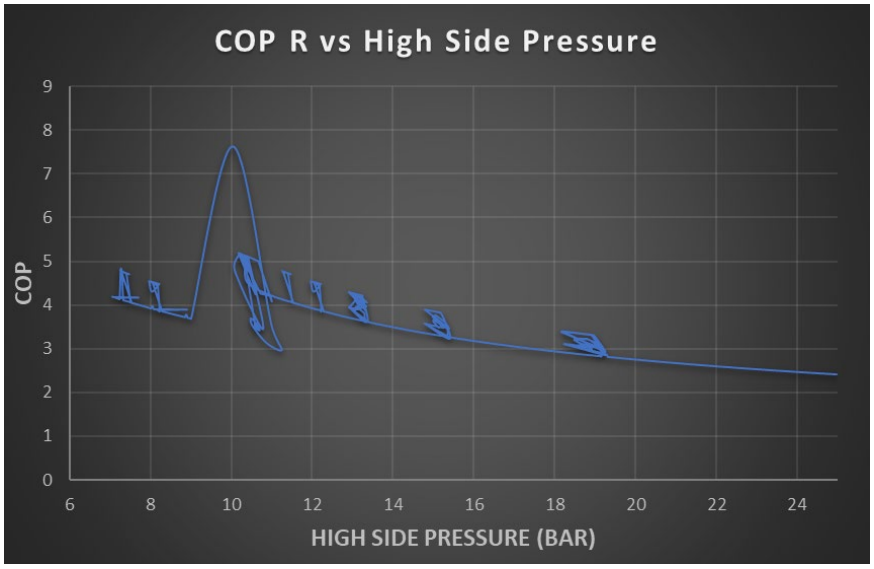

Figure 45: *Variation of COP with discharge pressure – system 1*

In **Figure 45**, the observed fluctuations in the COP as pressure varies could be indicative of underlying system inefficiencies or control challenges. Such inconsistent operation, especially in the critical range of 7-10 bar, could lead to sub-optimal cooling performance and higher energy usage, particularly if the system struggles to stabilize around the ideal operation point. Around 11 bar, the system appears to stabilize somewhat, suggesting this may be a more optimal operating point. However, periodic disruptions are still observed, indicating intermittent issues with system stability. These could potentially be due to either of the compressors failing to maintain a consistent speed, suggesting an area for further study and potential system optimization (discussed later).

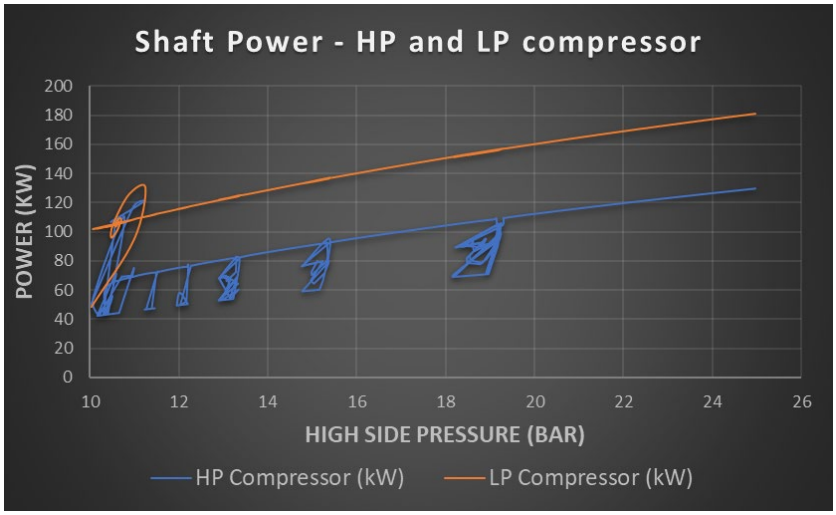

Figure 46: *Variation of shaft power for both compressors in relation to high side pressure – system 1*

As evident from **Figure 46**, the High-Pressure (HP) compressor seems to be facing difficulties in achieving an optimal rotational speed, reflected in its inconsistent power consumption patterns as the high side pressure varies. This issue may be attributed to a range of factors, including mechanical inefficiencies, control system challenges, or other operational variables not yet considered. Such instability in the HP compressor operation could potentially affect the system's overall energy efficiency and reliability. Therefore, it is crucial to further investigate these discrepancies, identify the root causes, and devise appropriate solutions. A detailed analysis of the possible issues will follow in the discussion section.

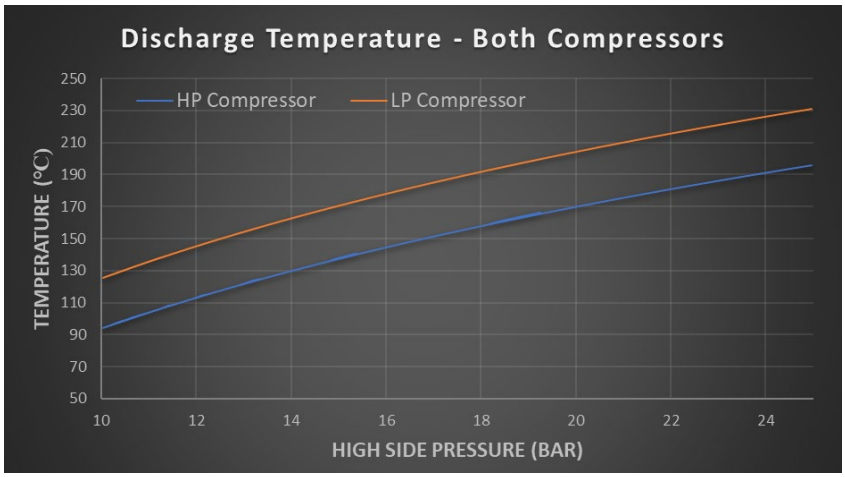

Figure 47: *Comparison of discharge temperature versus high side pressure for both compressors*

From **Figure 47**, it is evident that the discharge temperature for both compressors increases with the high side pressure. This is a typical behaviour since a higher-pressure ratio generally leads to increased compression work, thereby raising the temperature of the refrigerant at the compressor's discharge. HP compressor is likely to show a lower increase in discharge temperature with pressure compared to the LP compressor due to its lower compression ratio. This could indicate a higher workload and potentially higher internal losses in the HP

compressor. High discharge temperatures can lead to issues such as oil breakdown, motor insulation failure, and excessive wear on compressor components. Therefore, careful monitoring and control of these temperatures are vital for reliable and efficient system operation.

4.1.3.2 Seasonal operation – summer and winter

The findings from section 4.1.3.1 led to the identification of an optimal discharge pressure of 12 bar for System 1. Notably, the system demonstrated irregular behaviour under different conditions, which prompted a reassessment and refinement of the PI controllers and other components specifically for a 12 bar discharge pressure condition.

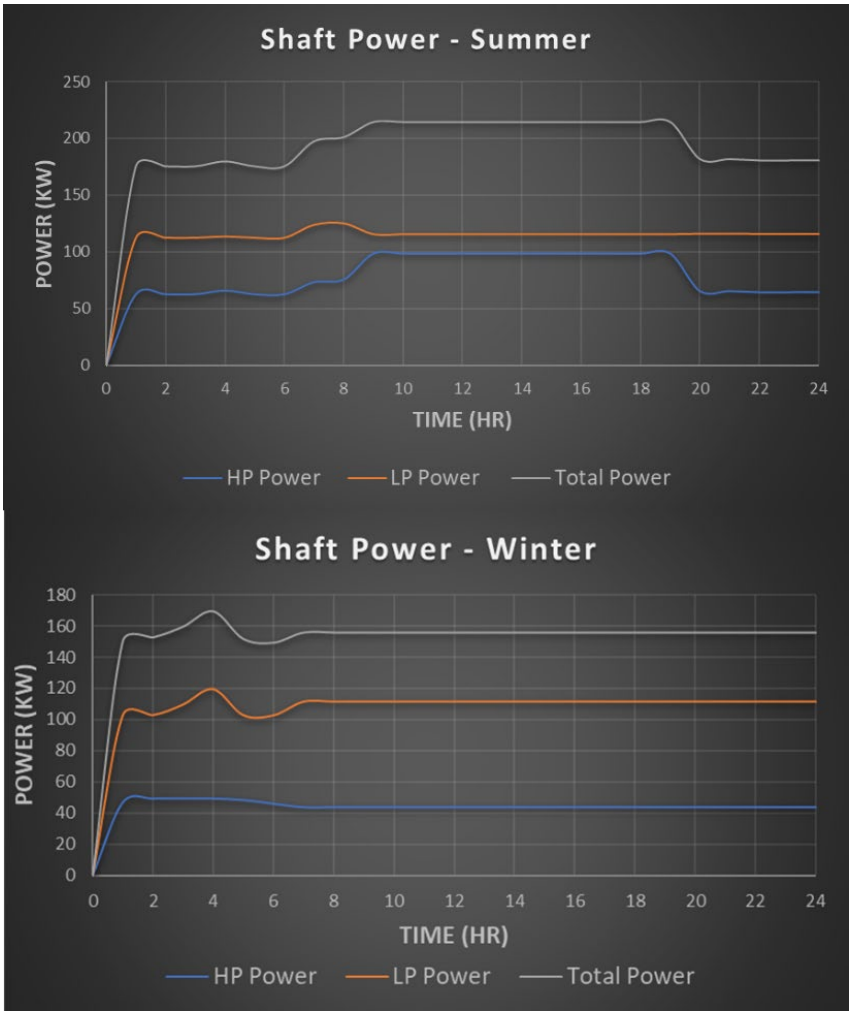

Figure 48: *Temporal variation of shaft power for individual separators and total system across seasons*

Figure 48 offers a profound insight into the efficient operation of the compressors in response to the system's demands. It plots the temporal evolution of shaft power for the individual separators and the total system, painting a vivid picture of the power dynamics at play across different seasons. Observing the fluctuations, it is evident that the compressors and separators are finely tuned to respond to the varying environmental conditions, thereby

ensuring optimal performance throughout the year. The adaptability of the compressors to maintain a balanced load distribution between the separators is commendable, establishing the robustness and resilience of the system's design.

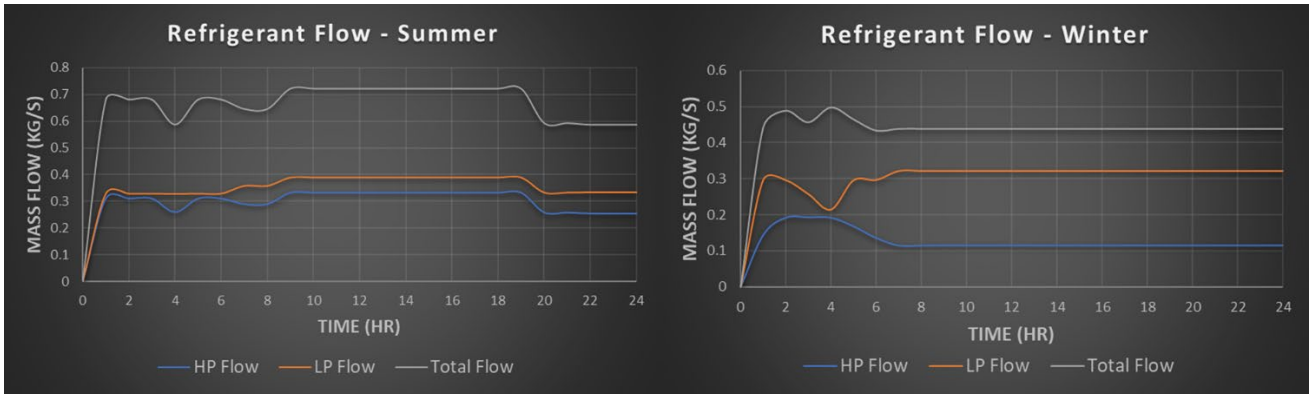

Figure 49: *Variation of refrigerant mass flow rate through HP and LP compressors over time for both seasons*

Figure 49 shows the system's ability to modulate the refrigerant flow in response to changing external conditions highlighting its adaptability and resilience. The total flow is the cumulative effect of the flow through both compressors. It's interesting to observe how the system balances the flow between the HP and LP compressors to maintain overall performance, ensuring a continuous and efficient operation.

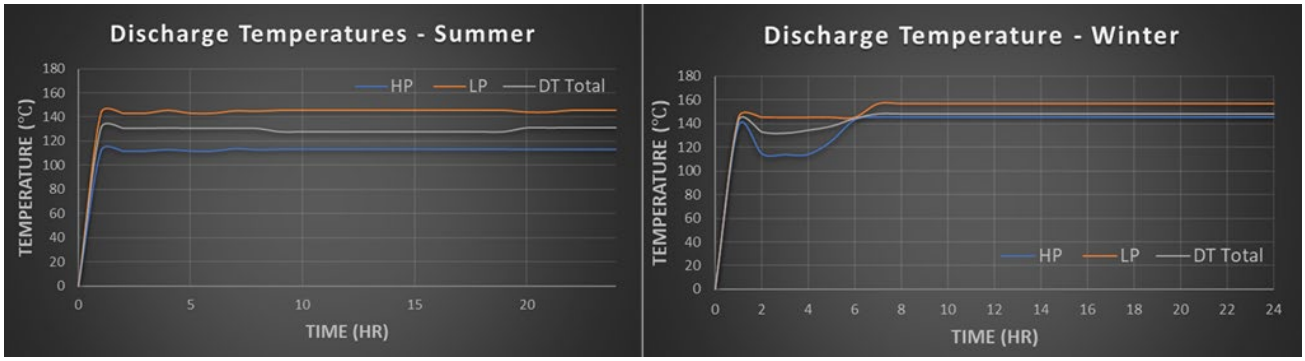

Figure 50: *Seasonal variation in discharge temperatures from HP and LP compressors, and combined discharge temperature before entering the condenser.*

As observed in Figure 50, the discharge temperatures are significantly high but remain fairly stable throughout the day, in both seasons. These elevated temperatures indicate the presence of substantial thermal energy, which, instead of being discharged into the environment, could potentially be harnessed for other applications, thereby augmenting the overall efficiency of the system. This idea of waste heat recovery could form a significant part of future work in improving the system's performance.

Table 16: *Daily parameters comparison for summer and winter seasons – System 1*

Parameters (units)	Summer	Winter	Percentage difference (%)
$\dot{W}_{HP}$ (kWh)	1912	1060	44.56
$\dot{W}_{LP}$ (kWh)	2715	2598	4.31
$\dot{W}_{LP} + \dot{W}_{HP} + \dot{W}_{Pu1}$ (kWh)	4633	3664	20.92
Discharge pressure (bar)	12	12	-
Typical DT – HP Comp. (°C)	113	140	-23.89
Typical DT – LP Comp. (°C)	145	154	-6.21
Typical DT - System (°C)	130	146	-12.31
Typical $\dot{m}_f$ (kg/s)	0.305	0.129	57.70
Typical $\dot{m}_l$ (kg/s)	0.359	0.311	13.37
Typical $\dot{m}_t$ (kg/s)	0.673	0.444	34.03
Seawater outlet temperature (°C)	26.2	23	12.21
Seasonal COP (Refrigeration)	3.98	3.22	19.09

4.1.3.3 Circulation pump flow rate analysis – Summer daily load

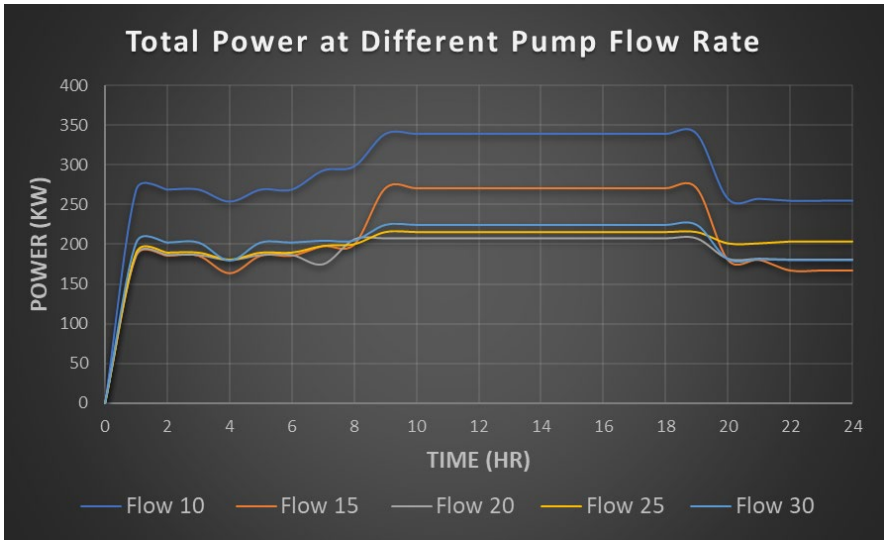

Figure 51: *Comparison of total power consumption at varied pump flow rates during a typical summer day – system 1*

Figure 51 illustrates the total power consumed by the system at varying pump flow rates during the peak summer season. Interestingly, the power consumption is not linearly proportional to the pump flow rate. The system consumes the least power at 10 kg/s flow rate and the most at 30 kg/s. One possible explanation for this could be due to the efficiency of the pump at different operating points. The pump may operate more efficiently at lower flow rates, leading to lower total system power consumption. Additionally, the system's total thermal load and the characteristics of other components may also influence this trend. For

instance, at higher flow rates, other system components may require more power to handle the increased refrigerant flow, thus increasing the total power consumption.

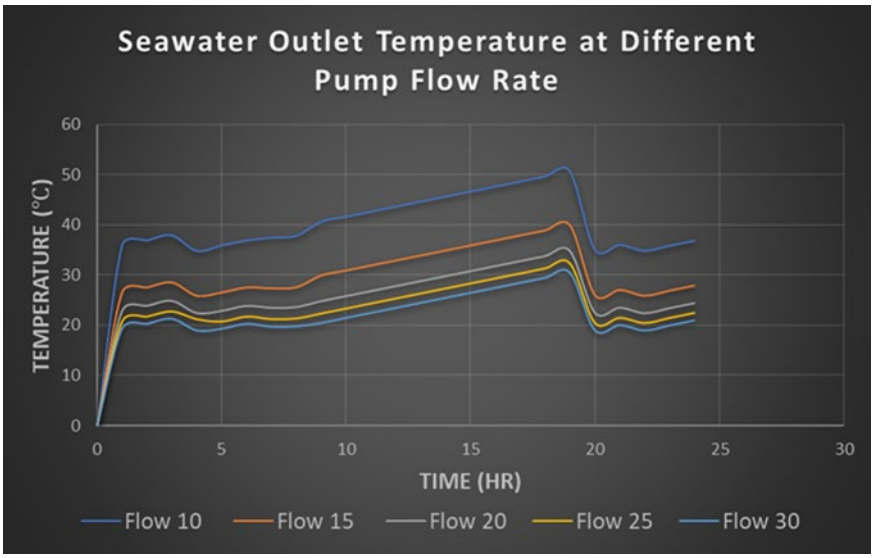

Figure 52: *Seawater outlet temperature at varying pump flow rates – System 1*

Figure 52 showcases the relationship between seawater outlet temperature and pump flow rate. As the flow rate decreases, the seawater spends more time in the condenser, absorbing more heat and exiting at a higher temperature. This is a testament to the efficiency of the heat transfer process in the condenser. However, this relationship also poses a potential risk to the condenser. If the seawater outlet temperature becomes too high due to a low flow rate, it could damage the condenser over time due to thermal stresses. It's essential to strike a balance as lower flow rates also increase pump power, potentially affecting the system's COP. Therefore, while the outlet temperature might not be of primary concern as the seawater is discharged back into the sea, it's still a crucial factor to consider.

Table 17: *Daily parameters comparison at different pump flow rates – System 1 (summer daily load profile)*

Parameters	**Pump Flow Rate (kg/s)**				
	10	**15**	**20**	**25**	**30**
Energy consumed per day (kWh)	7073	5261	4584	4806	4893
Typical seawater outlet temperature (°C)	41	31	26	24	22
Typical COP (Refrigeration)	2.63	3.61	4.02	3.83	3.78

4.1.4 System visualization using DaVE

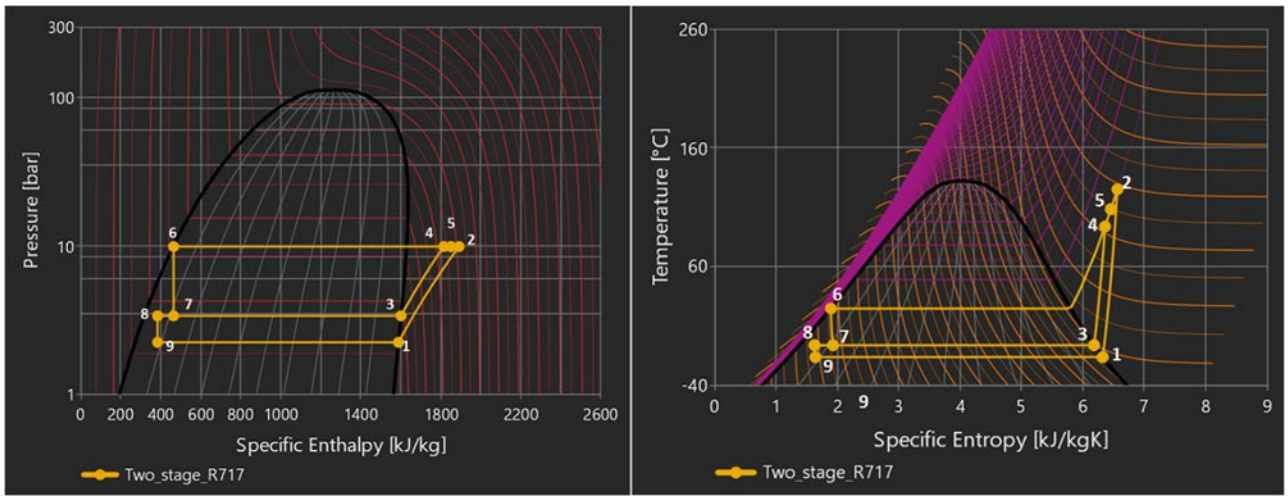

Figure 53: *Thermodynamic state analysis of the R717 system: P-h (left) and T-s (right) diagrams.*

The visual representation of the Dymola simulation results was achieved using the DaVE tool, which offers a detailed view of the prevailing temperature and pressure conditions in the system. Notably, state points 6 and 8 in the system emerge as areas of concern. At state point 8, the refrigerant leaving liquid separator 1 is anticipated to be in a fully saturated liquid state. However, observations from the simulation may suggest otherwise, indicating a potential issue with the operation or performance of liquid separator 1 or the upstream components that could be causing this discrepancy.

Simultaneously, at state point 6 in the condenser, the refrigerant is expected to undergo subcooling due to the influx of seawater. Yet, the data might be suggesting that the anticipated level of subcooling is not being achieved. This could point to possible inefficiencies in the heat exchange process within the condenser, or perhaps an issue with the seawater's temperature or flow rate. A detailed exploration of these identified issues is presented in Section 4.1

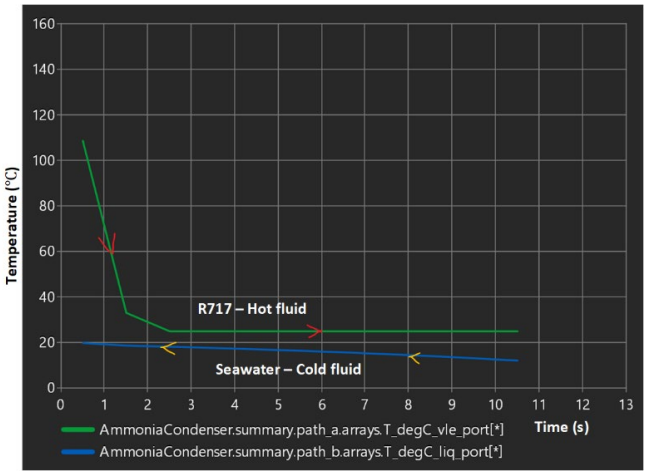

Figure 54: *Depiction of counterflow heat exchange mechanism in the condenser: hot refrigerant interacting with the cold seawater.*

4.2 System 2

4.2.1 Static simulations

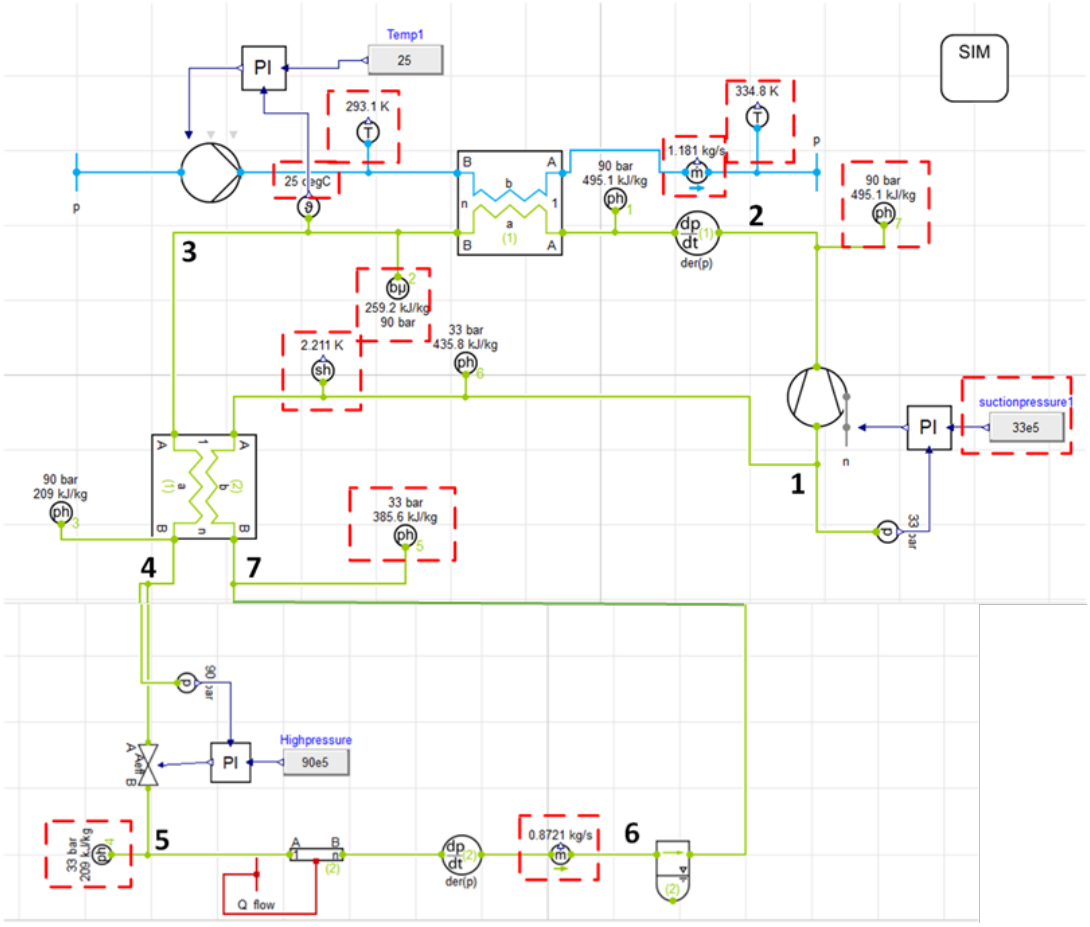

Figure 55: *Results obtained from the static simulation of the R744 RSW system.*

As previously stated, the cooling loads on the evaporator tube and the heating load on the gas cooler were key inputs for the system. The high side pressure was measured at 90 bar, and the mass flow into the compressor was calculated by the evaporator heat load. With an enthalpy of 495.1 kJ/kg, the refrigerant entered the gas cooler and began rejecting heat at the gliding temperature. It was then subcooled further to state 3 with an enthalpy of 259.2 kJ/kg. The rejected heat was absorbed at an entrance water temperature of 20°C from the 70HS, resulting in a return water temperature of 62°C.

A PI controller connected to the pump regulated the water mass flow rate, aiming for a CO_2 gas cooler outlet temperature of 25°C with a specified water mass flow rate of 1.18 kg/s. The working fluid then entered the internal heat exchanger (upper side), where heat was transferred to the refrigerant entering the suction line of the compressor. This subcooled the refrigerant further to state 4 with an enthalpy of 209 kJ/kg. Further throttling occurred at state point 5, maintaining the enthalpy constant due to isenthalpic expansion.

Table 18: *Key performance indicators obtained from the static simulations of the R744 system*

Parameters (units)	**Dymola**
$\dot{Q}_{GC}$ (kW)	205.77
$\dot{Q}_{IHX}$ (kW)	43.73
$\dot{m}_c$ (kg/s)	0.873
$\dot{m}_w$ (kg/s)	1.182
$\dot{W}_C$ (kW)	51.77
$\dot{W}_{Pu2}$ (kW)	0.0169
Suction pressure (bar)	33
Discharge pressure (bar)	90
Pressure ratio	2.73
$COP_{R744\ HP}$	3.97
Electricity consumed in a day – 23hrs (kWh)	1191

The heat load was provided by the 154kW evaporator capacity, which caused the CO_2 to evapourate at a constant temperature of -2°C and reach state point 6 with an enthalpy of 385.6 kJ/kg. The fluid gathered in the liquid receiver, but only the gas part made it to state point 7 at the suction side of the IHX. The major goal was to superheat the refrigerant, absorbing the heat lost during top-side flow and attaining state point 1. The actual superheat was 2.2K greater than projected. Finally, the compressor squeezed the superheated refrigerant to state point 2.

4.2.2 Dynamic simulations

4.2.2.1 Dynamic discharge pressure - maximum and average load

As previously stated, the analysis considered four load cases: average and peak load for both summer and winter conditions.

	Max (kW)	Average (kW)
Summer	435	257
Winter	194	154

It is possible to get insights into the system's behaviour under varied amounts of demand by monitoring the transient pressure under certain load scenarios. For each load situation, the pressure variations, reaction time, and system stability may be evaluated and assessed.

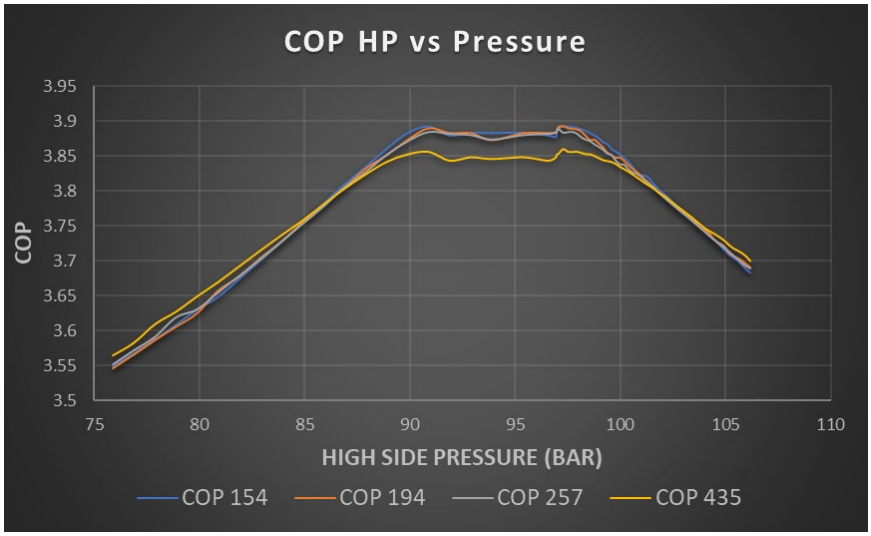

Figure 56: *Variation of COP with pressure for each load case*

It is important to note that the discharge pressure range was from 75 to 106 bar. Throughout the simulations, one critical limitation was maintained: the necessity to produce hot water at a temperature of 70°C. Analysing **Figure 56** reveals that 95-97 bar is the ideal discharge pressure for the system to work properly and successfully. Within the pressure range of 90 to 97 bar, the COP stabilizes. This means that the system achieves an optimal mix of energy efficiency and performance within this range. The stabilizing trend suggests that further increasing the pressure may not significantly improve the COP, and other factors should be considered for system optimization.

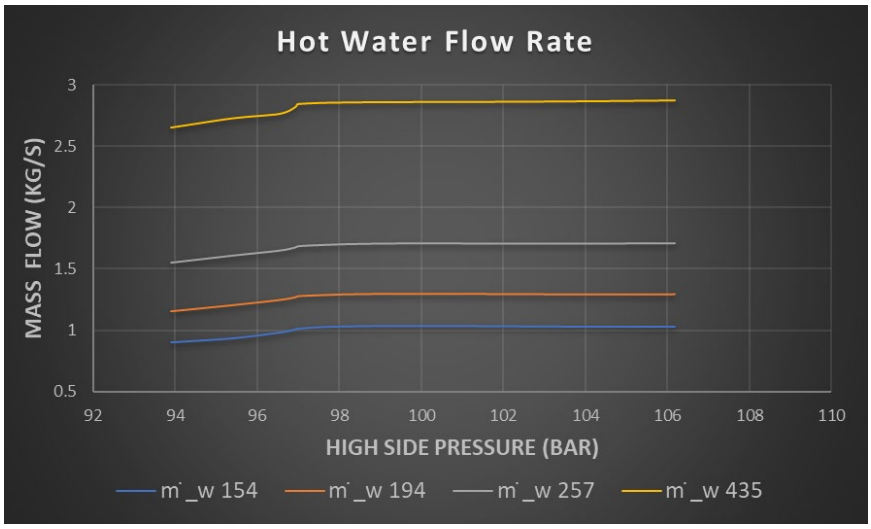

Figure 57: *Hot water production rate variation with pressure*

At pressures lower than 93 bar, the system had severe difficulties in producing 70°C water. The compressor and pumps had negative values, suggesting that they were unable to satisfy the load requirement properly. **Figure 57** shows that raising the system pressure results in increased hot water output. This is due to the higher load on the evaporator side, which produces a bigger mass of hot water. However, the trade-offs associated with increasing

pressures must be considered. As the pressure increases, the COP of the system lowers, and there is more stress and strain, thereby limiting component lifespan, and so on.

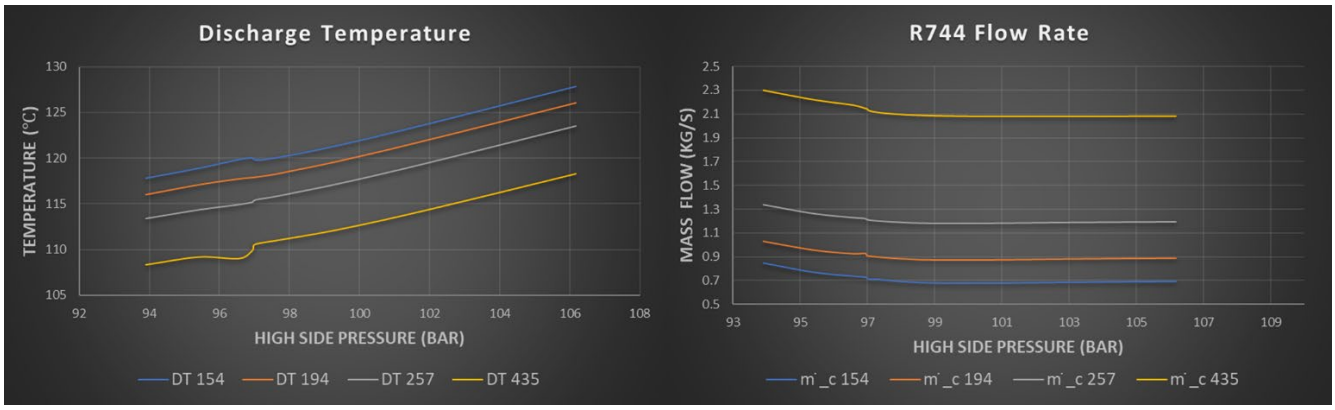

Figure 58: *Compressor discharge temperature (left) and refrigerant flow rate variation (right) with respect to the pressure increase.*

Figure 58 on the left shows that the discharge temperature rises in direct proportion to the pressure. This discovery is consistent with the system's predicted behaviour. These findings are critical since they provide significant insights into the complex relationship between pressure and discharge temperature. Surprisingly, the discharge temperature is highest in the lowest load condition. This unanticipated development might be attributable to operational factors and system dynamics. It is also evident from the graph on the right that the highest load case corresponds to the highest mass flow rate, indicating a direct relationship between the load demand and the refrigerant flow. As the pressure increases, the mass flow rate gradually stabilizes, reaching a plateau after reaching 97 bars. This stabilization suggests that the desired hot water output has been achieved, and further pressure increase does not significantly impact the mass flow rate.

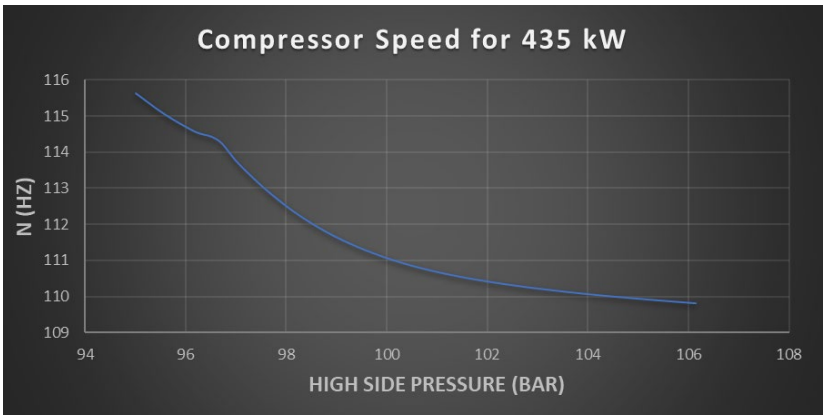

Figure 59: *Variation of compressor frequency with pressure*

Figure 59 depicts the inverse connection that exists between pressure and the compressor's operational parameters. When the pressure is high, the compressor has to use more energy to overcome the higher resistance and keep the ideal pressure levels. As a result, the compressor's speed is reduced to guarantee efficient functioning. The reduction in

compressor speed aids in optimizing the rate of work input into the compressor, ensuring that it performs within the parameters that were specified. It underscores the need for precise control systems that can adapt the compressor speed in response to varying pressure conditions.

4.2.2.2 Seasonal operation – summer and winter

Following extensive simulations (4.2.2.1) with dynamically fluctuating pressures, it was established the best discharge pressure for summer operation is 97 bar, whereas the best pressure for winter operation is 95 bar. This significant finding has a practical implication for the simulation process, as it allows for a more streamlined approach by focusing solely on the specific pressure point that yields the best performance.

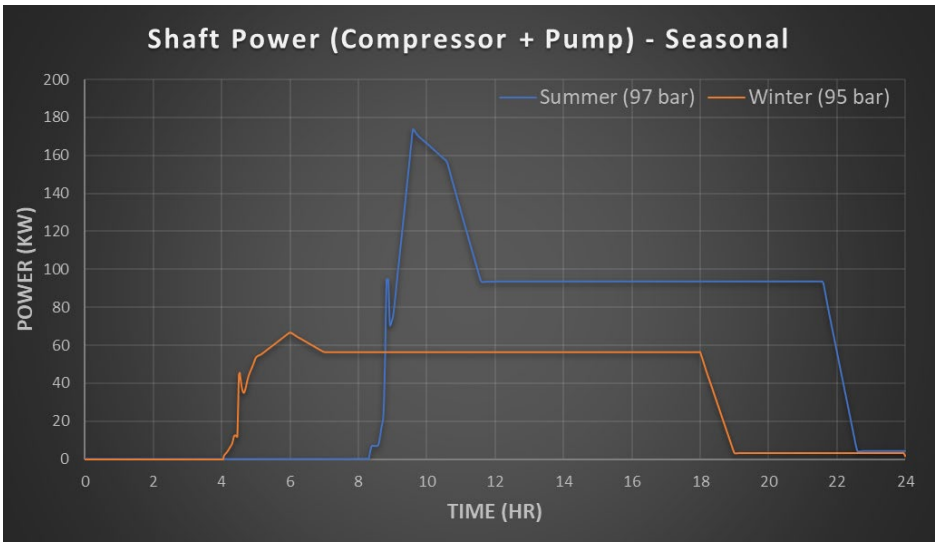

Figure 60: *Shaft power vs Time during summer and winter (System 2)*

Figure 60 and **Figure 61** demonstrates the change in shaft power and gas cooler heat flow during the summer and winter season. Both parameters display a similar pattern of fluctuations, which can be traced to the system's seasonal load profile. The observed similarity in the variable pattern of shaft power and gas cooler heat flow can be attributed to their mutual dependency. The cooling requirement rises as the system load rises, necessitating the compressor to work harder and consume more electricity. As a result, the gas cooler must dissipate more heat to maintain the desired temperature levels. The heat flow in the gas cooler is closely tied to the cooling load and the temperature difference between the refrigerant and the cooling medium.

Higher values in the summer emphasize the system's ability to manage increased cooling needs, while lower values in the winter demonstrate the system's adaptability to decreased cooling loads. These observations highlight the system's response to changing seasonal conditions and its capacity to successfully meet cooling demands while remaining efficient.

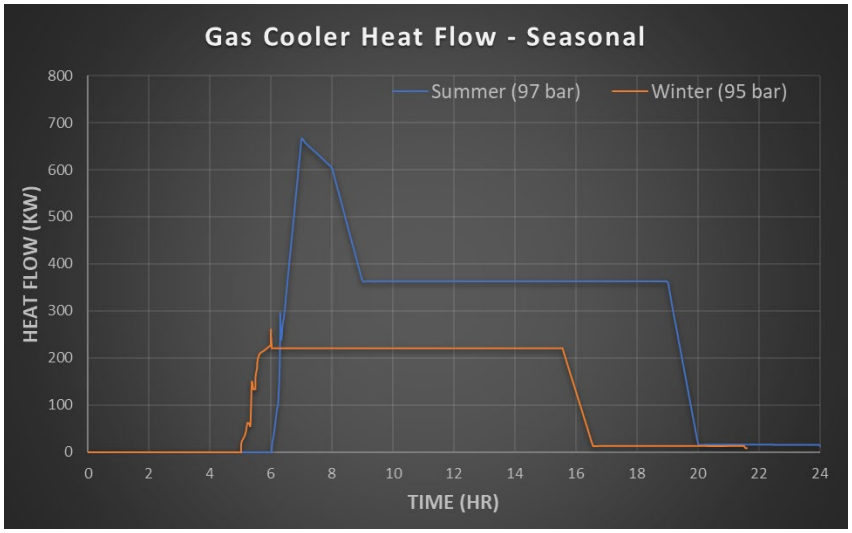

Figure 61: *Gas cooler heat flow vs Time during summer and winter (System 2)*

Understanding the relationship between shaft power and gas cooler heat flow is crucial for optimizing system performance and energy efficiency.

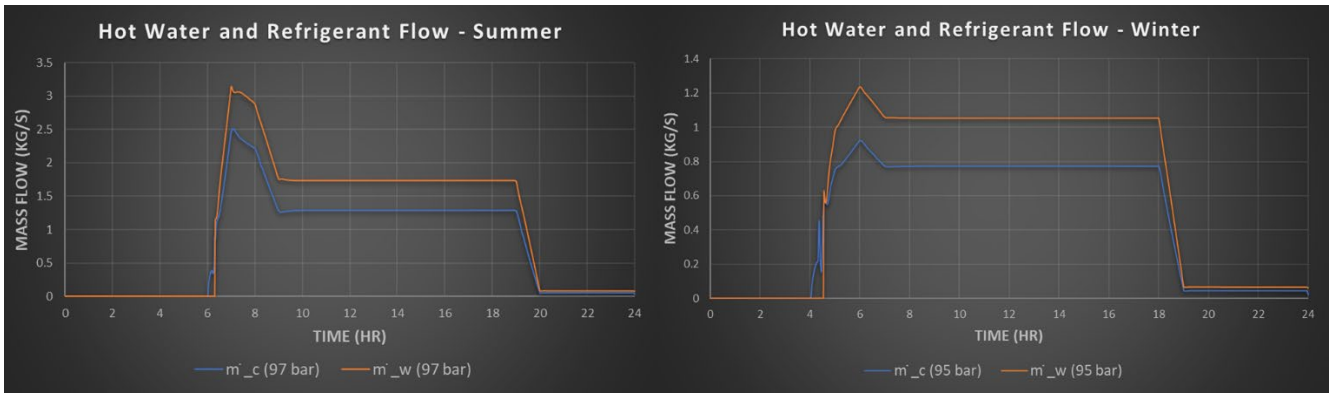

Figure 62: *Hot water and refrigerant flow vs Time for summer (left) and winter (right) – System 2*

Figure 62 shows that both parameters have a synchronized pattern of variation as the produced hot water follows a similar trend as the refrigerant mass flow, indicating that the system is running smoothly by appropriately adjusting the mass flow rate to meet the heating demand. When heating demand rises, the system responds by increasing refrigerant mass flow to transfer more heat to the water, resulting in increased hot water production. When heating demand falls, the system reduces refrigerant mass flow to optimize energy consumption while still meeting the required heating load. The close alignment of produced hot water and refrigerant mass flow is due to the system's control approach, which assures a balanced and optimum functioning. To achieve the desired hot water output, the control system dynamically regulates the refrigerant mass flow rate.

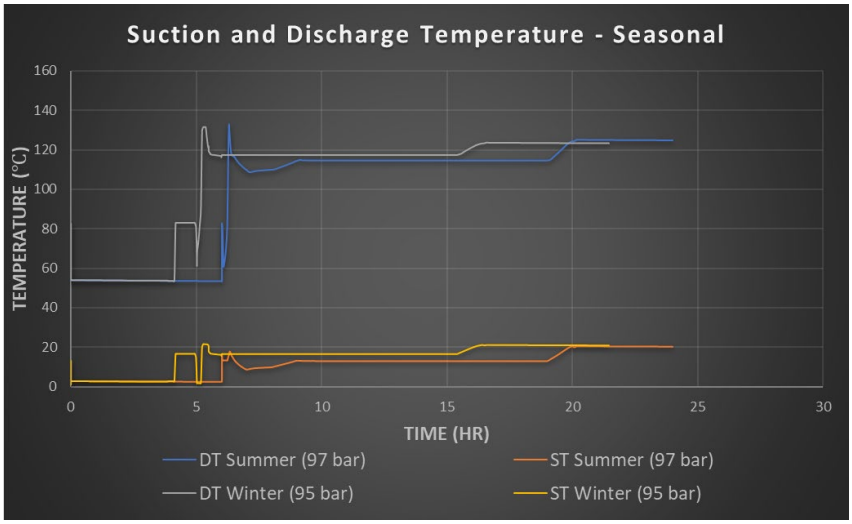

Figure 63: *Suction and discharge temperature vs time during summer and winter (System 2)*

Figure 63 depicts the compressor's capability in efficiently raising refrigerant temperatures as part of the heat transfer process. The ability of the compressor to maintain steady suction and discharge temperatures throughout the season reflects the system's design and control. This consistency allows a consistent heat transfer technique, eliminating variations and ensuring dependable operation.

Table 19: *Daily parameters comparison for summer and winter seasons – System 2*

Parameters (units)	Summer	Winter	Percentage difference (%)
Energy consumed per day (kWh)	1386	813	41.34
Gas cooler heat flow per day (kWh)	5359	3168	40.88
Hot water produced per day (litre)	95771	57720	39.73
Typical suction temperature (°C)	13	16.5	-26.92
Typical discharge temperature (°C)	114.7	117.4	-2.35
Discharge pressure (bar)	97	95	2.06
Typical superheating in IHX (°C)	13	17	-30.77
Pressure ratio	2.94	2.88	2.04
Seasonal COP of the HP	3.91	3.93	-0.51

4.2.2.3 Dynamic increase of required water temperature – winter daily load profile

The goal was to gradually raise the required hot water temperature and evaluate the system's effectiveness in providing water above 70°C with a maximum temperature of 90°C. The day began with a demand for hot water at 70°C (5 am – 8 am) in the morning, which quickly increased to 80°C (9 am – 4 pm) in the afternoon. The temperature requirement further increased to 90°C (5 pm – 12 am) in the evening. This scenario simulated the real-world volatility in hot water requirements throughout the day.

It is crucial to note that during the winter season, the system is turned on at 4:45 am, resulting in the start of water production at 5 am.

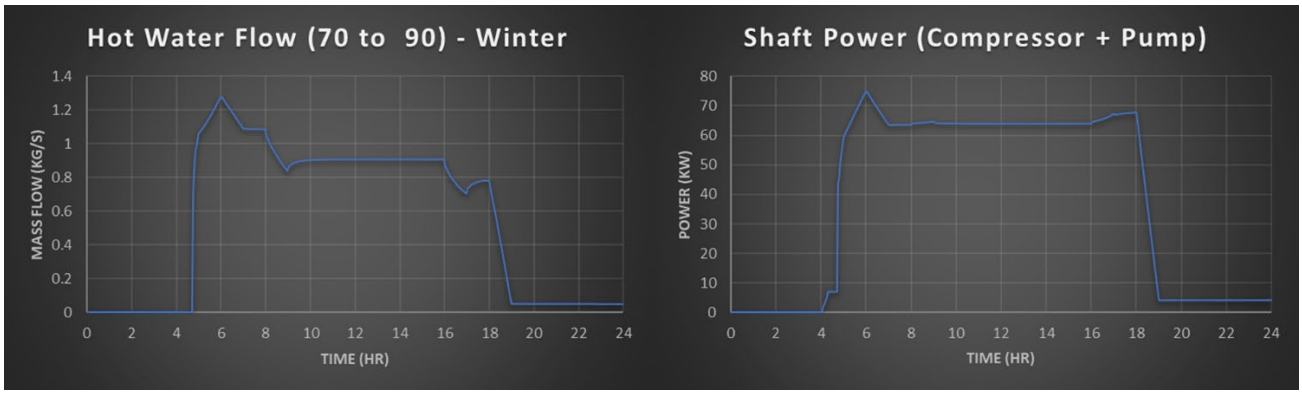

Figure 64: *Hot water flow (left) and power consumption (right) vs Time (70-90HW System 2)*

Figure 64 depicts the system's capacity to provide a continuous and dependable hot water supply throughout the day while efficiently adjusting to fluctuating temperature requirements. Another interesting aspect is the compressor's relatively consistent shaft power consumption. This indicates that the compressor adjusts well to shifting load needs while consuming minimal energy.

Table 20: *Variation of parameters with water outlet temperature during winter*

Parameters (units)	Water Outlet Temperature		
	70 °C (5am – 8 am)	80 °C (9am – 4pm)	90 °C (5pm – 12am)
Hot water produced (litre)	15802	25673	10019
Energy consumed (kWh)	213	498	181
COP	3.59	3.56	3.46

4.2.3 System visualization using DaVE

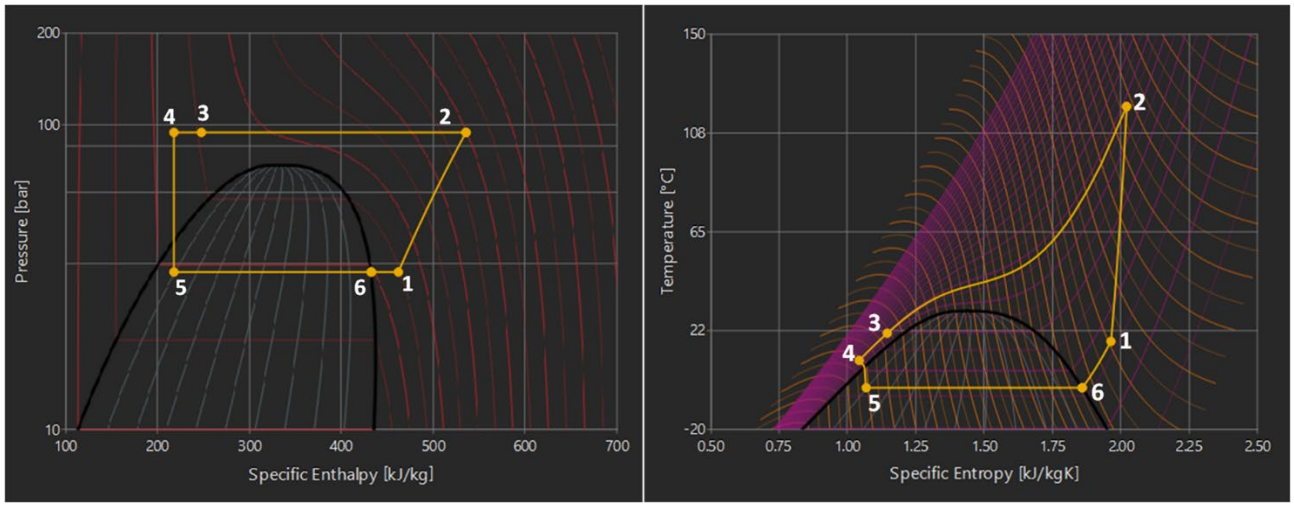

Figure 65: *P-h (left) and T-s (right) diagram - thermodynamic behaviour of the R744 system during winter.*

Figure 65 represents the optimal performance of the transcritical R744 heat pump throughout the winter season. During the heat transfer process, the refrigerant passes through a transcritical cycle, where it encounters both subcritical and supercritical states. An internal heat exchanger is noticeable in the system. The diagram shows amazing heat transfer in the internal heat exchanger, as demonstrated by substantial refrigerant superheating and subcooling. The p-h diagram of the system reflects the liquid separator's successful operation. It demonstrates that the refrigerant entering the IHX is in a gaseous condition, showing that the liquid separator properly separated the liquid phase from the refrigerant stream. This is significant because putting liquid refrigerant into the IHX might result in problems such as decreased heat transfer efficiency, higher pressure drops, and potential damage to the downstream components.

The t-s graphic shows that R744 remains supercritical as it flows through the system during the heat rejection phase. Condensation does not occur in the R744 heat pump cycle, unlike usual heat pump cycles employing refrigerants such as Freon. The lack of phase change eliminates the risk of refrigerant leakage due to condensate formation. However, the heat transfer coefficients and specific heat capacity of R744 can vary significantly in the supercritical region.

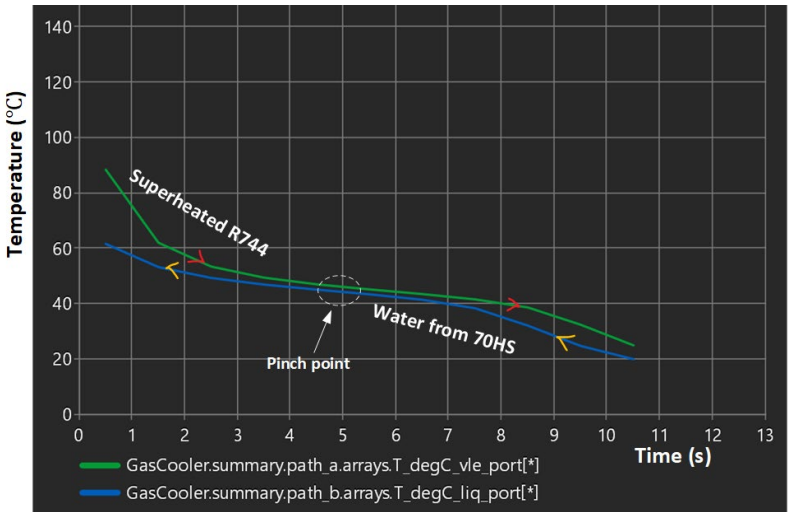

Figure 66: *Temperature glide inside the gas cooler (pinch point indicated)*

The graph in Figure 66 above depicts an important phenomenon known as the pinch point. The occurrence of a pinch point in a water-cooled CO_2 gas cooler is predicted due to the large nonlinear fluctuation of supercritical CO_2's specific heat capacity with temperature.

4.3 Electricity consumption – System 1 and System 2

Building upon the insights provided in section 3.6 and the key factors outlined in **Table 13**, the annual electricity consumption for both System 1 and System 2 was determined by using equation 3.13.

Table 21: *Seasonal and annual energy costs for System 1*

Key Findings	Summer	Winter
Operational days per year	96	135
Energy consumed per day (kWh)	4633	3664
Energy Cost (NOK)	221,050	245,836
Annual energy cost of system 1	**466,886 NOK**	

Table 22: *Seasonal and annual energy costs for System 2*

Key Findings	Summer	Winter
Operational days per year	96	135
Energy consumed per day (kWh)	1386	813
Energy Cost (NOK)	66,129	54,548
Annual energy cost of system 2	**120,677 NOK**	

Table 21 and **Table 22** depict the annual energy costs for System 1 and System 2 respectively. Hence, the total annual energy cost for the SPP stands at **587,563 NOK**. It's crucial to note that this cost is an aggregation of the costs associated with both systems only.

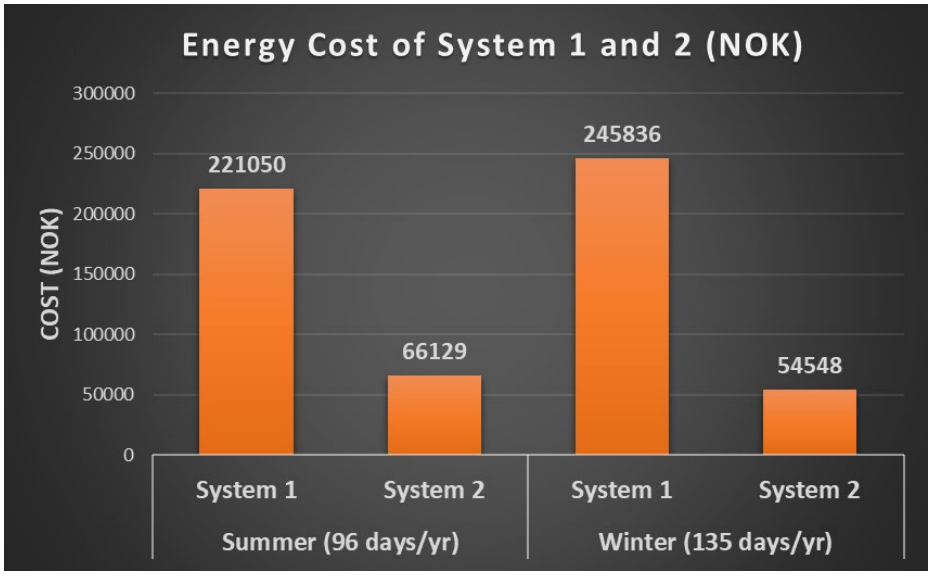

Figure 67: *Comparison of the seasonal energy costs associated with System 1 and System 2.*

Chapter 5: Discussion

This chapter is dedicated to analysing and interpreting the results obtained from the modelling and simulation of both systems. By examining these results in detail, we can gain a deeper understanding of the systems' behaviour and uncover valuable insights. This analysis is essential for evaluating system performance, identifying areas for improvement, and contributing to the existing knowledge in the field of refrigeration systems.

5.1 System 1 – Two stage parallel compression (R717)

- The representation of liquid separators 1 and 2 in the simulation model has presented notable challenges. It is a fundamental principle of flooded evaporators that a specific volume of liquid refrigerant should always be available to meet the cooling requirement at any given moment. In the simulation model, however, this principle was not adhered to, leading to a division of the total charge of refrigerant entering Separator 1 between the HP compressor and Separator 2. In **Figure 53**, the refrigerant moving towards the state point is not fully saturated. This issue arises from the control of the PI controller over the area of Expansion Valve 2 (**Figure 32**). In an ideal situation, the desired input signal should be the mid-pressure level (3.412 bar). However, due to constraints in time, an enthalpy value based on theoretical simulations was used, which may not accurately reflect actual system behaviour. Separator 2 encounters a similar issue. Ideally, the entire refrigerant entering the receiver should be saturated after catering to a cooling demand and then be drawn out by the LP compressor in the simulation model. This would ensure the operation of a flooded evaporator, while also increasing the power consumption of the LP compressor. Interestingly, if the LP compressor only removed a portion of the refrigerant (flash gas), it could potentially be under less strain and therefore have a longer lifespan. These findings underscore the importance of accurate system component representation in simulation models. Any inconsistencies could lead to unintended consequences, as seen in this case (S., 2011).

- The irregularities in **Figure 45**, particularly in the critical range of 7-10 bar, suggest the presence of system inefficiencies or control challenges that could impair the system's cooling performance and escalate energy consumption. At around 11 bars, the system appears to attain some stability, indicating this pressure level could potentially serve as a more optimal operating point. However, the periodic disruptions that persist even at this level suggest intermittent stability issues within the system.
    a) These disruptions could be the inability of either the HP or LP compressor to maintain a consistent speed. This inconsistency might lead to fluctuations in the pressure and subsequent variations in the COP. This observation provides a valuable direction for future investigations. By focusing on compressor speed control, it might be possible to reduce these COP fluctuations, increase system

stability, and optimize performance. Lin et al., 2019 developed an optimization control strategy for HVAC systems with a focus on energy conservation.

- Upon analysing **Figure 46**, fluctuations in power consumption patterns, which are contingent on high-side pressure variations, indicate that the HP compressor struggles to maintain an optimal rotational speed. Talib and Nassif, 2021 introduced an innovative two-level optimization approach aimed at reducing total energy consumption. Several factors might be responsible for this observed inconsistency:
    a) There could be mechanical inefficiencies inherent to the compressor. These could be due to the wear and tear of components over time, or possibly design limitations that restrict optimal performance.
    b) The control system managing the compressor's operation might be encountering challenges. This could include issues with the programming or control logic that regulates the compressor's function.
    c) Operational variables not considered in the current study might be influencing the compressor's performance.

  These irregularities in the HP compressor's operation could negatively impact the overall energy efficiency and reliability of the system. Therefore, further investigation is needed to pinpoint the causes and develop appropriate solutions.

- The behaviour in **Figure 47** aligns with the understanding that a higher-pressure ratio leads to an increased workload on the compressor, and consequently, a rise in the discharge temperature of the refrigerant. This is a common occurrence as high pressure requires more work from the compressor, leading to increased electrical consumption and added heat energy. School, 2019 proves that the higher the pressure, the higher the temperature due to the basic physics of pressure and temperature relationships.
    a) The HP compressor shows a slower increase in discharge temperature with pressure compared to the LP compressor. This could suggest that the HP compressor is operating at a higher workload, leading to potentially higher internal losses. High discharge temperatures, if not carefully managed, can induce a variety of issues such as oil breakdown, motor insulation failure, and excessive wear on compressor components. As such, close monitoring of these temperatures is crucial for system reliability and efficiency.
    b) School, 2019 found that if the discharge temperature, as measured at the compressor, surpasses 225°, it is an indication of a problem, as temperatures at this level can cause the oil to break down. Additionally, high discharge temperatures can be a result of various factors such as low refrigerant charge, severe overcharge, low condenser airflow, restrictions in the system, and low mass flow rate due to high suction temperature or restrictions in the system.

- Simulation 4.1.3.2 proves the adaptability of system 1. It is a crucial aspect in terms of maintaining balanced load distribution between separators. Throughout the year, the system dynamically adjusts its operations to cater to varying environmental conditions and user demands. This adaptability serves as a testament to the system's resilience and robustness, allowing it to sustain its performance under various circumstances. To optimize performance and energy efficiency, temperature management systems can employ a host of strategies (Lin et al., 2019):
    a) The best strategy – involves the deployment of a dynamic temperature setting for the fan coil unit. This strategy allows for adjustments to the FCU temperature in harmony with changes in outdoor temperature, ensuring that the indoor thermal comfort of occupants is maintained. Alongside this, a genetic algorithm can be employed, serving to calculate the minimum energy consumption for the temperature management system. The algorithm is capable of determining the operating frequency of the pump that corresponds to the minimum energy consumption.

  Despite the insights gained from existing research, there remains a need to further investigate the specific role of individual separators in maintaining the balance of load distribution.

- The power consumption of refrigeration systems in relation to pump flow rates is a complex issue that is influenced by a variety of factors. These variables help to explain the complicated relationship depicted in **Figure 51**.
    a) Pump Efficiency – The efficiency of a pump fluctuates across different operational points. It is plausible that systems may display lower power consumption at reduced flow rates if the pump exhibits heightened efficiency under these conditions (Papa et al., 2015).
    b) Total Thermal Load – that the refrigeration system is required to manage can significantly impact its power consumption. An increased pump flow rate escalates the thermal load, potentially resulting in augmented power usage (KATIPAMULA and LU, 2006).
    c) Component Characteristics: The attributes of the other components in the refrigeration system, such as the compressor and evaporator, can profoundly influence power consumption. An elevated flow rate may increase the power demanded by these components to manage the heightened refrigerant flow, consequently boosting overall power consumption.

- As the flow rate diminishes, the seawater remains longer in the condenser, gaining additional heat and consequently exiting at an elevated temperature. **Figure 52** underscores the efficiency of the heat transfer process within the condenser. However, there are many implications of this inverse relationship (Liu et al., 2022):

a) The efficient heat transfer, implied by the heightened outlet temperature at lower flow rates, validates the system's heat rejection capabilities. The system manages to offload a significant portion of its thermal load into the seawater, thereby maintaining the cooling process's effectiveness.
b) The elevated outlet temperature hints at the possibility of the condenser encountering heightened thermal stress. The concern here lies with the material integrity of the condenser. Excessive heat could induce thermal expansion and contraction cycles in the condenser's material, potentially leading to mechanical fatigue over time (Llopis et al., 2008).
c) Lower flow rates might increase the pump's power requirements, thereby compromising the system's overall COP. Hence, even though the seawater is eventually discharged back into the environment, its outlet temperature serves as an indirect indicator of performance aspects.

5.2 System 2 – RSW heat pump (R744)

- Section 4.2.1 and **Figure 66** show the proficient heat exchange process of System 2's gas cooler, demonstrating its effectiveness even while operating at maximum capacity. The incoming water at 70HS undergoes significant heating, underscoring the efficiency of the heat transmission between the two interacting fluids. The system is presently governed by a control strategy reliant on the desired water outlet temperature. The effectiveness of this control strategy is further evidenced by the rapid stabilization of the PI controller, demonstrating the successful tuning of the controller. This indicates a finely tuned control system that contributes to the stability and reliability of System 2's operation. However, the fast stabilization should not preclude the exploration of alternative control strategies aimed at further optimizing the system's performance. Raman et al., 2020 investigated the use of a Model Predictive Control (MPC) strategy for improving the energy efficiency of HVAC systems. MPC is a control strategy that uses a model of the system to predict its future behaviour and uses this prediction to optimize system performance.

- **Figure 66** also provides some exploration of the heat transfer dynamics within the gas cooler of System 2. The pinch point (at 45°C), a characteristic feature in heat exchange processes involving supercritical fluids, is significant as it demarcates the narrowest gap between the hot and cold fluid's temperature profiles, thereby dictating the effectiveness of heat transfer. The pinch-point phenomenon also poses a challenge. The heat transfer process can be severely limited by the pinch point, constraining the overall system performance. This constraint can lead to a lower-than-desired outlet water temperature, causing the system to miss its primary objective: heating the water to a specific temperature. Ladislav et al., 2016 provide a comprehensive analysis of the pinch point

phenomenon in systems utilizing supercritical CO_2. The research offers valuable insights into how to best manage the pinch point in the context of System 2's gas cooler.

- The IHX in the suction line of system 2 is crucial in enhancing the system's performance. The exceptionally high degree of superheat (10-14K) observed in both summer and winter seasons (**Table 19**) could be attributed to the efficient heat transfer properties of CO_2, coupled with an effective IHX design. Boewe et al., 2001 explored the role of the IHX in augmenting the performance of a transcritical R744 heat pump. The study found:
    a) A significant correlation between the integration of the IHX and the enhancement of the system's performance. When an IHX was incorporated, the heat pump's efficiency witnessed an impressive increase of up to 25%.
    b) The performance boost was particularly pronounced when the heat pump was operating in idle mode under high ambient temperatures.
    c) In heat pump systems that don't incorporate an IHX, there is a substantial disparity between the pressures that optimize capacity and those that maximize efficiency.
    d) The IHX creates the potential for the implementation of simpler and less precise control systems and strategies. This is because it creates a more harmonious balance between capacity and efficiency, reducing the need for meticulous control over these parameters.
    e) Counterflow IHX was compared with a parallel IHX. The counterflow arrangement was superior in enhancing the heat pump's performance. This outcome was in line with expectations, as the counterflow design is generally more efficient due to its ability to maximize the temperature gradient between the two fluids involved in the heat exchange process.

- As shown in **Figure 57**, increasing the system pressure enables a larger output of hot water due to the increased load on the evaporator. However, due to potential trade-offs, raising pressure levels should be approached with prudence. Notably, the system's COP drops as pressure is increased. This signal decreased energy efficiency, which may result in increased long-term operational expenses. Lee et al., 2020 conducted a study on heat pump systems with high-pressure side chillers. They found that under certain conditions, increasing pressure and compressor speed could lead to a decrease in system efficiency by 16.4% on average. However, the cooling capacity increased by 8.0% on average, indicating a trade-off between efficiency and capacity. Furthermore, higher pressures can put excessive stress on the system components, potentially reducing their lifespan.

- **Figure 59** shows the inverse relationship between pressure and compressor operation but it is important to highlight that high pressure can lead to increased energy demand on the compressor.

a) Choi et al., 2021 studied the effects of compressor frequency on the dynamic performance of heat pumps and concluded that he performance of a compressor is usually defined by curves of delivery pressure against mass flow rate for various fixed values of rotational speed and inlet temperature. This underscores the importance of precise control systems that can adjust compressor speed in response to varying pressure conditions to optimize the rate of work input into the compressor.
b) Ge and Tassou, 2011 investigated the potential consequences of excessive discharge pressure in a heat pump. These issues include air contamination in the refrigerant system, blocked air flow, clogged filters, and contaminants on the compressor valves, among others. Each of these can impact the compressor's operational parameters and the overall system performance in different ways.

- **Figure 62** is evidence that the system's 2 control approach plays a crucial role in maintaining the balance between the refrigerant mass flow and the produced hot water. The synchronized pattern of variation between these two parameters is a clear indication of the system's efficiency in dynamically adjusting to the heating demand. Smitt et al., 2020 studied an integrated R744 heat pump to produce hot water for hotels. The synchronisation can be attributed to various factors:
  a) Thermodynamic properties of R744 (2.1.4.3) – due to its high specific heat capacity and latent heat can absorb and transfer more heat, leading to increased hot water production. As the heating demand rises, the system responds by increasing the mass flow rate of the refrigerant, which has a high capacity for heat transfer, resulting in increased hot water production.
  b) Efficient heat exchanger design – An efficient heat exchanger allows for optimal heat transfer between the refrigerant and the water. When the heating demand increases, the heat exchanger facilitates the transfer of more heat from the refrigerant to the water (Junqi et al., 2021).
  c) System's load matching capability – Fahlén, 2012 study on the role of control systems in R744 heat pumps underscores the importance of a well-tuned control system in managing the dynamic adjustments of the refrigerant mass flow rate. System 2's controllers are finely tuned to respond to changes in heating demand, ensuring that the system can dynamically adjust the refrigerant mass flow rate as needed.

- Based on the findings from Muhssin et al., 2018 and Artuso et al., 2021, the significance of dynamic adjustment capability (demonstrated by System 2 - 4.2.2.2) can be articulated as follows:
  a) Energy use optimization – dynamic adjustment allows the system to modulate the refrigerant mass flow rate in response to real-time heating demand. This ability

ensures that the system operates at peak efficiency, minimizing energy waste and reducing operational costs.

b) Responsiveness to load changes – the capacity to dynamically adjust to changes in heating demand ensures that the system can promptly and accurately meet varying heating needs. This responsiveness contributes to maintaining a consistent and comfortable environment.

c) System reliability and longevity – By enabling the system to operate within its optimal range, dynamic adjustment enhances system reliability. It helps prevent potential issues related to overheating or underheating, thereby extending the system's lifespan.

d) Versatility – A well-tuned control system can adapt to varying conditions, making the system more versatile. Whether the heating demand increases due to colder weather or decreases due to energy conservation measures, the control system can adjust the refrigerant mass flow rate, accordingly, ensuring that the system continues to operate effectively.

- Section 4.2.2.3 depicts system 2's fantastic capacity to overcome the challenge of meeting fluctuating hot water demands, especially in a scenario where the temperature requirement increases over the course of a day, is a complex one. System 2 being a simulation model indicates that further research and analysis are required to understand the feasibility of implementing such a system in the real world to address the complex issue of fluctuating temperature demands. To gain insights into the existing systems available a literature review was conducted on several types of boilers. Since boilers are not in the scope of this thesis, the review can be articulated as follows (Miura, 2022):

  a) There are several types of boiler systems that can potentially meet these demands, including fire tube boilers, modular water tube boilers, condensing boilers, and electric boilers.

  b) Fire tube boilers, the most common type, are less efficient at handling fluctuating loads due to the time it takes to produce steam and then cool down. They tend to have lower Annual Fuel Utilization Efficiency (AFUE) ratings, which is the ratio of how much heat transfers to the water versus how much goes out of the flue. Newer models of the fire tube design are more energy efficient, averaging AFUE ratings around 80% or higher.

  c) Modular water tube boilers can convert water to steam more quickly, consuming less fuel in the process while typically achieving an AFUE rating of 83-85%. Their design allows the pipes to expand and contract freely in response to the cold water inside and the heat outside without the risk of thermal shock.

  d) Condensing boilers can reuse the heat from the flue gases to heat the cold water, thus saving energy. They typically have AFUE ratings between 85-95%.

Chapter 6: Conclusion

The research involved exploration and analysis of the diverse energy systems deployed in multiple stages of onshore salmon processing. The systems were systematically studied based on their functional roles. This in-depth investigation was ultimately aimed at understanding the nuanced heating and cooling demands unique to each system and developing a temperature management system to effectively address these requirements.

The main objective was to develop a simulation tool that can investigate various system configurations for similar industrial process plants based on realistic daily load profiles provided by PTG. Therefore, an actual SPP located in Northern Norway was selected and its load profiles encompass both heating and cooling demands during a typical day in the summer and winter months were obtained. Further, it led to the identification and exploration of two potential solutions. The first solution proposed a single heat pump system to fulfil all the requirements of the SPP. The second solution involved the deployment of two distinct systems: a two-stage parallel compression R717 refrigeration system and an R744 RSW system. Upon a thorough assessment of the advantages and disadvantages of each solution, the dual-system approach was chosen as the optimal choice. Both these systems were extensively analysed to comprehend their operation and mechanism. Subsequently, the systems were dissected into various sections for further investigation and designed and modelled using Dymola (using certain assumptions).

The simulation process in Dymola was divided into static and dynamic simulations. Static simulations gave a comprehensive understanding of the system's performance under various operating conditions. By inputting fixed parameters, the system's behaviour, efficiency, and feasibility were assessed. These simulations served as a foundation for the subsequent dynamic simulations. The initial dynamic simulations were run to find the optimal parameters such as high side pressure, etc and the models' control system and other components were carefully configured to meet the dynamically changing demands throughout the year.

System 1 (R717) exhibited a maximum cooling capacity of 890 kW. The high, medium, and low sides were set at 12 bar, 3.412 bar, and 2.26 bar respectively. Cold seawater was used to cool down the high-temperature refrigerant in the condenser. The system consumed **4633 kWh** on a typical summer day, whereas in winter, the energy consumption was slightly lower at **3664 kWh**. The annual energy cost associated with the operation of System 1 was calculated to be **466,886 NOK**. In the summer, System 1's SCOP was found to be **3.98** and, in the winter, the SCOP dropped to **3.22**.

System 2's (R744) pressure levels were maintained between 33 bar and 97 bar during the summer. The high-side pressure was slightly reduced to 95 bar during the winter season. These pressure adjustments were made to fulfil the requirement of providing hot water at 70°C. On analysing the energy consumption, it was found that the system utilized **1386 kWh** on an average summer day and **813 kWh** on a typical winter day. The system has the

capability to produce approximately **95,771 litres** of hot water on a typical summer day and **57,720 litres** on a typical winter day. The annual energy costs associated with the operation of the R744 system amounted to **120,677 NOK**. In the summer, System 2's SCOP was found to be **3.91** and, in the winter, the SCOP was **3.93**.

Following the acquisition and assessment of key performance indicators for both systems, specialized simulations were conducted that were tailored to each system's specific use case. These simulations were crucial in gaining a more nuanced understanding of the underlying physics that drive the performance of each system. Each set of results was meticulously examined and discussed to discern the intricate mechanisms that led to the observed outcomes. A comprehensive review of the existing literature was also carried out to further delve into the 'why' and 'how' behind these results. This approach allowed for a more thorough and insightful analysis.

It is crucial to acknowledge that these simulations were performed under specific assumptions and conditions. The real-world implementation of these systems might yield different results due to a variety of factors such as environmental conditions, equipment malfunctions, etc. The main objective of this study—to create a comprehensive simulation tool capable of investigating various system configurations—was successfully achieved. This tool will serve as a significant resource for PTG in their future efforts aimed at optimizing similar systems, underpinning informed decision-making and facilitating the development of more efficient, sustainable industrial processes.

Chapter 7: Further Work

Given the constraints of time and resources on this project, numerous topics and ideas were left unexplored. This chapter focuses on potential avenues for improvement and further investigation, most of which are extensions of the current work. These suggestions offer a roadmap for future research to build upon the foundation laid by this project.

- **System 1 - Two stage R717 refrigeration system.**
  a) Recreate the whole system within the simulation model, encompassing all three loops (Figure 32). This goes beyond simply setting the cooling load as input for the liquid separators, it involves directing the refrigerant appropriately into each individual loop. This enhancement would generate new obstacles, such as controlling the mass flow rate and managing the refrigerant's saturation level across each loop.
  b) Better modelling of the liquid separators is crucial. It's important to adhere to the principles of the flooded evaporator, ensuring that the separators always maintain a certain volume of refrigerant to satisfy the cooling needs.
  c) Enhancements to the control system are needed to better adapt to shifting dynamic loads. Enhancement of the management of suction and discharge pressures can be achieved by fine-tuning the HP and LP compressors.
  d) The system's design should be responsive, adjusting the pressure levels proactively to meet demand and not vice versa.
  e) The current system relies on seawater for cooling, but other methods of heat rejection could be explored. This could lead to more efficient operations and reduced environmental impact.
  f) Further comprehensive investigations are needed to discern the impact of an array of variables. These include the temperature of condensation, the flow rate of the sea water pump, the design and efficiency of the heat exchanger, the properties and volume of the refrigerant, the operating conditions of the compressors, etc. These investigations should be carried out using dynamic simulations that mimic the conditions of seasonal operations.
  g) The condenser currently expels a significant quantity of heat, resulting in a substantial waste of energy, much of which is cooled using seawater. Upon reflection, it's possible that the system proposed in Solution 1 (Figure 31) may indeed offer superior outcomes in terms of both cost-effectiveness and overall system performance. Therefore, detailed modelling and simulation of this system could be beneficial. This would allow a comparison of the two systems, potentially highlighting areas for efficiency gains and providing insights into alternative methods for heat management and energy use.

- **System 2 – Transcritical R744 heat pump**
  a) R744 heat pumps are the best choice when it comes to producing hot water due to a lot of favourable properties of the system. Though this study used R744, the exploration of other refrigerants could provide valuable insights into system performance and efficiency.
  b) An in-depth analysis of the relationship between compressor parameters and system efficiency could lead to significant improvements in system operation. A focus could be placed on varying discharge temperatures and the frequency of the compressor.
  c) Further investigation into the dynamic adjustment of pressure to meet varying loads could improve system efficiency and performance.
  d) Future research could explore the longevity of system components under various operating conditions and strategies for preventative maintenance.
  e) A detailed study of how varying temperatures of the incoming water, both on the gas cooler and evaporator sides, impact the COP and other key metrics of the system is necessary.
  f) Deep investigation whether the system can heat the incoming water from various systems to temperatures significantly higher than 70°C, potentially reaching 80°C, 90°C, or more. This may involve refining the control system to dynamically adjust the pressure levels based on the desired water temperature.

- **Common to both systems**
  a) While the study focused on system performance, future research could explore the longevity of system components under various operating conditions and strategies for preventative maintenance.
  b) The study focused on summer and winter conditions. However, the system's response to spring and autumn conditions and extreme weather events could be investigated.
  c) Future work could also explore how these temperature management systems could be integrated with renewable energy systems, such as solar or wind energy, to create a more sustainable and efficient energy solution.
  d) A detailed evaluation should be carried out to understand the financial implications of this system. This analysis should not only consider the initial investment costs of equipment but also the operational and maintenance expenses associated with running the system efficiently. Each component should be assessed for its cost and source, potentially leading the way towards real-world implementation.

Bibliography

Artuso, P., Tosato, G., Rossetti, A., Marinetti, S., Hafner, A., Banasiak, K., Minetto, S., 2021. Dynamic Modelling and Validation of an Air-to-Water Reversible R744 Heat Pump for High Energy Demand Buildings. Energies 2021, Vol. 14, Page 8238 14, 8238. https://doi.org/10.3390/EN14248238

ASHRAE, 2011. ASHRAE Position Document on Natural Refrigerants [WWW Document]. ASHRAE Position documents. URL https://www.epa.gov/greenchill/ashrae-position-document-natural-refrigerants

Ates, B., Widell, K.N., Nordtvedt, T.S., Cojocaru, A.L., 2017. Energy consumption for salmon slaughtering processes. Refrigeration Science and Technology 256–263. https://doi.org/10.18462/IIR.NH3-CO2.2017.0014

Automatic Heating, 2022. History of Heat Pumps [WWW Document]. URL https://www.automaticheating.com.au/complete-guide-to-heat-pumps/history-of-heat-pumps/ (accessed 12.14.22).

Badri, D., Toublanc, C., Rouaud, O., Havet, M., 2021. Review on frosting, defrosting and frost management techniques in industrial food freezers. Renewable and Sustainable Energy Reviews 151, 111545. https://doi.org/10.1016/j.rser.2021.111545

Bamigbetan, O., Eikevik, T.M., Nekså, P., Bantle, M., 2017. Review of vapour compression heat pumps for high temperature heating using natural working fluids. International Journal of Refrigeration 80, 197–211. https://doi.org/10.1016/J.IJREFRIG.2017.04.021

Bid-On-Equipment, 2016. Bid on Equipment | What's the Difference Between a Continuous and a Batch Freezer? [WWW Document]. URL https://www.bid-on-equipment.com/blog/post/what-s-the-difference-between-a-continuous-and-a-batch-freezer (accessed 5.26.23).

Bodys, J., Hafner, A., Banasiak, K., Smolka, J., Ladam, Y., 2018. Design and simulations of refrigerated sea water chillers with CO2 ejector pumps for marine applications in hot climates. Energy 161, 90–103. https://doi.org/10.1016/J.ENERGY.2018.07.126

Boewe, D.E., Bullard, C.W., Yin, J.M., Hrnjak, P.S., Boewe Bullard, D.C., Yin, J., Hrnjak, P., ASHRAE Member ASHRAE, M., 2001. Contribution of internal heat exchanger to transcritical R-744 cycle performance. HVAC and R Research 7, 155–168. https://doi.org/10.1080/10789669.2001.10391268

Bogh-Sorensen, Leif., 2006. Recommendations for the processing and handling of frozen foods 174.

Bolaji, B.O., 2020. Theoretical assessment of new low global warming potential refrigerant mixtures as eco-friendly alternatives in domestic refrigeration systems. Sci Afr 10. https://doi.org/10.1016/J.SCIAF.2020.E00632

Bravo, F., Durán, G., Lucena, A., Marenco, J., Morán, D., Weintraub, A., 2013. Mathematical models for optimizing production chain planning in salmon farming. International Transactions in Operational Research 20, 731–766. https://doi.org/10.1111/ITOR.12022

Brodal, E., Jackson, S., Eiksund, O., 2018. Transient model of an RSW system with CO2 refrigeration – A study of overall performance. International Journal of Refrigeration 86, 344–355. https://doi.org/10.1016/J.IJREFRIG.2017.11.002

Çengel, Y.A., Boles, M.A., 2008. Thermodynamics : an engineering approach 1018.

Chen, Y., Gu, J., 2005. The optimum high pressure for CO2 transcritical refrigeration systems with internal heat exchangers. International Journal of Refrigeration 28, 1238–1249. https://doi.org/10.1016/J.IJREFRIG.2005.08.009

Cho, H., Ryu, C., Kim, Y., 2007. Cooling performance of a variable speed CO2 cycle with an electronic expansion valve and internal heat exchanger. International Journal of Refrigeration 30, 664–671. https://doi.org/10.1016/J.IJREFRIG.2006.10.004

Choi, J.Y., Lee, D.C., Park, M.H., Lee, Y., Kim, Y., 2021. Effects of compressor frequency and heat exchanger geometry on dynamic performance characteristics of heat pump dryers. Energy 235, 121391. https://doi.org/10.1016/J.ENERGY.2021.121391

Coker, A.K., 2015. Refrigeration Systems. Ludwig's Applied Process Design for Chemical and Petrochemical Plants 623–727. https://doi.org/10.1016/B978-0-08-094242-1.00017-6

Colt, J., Summerfelt, S., Pfeiffer, T., Fivelstad, S., Rust, M., 2008. Energy and resource consumption of land-based Atlantic salmon smolt hatcheries in the Pacific Northwest (USA). Aquaculture 280, 94–108. https://doi.org/10.1016/J.AQUACULTURE.2008.05.014

Danfoss, 2018. HCFC and CFC phase out | Learn about sustainable energy | Danfoss [WWW Document]. URL https://www.danfoss.com/en/about-danfoss/our-businesses/cooling/refrigerants-and-energy-efficiency/hcfc-and-cfc-phase-out/ (accessed 12.2.22).

Danfoss, 2013. Cold storage room "what you need to know about refrigeration" – part 2 [WWW Document]. URL https://www.danfoss.com/en/service-and-support/case-stories/dcs/cold-storage-room-what-you-need-to-know-about-refrigeration-part-2/ (accessed 12.12.22).

Dempsey, P., Bansal, P., 2012. The art of air blast freezing: Design and efficiency considerations. Appl Therm Eng 41, 71–83. https://doi.org/10.1016/j.applthermaleng.2011.12.013

Dincer, I., Kanoglu, M., 2010. Refrigeration Systems and Applications, วารสารวิชาการมหาวิทยาลัยอีสเทิร์นเอเชีย.

Duarte, M. v., Pires, L.C., Silva, P.D., Gaspar, P.D., 2017. Experimental comparison between R409A and R437A performance in a heat pump unit. Open Engineering 7, 77–90. https://doi.org/10.1515/ENG-2017-0011

Eckert, M., Kauffeld, M., Siegismund, V., VDE Verlag, 2022. Natural Refrigerants: Applications and Practical Guidelines.

Eikevik, T. M., 2021a. Chapter 1 : Introduction Chapter 1 : Introduction. NTNU Heat Pumping Compendium 1–16.

Eikevik, Trygve M, 2021a. Chapter 4 : Working Fluids - TEP 4255 Heat Pumping Course 1–76.

Eikevik, T. M., 2021b. Chapter 2 One stage vapor compression cycle. NTNU Heat Pumping Compendium.

Eikevik, Trygve M, 2021b. Chilling , freezing and thawing equipment - TEP 4265 Compendium.

Eikevik, T. M., 2021c. Chapter 3 Thermodynamic Principles. NTNU Heat Pumping Compendium 1–45.

ENOVA, 2010. Enovas industriaktiviteter 2010.

ENOVA, 2009. Enovas industriaktiviteter – med resultater fra 2008.

ENOVA, 2008. Enovas industriaktiviteter - med resultater fra 2007.

EU Commission, 2021. Energy-intensive industries [WWW Document]. URL https://single-market-economy.ec.europa.eu/industry/strategy/energy-intensive-industries_en (accessed 6.8.23).

Fahlén, P., 2012. Capacity control of heat pumps [WWW Document]. URL https://www.rehva.eu/rehva-journal/chapter/capacity-control-of-heat-pumps (accessed 6.9.23).

Fellow, P.J., 2010. Freezing - TEP 4506 Compendium.

Feng, F., Zhang, Z., Liu, X., Liu, C., Hou, Y., 2020. The influence of internal heat exchanger on the performance of transcritical CO2 water source heat pump water heater. Energies (Basel) 13. https://doi.org/10.3390/en13071787

Fleming, J.S., 2003. Carbon dioxide as the working fluid in heating and/or cooling systems. Bulletin of the International Institute of Refrigeration 83, 7–15.

Food and Agriculture Organization of the United Nations, 2018. THE STATE OF AND AQUACULTURE WORLD FISHERIES [WWW Document]. URL https://www.fao.org/3/ca9229en/online/ca9229en.html#chapter-1_1

F-Tech, 2021. Avfukting [WWW Document]. URL https://f-tech.no/

F-Tech, 2020. Dehumidifiers for all purposes | Professional and private [WWW Document]. URL https://f-tech.no/ (accessed 12.8.22).

Ge, Y.T., Tassou, S.A., 2011. Performance evaluation and optimal design of supermarket refrigeration systems with supermarket model "SuperSim". Part II: Model applications. International Journal of Refrigeration 34, 540–549. https://doi.org/10.1016/J.IJREFRIG.2010.11.004

Gennitsaris, S., Oliveira, M.C., Vris, G., Bofilios, A., Ntinou, T., Frutuoso, A.R., Queiroga, C., Giannatsis, J., Sofianopoulou, S., Dedoussis, V., 2023. Energy Efficiency Management in Small and Medium-Sized Enterprises: Current Situation, Case Studies and Best Practices. Sustainability 2023, Vol. 15, Page 3727 15, 3727. https://doi.org/10.3390/SU15043727

Georges, L., Berner, M., Martin Mathisen, H., 2014. AIR HEATING OF PASSIVE HOUSES IN COLD CLIMATES: INVESTIGATION USING DETAILED DYNAMIC SIMULATIONS, Building and Environment. https://doi.org/10.1016/j.buildenv.2013.12.020

Getu, H.M., Bansal, P.K., 2008. Thermodynamic analysis of an R744–R717 cascade refrigeration system. International Journal of Refrigeration 31, 45–54. https://doi.org/10.1016/J.IJREFRIG.2007.06.014

González-Fandos, E., Villarino-Rodríguez, A., García-Linares, M.C., García-Arias, M.T., García-Fernández, M.C., 2005. Microbiological safety and sensory characteristics of salmon slices processed by the sous vide method. Food Control 16, 77–85. https://doi.org/10.1016/J.FOODCONT.2003.11.011

Hafner, A., 2019. The advantages of natural working fluids. Refrigeration Science and Technology 2019-Augus, 2456–2464. https://doi.org/10.18462/iir.icr.2019.1030

Hafner, A., Eikevik, T.M., 2016. R744_book chapter - TEP 4506 Specialization Course 2.

Hafner, Ing.A., Gabrielii, C.H., Widell, K., 2019. Refrigeration units in marine vessels. TemaNord. https://doi.org/10.6027/TN2019-527

Haiozan, H., Ritter, W., 1994. Transcritical CO2 - a new cycle. Austrian proposal for the working COHEPS Meeting, Trondheim, Norway, 20 August, 1994.

Heinen & Hopman, 2017. RSW System [WWW Document]. URL https://www.heinenhopman.com/products/rsw-system/ (accessed 12.5.22).

Hiran, 2022. Energy systems for salmon process plants.

Holmøy Maritime, 2022. Vi bygger nytt lakseslakteri i Holmen [WWW Document]. URL https://holmoy.no/bygger-nytt-lakseslakteri-i-holmen/ (accessed 12.12.22).

Hoşöz, M., 2005. Performance Comparison of Single-Stage and Cascade Refrigeration Systems Using R134a as the Working Fluid. Turkish Journal of Engineering and Environmental Sciences 29, 285–296.

Hu, B., Wang, X., Cao, F., He, Z., Xing, Z., 2014. Experimental analysis of an air-source transcritical CO2 heat pump water heater using the hot gas bypass defrosting method. Appl Therm Eng 71, 528–535. https://doi.org/10.1016/J.APPLTHERMALENG.2014.07.017

HVACR GUY, 2017. What is a Cascade Refrigeration System? All You Need To Know [WWW Document]. URL https://hvacrguy.com/what-is-a-cascade-refrigeration-system/ (accessed 12.4.22).

iLaks.no, 2020. Holmøy om nytt lakseslakteri [WWW Document]. URL https://ilaks.no/holmoy-om-nytt-lakseslakteri-vi-er-nesten-klare-til-a-gjore-beslutningen/ (accessed 12.12.22).

Illán-Gómez, F., Sena-Cuevas, V.F., García-Cascales, J.R., Velasco, F.J.S., 2021. Experimental and numerical study of a CO2 water-to-water heat pump for hot water generation. International Journal of Refrigeration 132, 30–44. https://doi.org/10.1016/J.IJREFRIG.2021.09.020

J., E., S., C.J., E., C., 2018. Cold Chain Technology Brief: Cold storage and refrigerated warehouse.

Judith A. Evans, 2009. Frozen Food Science and Technology, Frozen Food Science and Technology. https://doi.org/10.1002/9781444302325.ch7

Junqi, D., Yibiao, W., Shiwei, J., Xianhui, Z., Linjie, H., 2021. Experimental study of R744 heat pump system for electric vehicle application. Appl Therm Eng 183, 116191. https://doi.org/10.1016/J.APPLTHERMALENG.2020.116191

Kæling, 2019. RSW system - Refrigerated Sea Water system [WWW Document]. URL https://cooling.is/en/industry-cooling-equipment/rsw-system/ (accessed 12.5.22).

KATIPAMULA, S., LU, N., 2006. Evaluation of residential HVAC control strategies for demand response programs. ASHRAE Trans 535–546.

Kezza, H., 2022. Analyse av avfukter i CO2 transkritisk varmepumpe.

Kim, M.H., Pettersen, J., Bullard, C.W., 2004. Fundamental process and system design issues in CO2 vapor compression systems, Progress in Energy and Combustion Science. https://doi.org/10.1016/j.pecs.2003.09.002

Kuldeteknisk AS, 2011. SeaCool - RSW-anlegg med Co2 som kuldemedium [WWW Document]. URL https://kuldeteknisk.no/produkter/seacool/ (accessed 12.6.22).

Ladislav, V., Vaclav, D., Ondrej, B., Vaclav, N., 2016. Pinch Point Analysis of Heat Exchangers for Supercritical Carbon Dioxide with Gaseous Admixtures in CCS Systems. Energy Procedia 86, 489–499. https://doi.org/10.1016/J.EGYPRO.2016.01.050

Larsen Ringvall, J., Larsen Ringvall NTNU, J., 2020. Mobile slaughterhouses at sea - Do stun-and-bleed vessels meet Norwegian salmon farming requirements?

Lee, M.Y., Garud, K.S., Jeon, H.B., Lee, H.S., 2020. A Study on Performance Characteristics of a Heat Pump System with High-Pressure Side Chiller for Light-Duty Commercial Electric Vehicles. Symmetry 2020, Vol. 12, Page 1237 12, 1237. https://doi.org/10.3390/SYM12081237

Legacy Air, 2022. Can I Mix Different Refrigerants? [WWW Document]. URL https://legacyac.com/can-i-mix-different-refrigerants/ (accessed 12.1.22).

Lin, C.M., Liu, H.Y., Tseng, K.Y., Lin, S.F., 2019. Heating, Ventilation, and Air Conditioning System Optimization Control Strategy Involving Fan Coil Unit Temperature Control. Applied Sciences 2019, Vol. 9, Page 2391 9, 2391. https://doi.org/10.3390/APP9112391

Liu, Y., Zhuang, Z., Zhou, Y., Zhao, S., Wang, D., Liu, H., 2022. Heat transfer performance analysis of seawater heat exchange pipelines in deep seawater closed cooling air conditioning system. Appl Therm Eng 212, 118582. https://doi.org/10.1016/J.APPLTHERMALENG.2022.118582

Llopis, R., Cabello, R., Torrella, E., 2008. A dynamic model of a shell-and-tube condenser operating in a vapour compression refrigeration plant. International Journal of Thermal Sciences 47, 926–934. https://doi.org/10.1016/J.IJTHERMALSCI.2007.06.021

Lorentzen, G., 1995. The use of natural refrigerants: a complete solution to the CFC/HCFC predicament. International Journal of Refrigeration 18, 190–197. https://doi.org/10.1016/0140-7007(94)00001-E

Lorentzen, G., 1994. Revival of carbon dioxide as a refrigerant. International Journal of Refrigeration-revue Internationale Du Froid 17, 292–301. https://doi.org/10.1016/0140-7007(94)90059-0

MEHDIZADEH, M., 2021. CO2/NH3 Cascade Industrial Refrigeration Systems – ColdChainManagement.org [WWW Document]. URL

https://coldchainmanagement.org/2021/05/25/co2-nh3-cascade-industrial-refrigeration-systems/ (accessed 12.5.22).

Meyer, J.P., 2011. HEAT PUMPS. A-to-Z Guide to Thermodynamics, Heat and Mass Transfer, and Fluids Engineering. https://doi.org/10.1615/ATOZ.H.HEAT_PUMPS

Miura, 2022. Steam Boilers For Fluctuating Demands | Miura America [WWW Document]. URL https://miuraboiler.com/choosing-the-best-boiler-for-fluctuating-load-demands/ (accessed 6.9.23).

Muhssin, M.T., Cipcigan, L.M., Jenkins, N., Slater, S., Cheng, M., Obaid, Z.A., 2018. Dynamic Frequency Response from Controlled Domestic Heat Pumps. IEEE Transactions on Power Systems 33, 4948–4957. https://doi.org/10.1109/TPWRS.2017.2789205

Mumanachit, P., Reindl, D.T., Nellis, G.F., 2012. Comparative analysis of low temperature industrial refrigeration systems. International Journal of Refrigeration 35, 1208–1221. https://doi.org/10.1016/J.IJREFRIG.2012.02.009

Nistad, A.A., Pettersen, J.B., 2020. Current and Future Energy Use for Atlantic Salmon Farming in Recirculating Aquaculture Systems in Norway.

Norway Days, 2023. Working days in year 2023 in Norway [WWW Document]. URL https://norway.workingdays.org/workingdays_holidays_2023.htm (accessed 6.8.23).

Norwegian Seafood Council, 2017. Is Norwegian salmon sustainable [WWW Document]. URL https://en.seafood.no/301/is-norwegian-salmon-sustainable/ (accessed 10.3.22).

OECD, 2021. Fisheries and Aquaculture in Norway. OECD Review of Fisheries Country Notes i, 2015–2022.

Ouadha, A., En-Nacer, M., Imine, O., 2008. Thermodynamic modelling of a water-to-water heat pump using propane as refrigerant. International Journal of Exergy 5, 451–469. https://doi.org/10.1504/IJEX.2008.019115

Ouadha, A., En-nacer, M., Imine, O., Haddad, C., 2007. Exergy analysis and comparison of two-stage and cascade refrigeration cycles using natural refrigerants. Heat-SET, Heat Transfer in Components and Systems for Sustainable Energy Technologies Conference, 2007 853–860.

Papa, F., De Ferreira, R.C., Radulj, D., 2015. Pumps: Energy efficiency & performance indicators. Water Pract Technol 10, 872–885. https://doi.org/10.2166/WPT.2015.109

PTG AS, 2017. Bærekraftig kjøling, frysing, tining og oppvarming - PTG [WWW Document]. URL https://www.ptg.no/ (accessed 12.5.22).

Raman, N.S., Devaprasad, K., Chen, B., Ingley, H.A., Barooah, P., 2020. Model predictive control for energy-efficient HVAC operation with humidity and latent heat considerations. Appl Energy 279, 115765. https://doi.org/10.1016/J.APENERGY.2020.115765

REGLOPLAS, 2022. Water as a heat transfer fluid : Mould temperature control : Technologies [WWW Document]. URL https://www.regloplas.com/en/technologies/mould-temperature-control/water-as-a-heat-transfer-fluid/ (accessed 12.13.22).

Romero-Ayala, O., Chelech, A., Cannella, S., Miranda-Gonzalez, P.A., 2021. An empirical simulation study of a salmon production line in southern Chile. Aquac Eng 94, 102173. https://doi.org/10.1016/J.AQUAENG.2021.102173

Rosenberg, E., Risberg, T.M., Mydske, H.J., Helgerud, H.E., 2007. Store energipotensialer i næringsmiddelindustrien Energieffektivisering i næringsmiddelindustrien 138.

S., E., 2011. Flooded evaporator in small refrigeration and heat pump systems. Green new deal - green economy. The latest technology in refrigeration and air conditioning: energy issues and climate change, new refrigerants, new European regulations, new plants. XIV European Conference: June 10-11, 2011, Milan.

S., L.T., H., L.C., W., C.T., 2006. Thermodynamic analysis of optimal condensing temperature of cascade-condenser in CO2/NH3 cascade refrigeration systems.

Sahasranaman, K., 2005. Get the most from high-temperature heat-transfer-fluid systems: fluid selection, system design and maintenance are the keys to achieving the best performance. Chemical Engineering 112, 46–51.

Schobeiri, M.T., 2022. Advanced Fluid Mechanics and Heat Transfer for Engineers and Scientists. Advanced Fluid Mechanics and Heat Transfer for Engineers and Scientists. https://doi.org/10.1007/978-3-030-72925-7

School, B., 2019. Why Discharge Line Temperature is a Useful Reading - HVAC School [WWW Document]. URL https://hvacrschool.com/why-discharge-line-temperature-is-a-useful-reading/ (accessed 6.8.23).

Schudel, S., Prawiranto, K., Defraeye, T., 2021. Comparison of freezing and convective dehydrofreezing of vegetables for reducing cell damage. J Food Eng 293, 110376. https://doi.org/10.1016/J.JFOODENG.2020.110376

SFT, 2022. Blast Freezers | Air Blast Freezers [WWW Document]. URL https://www.sf.technology/en/productDetail?id=22719d256cc2c591016ce73ecc990006 (accessed 12.7.22).

Shaikh, N.I., Prabhu, V., 2007. Mathematical modeling and simulation of cryogenic tunnel freezers. J Food Eng 80, 701–710. https://doi.org/10.1016/j.jfoodeng.2006.04.065

Singh, J., 1985. Heat transfer fluids and systems for process and energy applications 283.

Smitt, S., Tolstorebrov, I., Hafner, A., 2020. Integrated CO2 system with HVAC and hot water for hotels: Field measurements and performance evaluation. International Journal of Refrigeration 116, 59–69. https://doi.org/10.1016/J.IJREFRIG.2020.03.021

Snøhetta, 2022. Projects - Snøhetta [WWW Document]. URL https://snohetta.com/projects (accessed 12.12.22).

Statistisk Sentralbyrå, 2023. Electricity prices in Norway [WWW Document]. URL https://www.ssb.no/en/energi-og-industri/energi/statistikk/elektrisitetspriser

Stene, J., 2005a. Residential CO2 heat pump system for combined space heating and hot water heating. International Journal of Refrigeration 28, 1259–1265. https://doi.org/10.1016/j.ijrefrig.2005.07.006

Stene, J., 2005b. Residential CO2 heat pump system for combined space heating and hot water heating. International Journal of Refrigeration 28, 1259–1265. https://doi.org/10.1016/j.ijrefrig.2005.07.006

Stene, J., 1999. Compression systems with natural working fluids : guidelines for design and operation of compression heat pump, air conditioning and retrigerating systems with natural working fluids.

Su, C., Madani, H., Liu, H., Wang, R., Palm, B., 2020. Seawater heat pumps in China, a spatial analysis. Energy Convers Manag 203, 112240. https://doi.org/10.1016/j.enconman.2019.112240

SWEP, 2019. Flooded evaporators [WWW Document]. URL https://www.swep.net/refrigerant-handbook/6.-evaporators/asas2/ (accessed 12.14.22).

Talib, R., Nassif, N., 2021. “Demand Control” an Innovative Way of Reducing the HVAC System’s Energy Consumption. Buildings 11. https://doi.org/10.3390/BUILDINGS11100488

Teknotherm, 2022. Horizontal Plate Freezer - Teknotherm Marine [WWW Document]. URL https://www.teknotherm.no/product/horizontal-plate-freezer/ (accessed 12.7.22).

Thermal Engineering, 2019. What is Vapor-compression Cycle - Refrigeration Cycle - Definition [WWW Document]. URL https://www.thermal-engineering.org/what-is-vapor-compression-cycle-refrigeration-cycle-definition/ (accessed 12.1.22).

Torp, T., 2012. RSW systems Teknotherm Marine [WWW Document]. URL https://www.teknotherm.no/fisheries/fisheries-systems/rsw-systems/ (accessed 12.5.22).

UNILAB, 2019. Carbon dioxide heat pump: from the condenser to the gas-cooler [WWW Document]. URL https://www.unilab.eu/articles/technical-articles/thermodynamic-engineering-articles/from-condenser-to-gas-cooler/ (accessed 12.13.22).

United Nations, 1998. Kyoto Protocol to the United Nations Framework Convention on Climate Change 58. https://doi.org/10.51663/pnz.58.2.07

University of Strathclyde, 2010. Potential development of air source Heat Pump in the UK [WWW Document]. URL https://www.esru.strath.ac.uk/EandE/Web_sites/10-11/ASHP_CO2/lit-design.html (accessed 12.11.22).

U.S.Department of State, 2015. The Montreal Protocol on Substances That Deplete the Ozone Layer - United States Department of State.

Wikipedia, 2022. Sortland [WWW Document]. URL https://en.wikipedia.org/wiki/Sortland#Shopping (accessed 12.13.22).

Yang, D., Li, Y., Xie, J., Wang, J., 2022. Exergy destruction characteristics of a transcritical carbon dioxide two-stage compression/ejector refrigeration system for low-temperature cold storage. Energy Reports 8, 8546–8562. https://doi.org/10.1016/j.egyr.2022.06.066

Zhang, X., Wu, Y., Ma, C., Meng, Q., Hu, X., Yang, C., 2019. Experimental Study on Temperature Distribution and Heat Losses of a Molten Salt Heat Storage Tank. Energies 2019, Vol. 12, Page 1943 12, 1943. https://doi.org/10.3390/EN12101943

Appendix A

Building the simulation models in Dymola

System 1

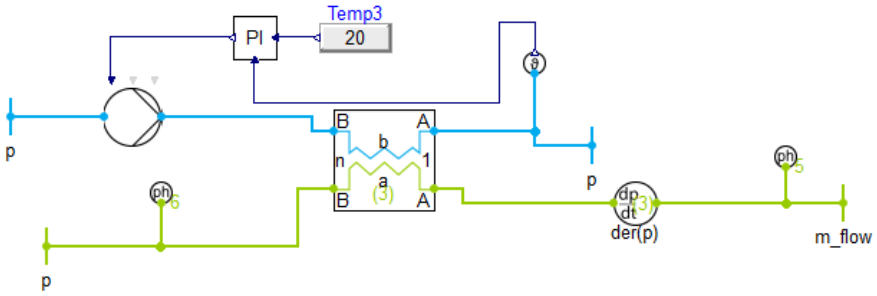

Figure: *Step 1*

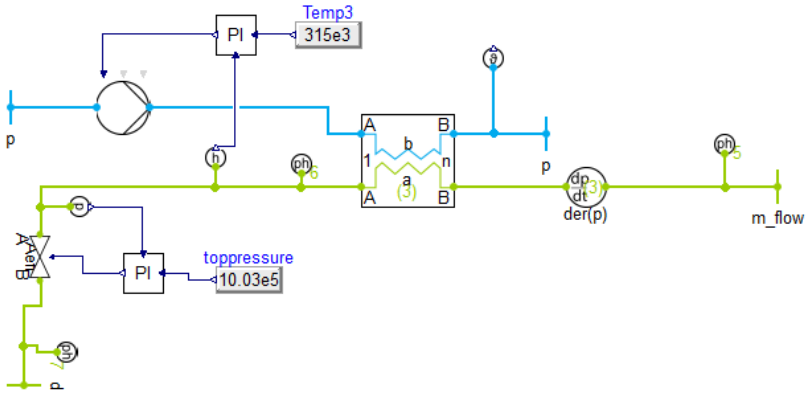

Figure: *Step 2*

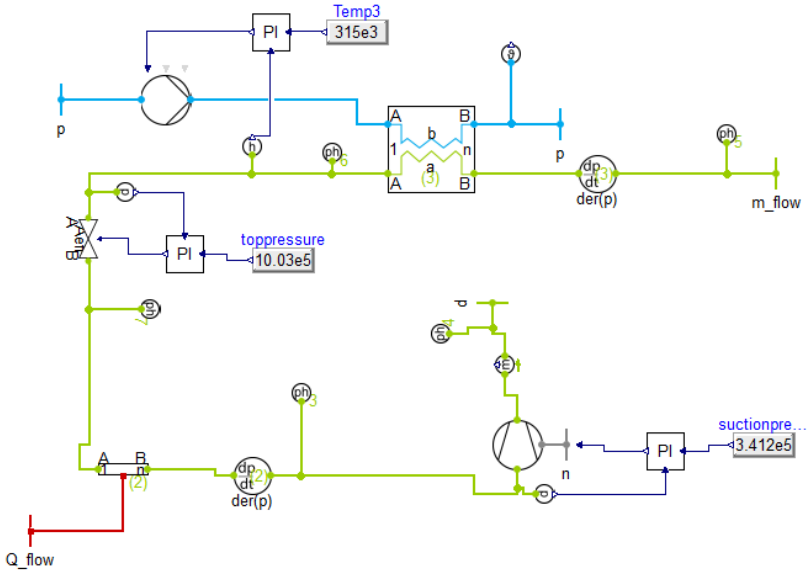

Figure: *Step 3*

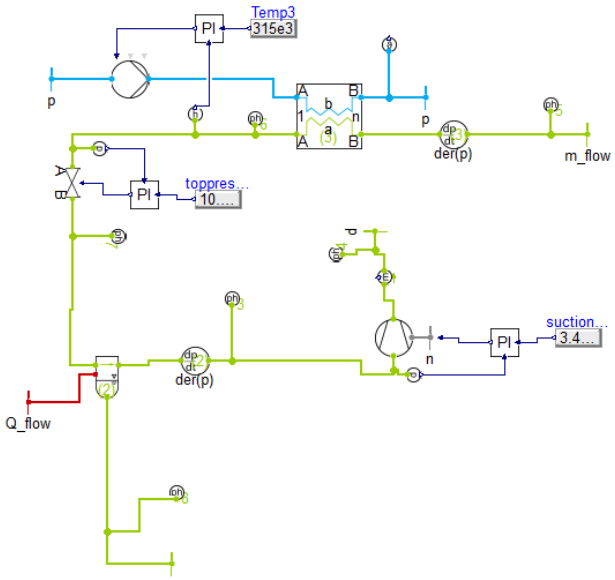

Figure: *Step 4*

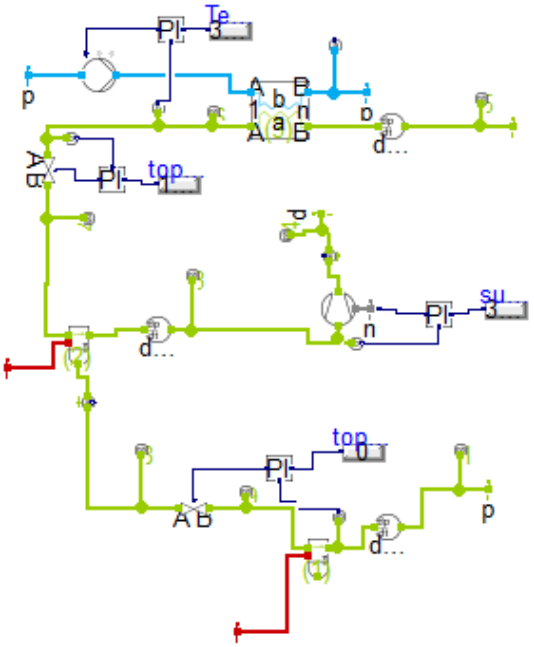

Figure: *Step 5*

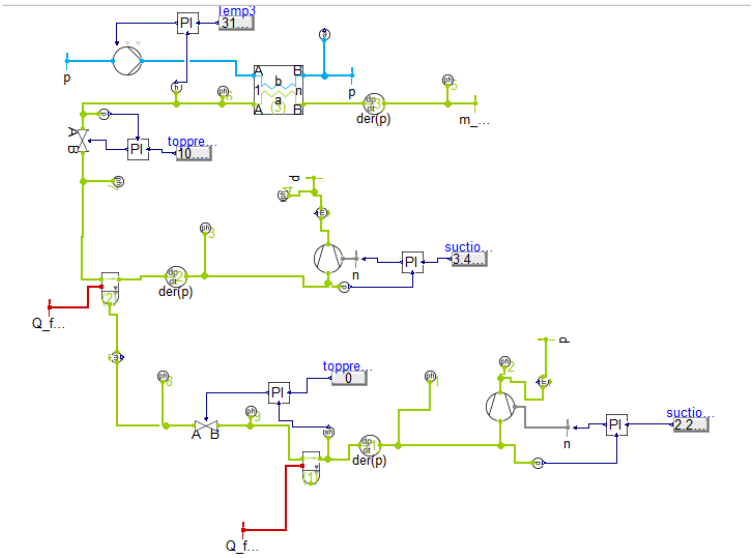

Figure: *Step 6*

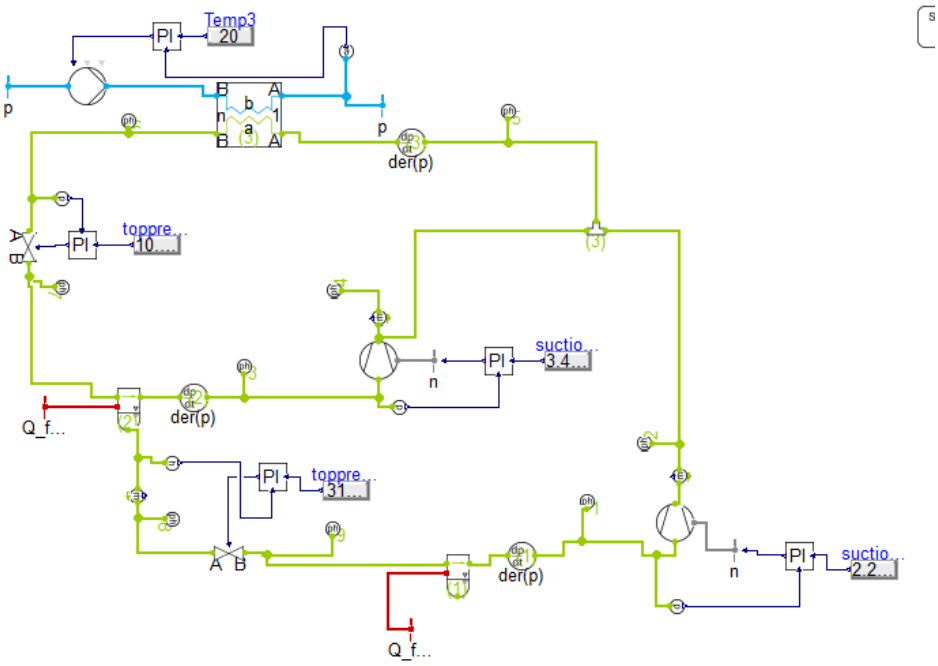

Figure: *Step 7*

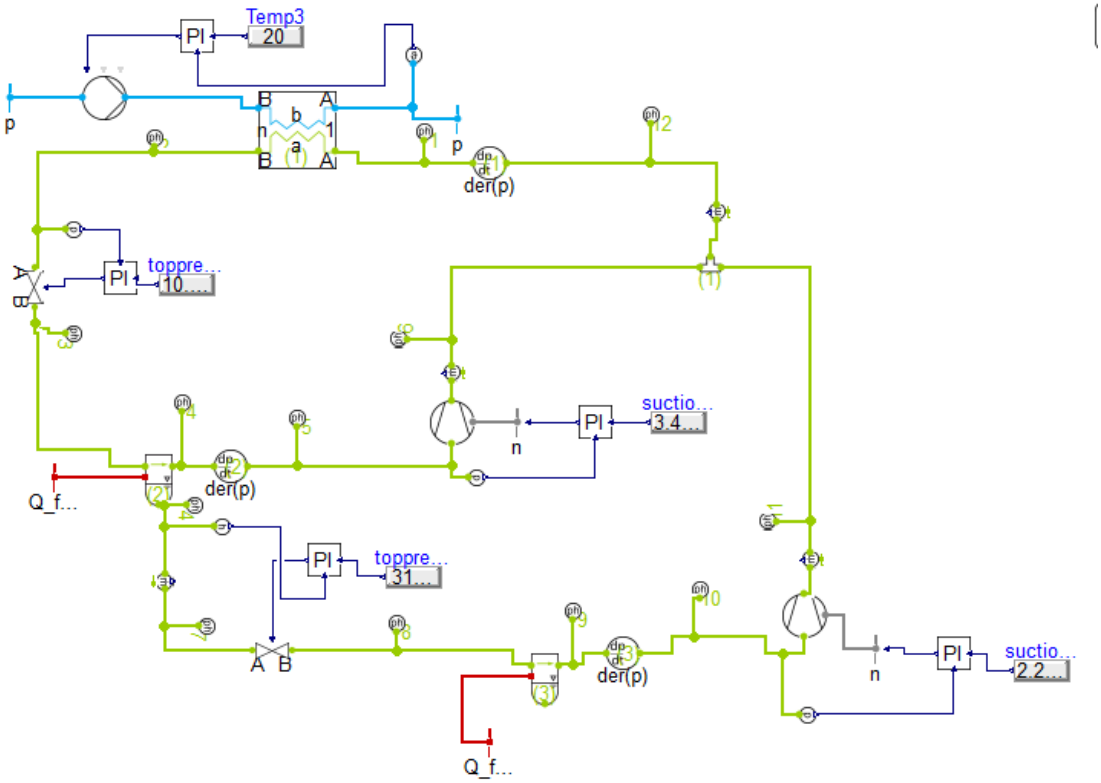

Figure: *Step 8*

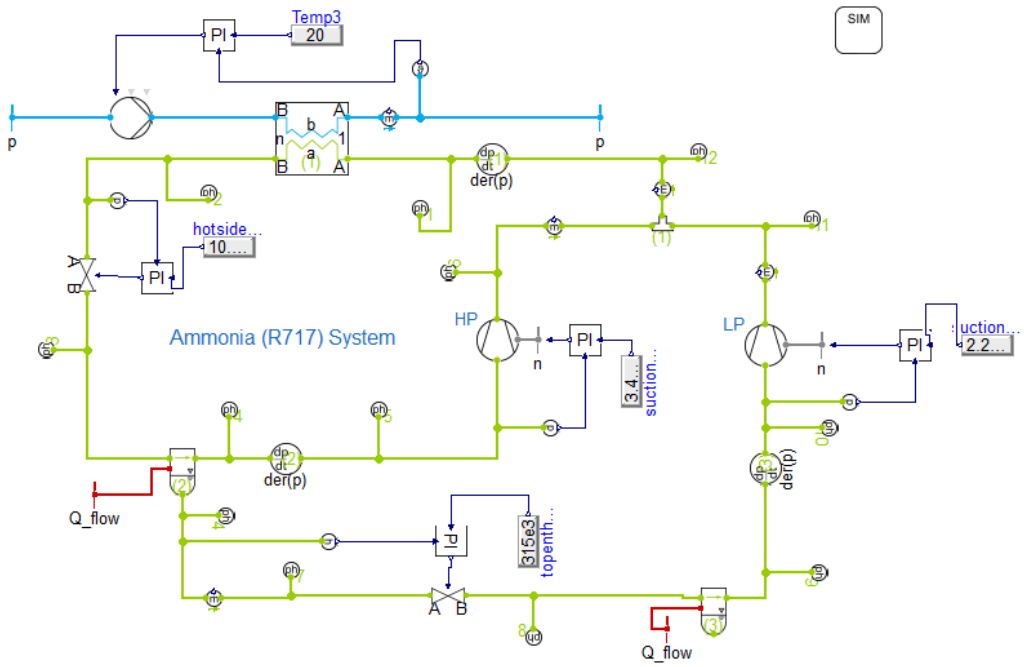

Figure: *Final step*

System 2

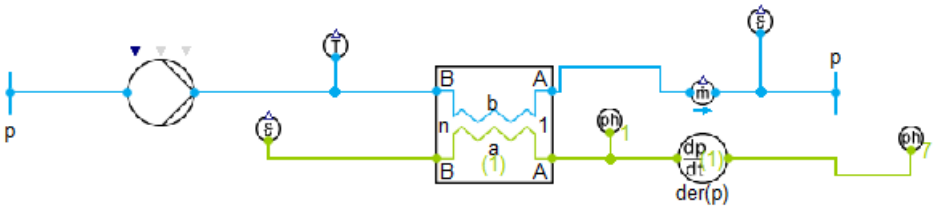

Figure: *Step 1 – Gas cooler and water pump*

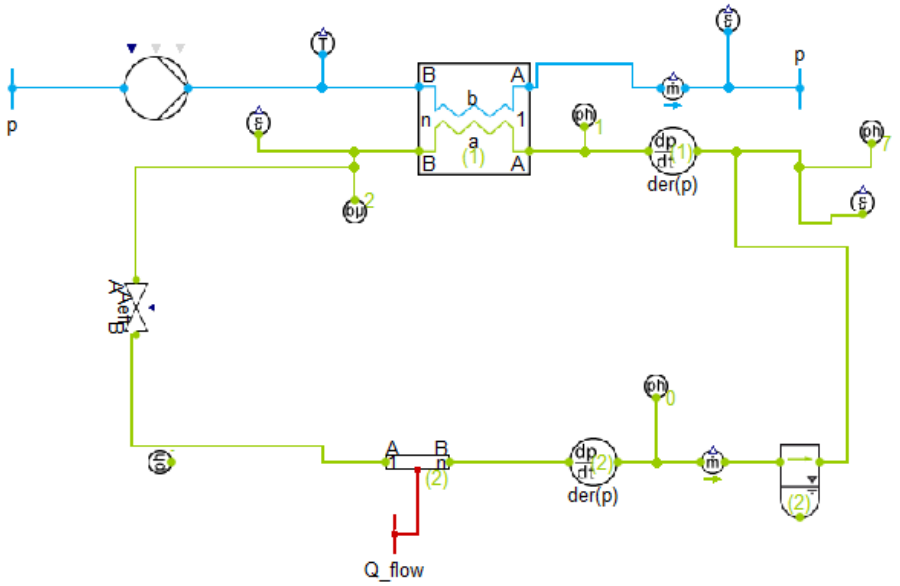

Figure: *Step 2 - Expansion valve and evaporator tube*

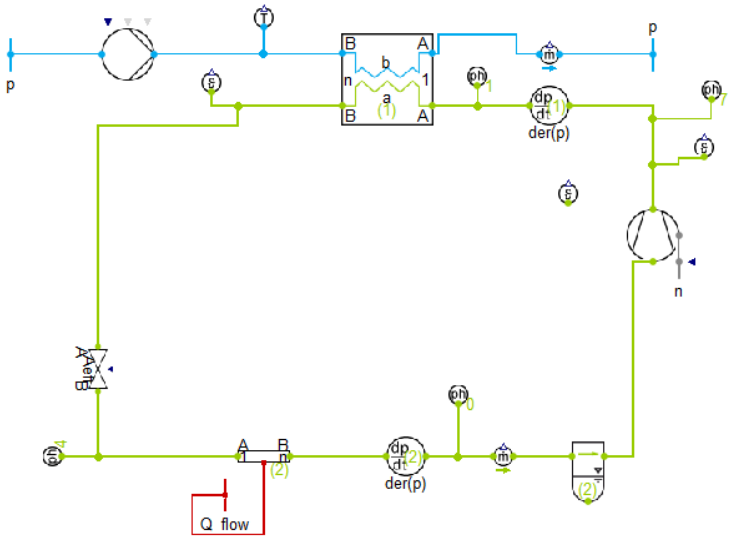

Figure: *Step 3*

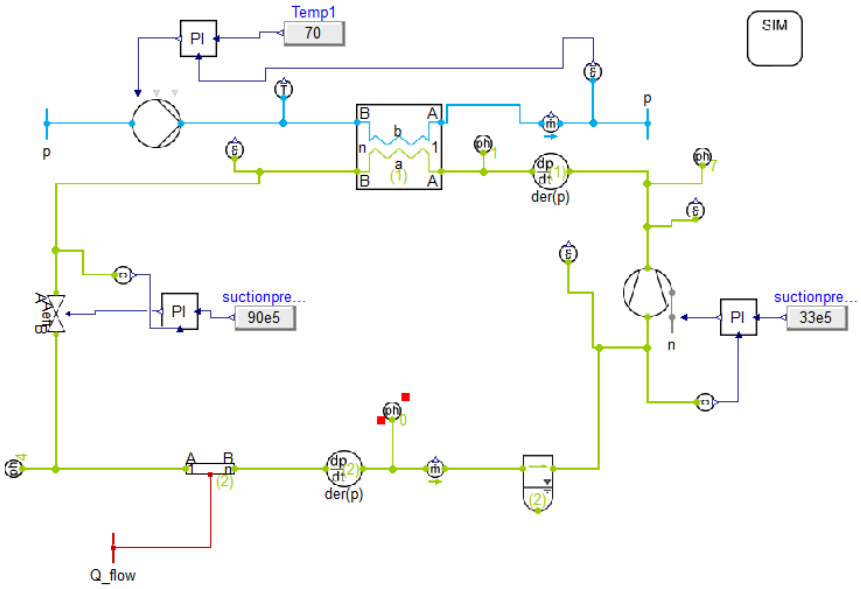

Figure: *Step 4*

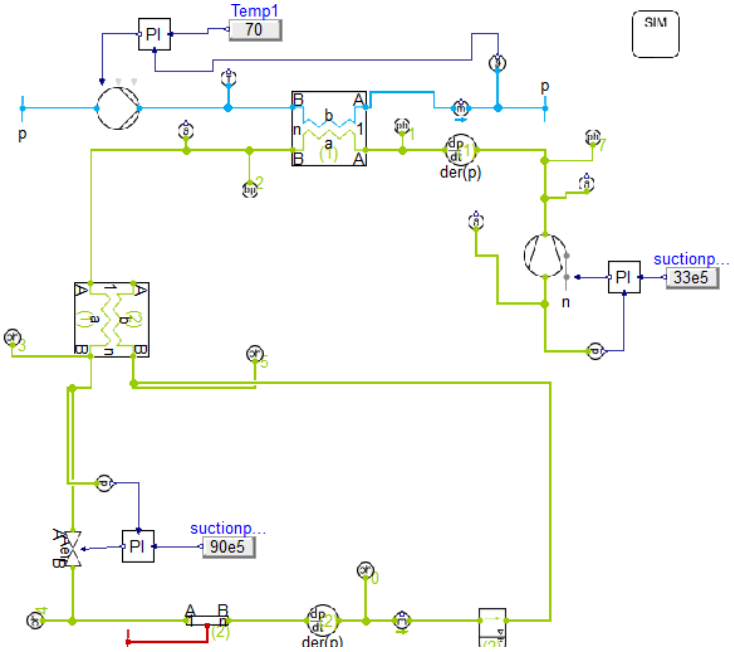

Figure: *Step 5*

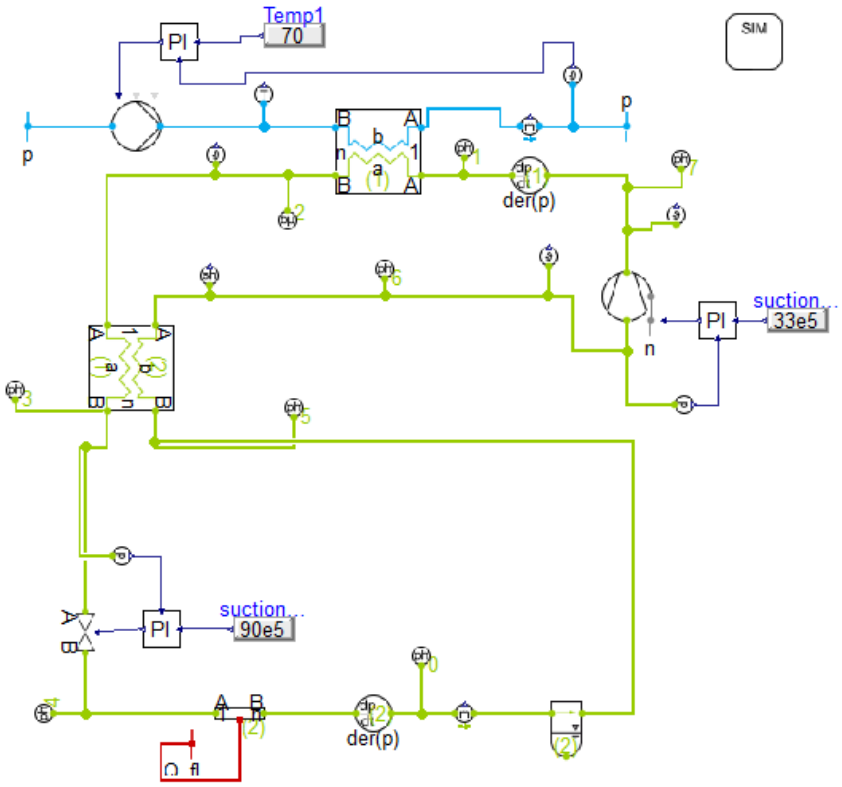

Figure: *Step 6*

Appendix B

1. EES Code and MATLAB

1.1 EES Code – System 1

```
"Point 1 - Lower Evaporating Temperature -16C "
 P[1]=2.263
h[1]=enthalpy(Ammonia,x=1,P=P[1])
s[1]=entropy(Ammonia,x=1,P=P[1])
s[2]=s[1]

"Point 2 - After Compressor 2 from 2.263 bar "
P[2]=10.03
h2s=enthalpy(Ammonia,s=s[2],P=P[2])
eff_is=0.7
h[2]=((h2s-h[1])/eff_is)+h[1]

"Point 3"
P[3]=3.412
h[3]=enthalpy(Ammonia,x=1,P=P[3])
s[3]=entropy(Ammonia,x=1,P=P[3])
s[4]=s[3]

"Point 4 - After Compressor 1"
P[4]=P[2]
h4s=enthalpy(Ammonia,s=s[4],P=P[4])
h[4]=((h4s-h[3])/eff_is)+h[3]

"Point 6 - Condensed Refrigerant from 3.412 bar"
P[6]=P[4]
h[6]=enthalpy(Ammonia,x=0,P=P[6])


"Point 7 - Throttling to Mid Evaporating Pressure at -6C , 3.412 bar"
P[7]=P[3]
h[7]=h[6]

"Point 8 - Condensed Refrigerant at -6C"
P[8]=P[3]
h[8]=enthalpy(Ammonia,x=0,P=P[8])

"Point 9 - Throttling to Lower Evaporating Pressure at  -16C , 2.263 bar"
P[9]=P[1]
h[9]=h[8]

"Vapour Fraction at Point 7 - Flash Gas"
x[7]=quality(Ammonia,T=-6,h=h[7])
```

"Tank B - Energy Balance"
Q_low=433
mdot_l=Q_low/(h[1]-h[9])

"Tank A - Energy Balance"
Q_high=457
mdot_t= (Q_high-(mdot_l*h[8])+(mdot_l*h[3]))/(h[3]-h[7])
mdot_f=mdot_t-mdot_l

"Total Mass Flow and Enthalpy entering Condenser"
P[5]=P[2]
h[5]=((mdot_f*h[4])+(mdot_l*h[2]))/mdot_t
Q_c=mdot_t*(h[5]-h[6])

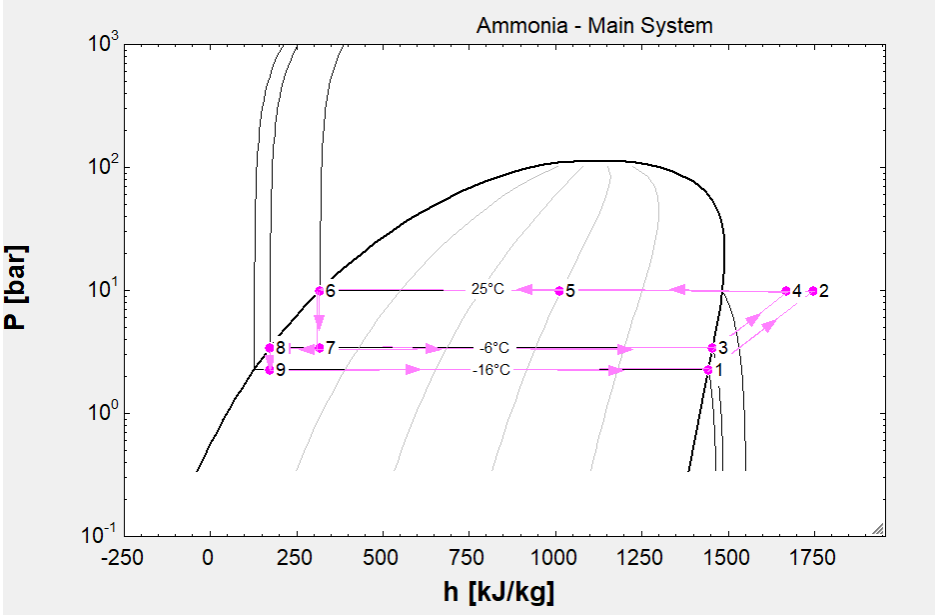

Figure: *p-h graph of system 1 obtained from EES*

1.2 EES Code – System 2

```
$Load Incompressible
"Point 1 - Condenser In at 90bar"
T[1]=88.34
P[1]=90
h[1]=494.4

"Point 2 - Condenser Out at 90bar"
T[2]=25
P[2]=90
h[2]=259.2

"Point 3 - IHX at 90 bar (Hot side)"
T[3]=5.787
P[3]=90
h[3]=209.1


"Point 4 - Throttling to 33bar"
T[4]=-2
P[4]=33
h[4]=209.1

"Point 5 - Evaporating at 33bar, -2C"
T[5]=-2
P[5]=33
h[5]=385.5

"Point 6 - IHX at 33 bar - Cold Side"
T[6]=0.07186
P[6]=33
h[6]=435.7
```

1.3 MATLAB code for cost analysis

```
clear all
close all

% Process with Freeze concentration and spray drying
interest_rate = 5/100;      % Rate of interest taken 5%
num_years = 20;  % Number of years
annuity_factor = (interest_rate/(1-(1+interest_rate)^-num_years));
      % Annuity factor
operating_energy_demand = 3183*5000;  % Operating energy demand per
year
energy_price = 0.36;  % Energy price in NOK
investment_cost_process1 = 63269910;  % Process 1 investment cost
maintenance_cost_process1 = investment_cost_process1*(5/100);     %
Maintenance cost 5 percent
net_annual_costs_process1 =
(investment_cost_process1*annuity_factor) +
(operating_energy_demand*energy_price) +
(maintenance_cost_process1);

% Additional equipment investment
investment_cost_freeze_concentrator = 14625000;  % Investment cost
of freeze concentrator in NOK
investment_cost_combined = 63269910;
operating_energy_demand_combined = 1245.3*5000;  % Operating energy
demand with combined equipment
maintenance_cost_combined = (investment_cost_freeze_concentrator +
investment_cost_combined)*(5/100);     % Maintenance cost 5 percent
net_annual_costs_combined =
(investment_cost_freeze_concentrator*annuity_factor) +
(investment_cost_combined*annuity_factor) +
(operating_energy_demand_combined*energy_price) +
(maintenance_cost_combined);
net_annual_savings = (operating_energy_demand*energy_price -
operating_energy_demand_combined*energy_price) +
(maintenance_cost_process1 - maintenance_cost_combined);     % Net
annual savings (annual cost reduction plus maintenance)
additional_investment_costs = (investment_cost_freeze_concentrator +
investment_cost_combined) - investment_cost_process1;  % Additional
investment costs
payback_time = additional_investment_costs / net_annual_savings;  %
Payback time detrmination

% FC with Drum Drying
interest_rate = 5/100;      % Rate of interest taken 5%
num_years = 20;  % Number of years
annuity_factor = (interest_rate/(1-(1+interest_rate)^-num_years));
      % Annuity factor
```

```
operating_energy_demand = 2958*5000;  % Operating energy demand per
year
energy_price = 0.36;  % Energy price in NOK
investment_cost_process2 = 61666110;  % Process with Drum dryer
investment cost
maintenance_cost_process2 = investment_cost_process2*(5/100);    %
Maintenance cost 5 percent of investment cost
net_annual_costs_process2 =
(investment_cost_process2*annuity_factor) +
(operating_energy_demand*energy_price) +
(maintenance_cost_process2);

% Additional equipment investment
investment_cost_freeze_concentrator = 14625000;  % Investment cost
of freeze concentrator in USD
investment_cost_combined = 61666110;
operating_energy_demand_combined = 1124.3*5000;  % Operating energy
demand with combined equipment
maintenance_cost_combined = (investment_cost_freeze_concentrator +
investment_cost_combined)*(5/100);    % Maintenance cost 5 percent
net_annual_costs_combined =
(investment_cost_freeze_concentrator*annuity_factor) +
(investment_cost_combined*annuity_factor) +
(operating_energy_demand_combined*energy_price)
```

1.4 MATLAB code for calculating system parameters – area under the curve.

1.4.1 System 1

1.4.1.1 Electricity consumed.

```
clc
clear all

PS1 = @(x) 112.05*x - 8.9925*x^2 + 0.545*x^3; %Break HP

s= PS1(6) - PS1(4); %4-6

PS2 = @(x) 128.65*x - 2.9975*x^2 + 0.181667*x^3; %Break LP

q = PS2(6)-PS2(4); %4-6

PS3= @(x) 240.96*x - 11.99*x^2 + 0.726667*x^3; %Break Total

a = PS3(6)-PS3(4); %Energy from 19-20
```

1.4.2 System 2

1.4.2.1 Summer – Electricity consumed.

```
clc
clear all

PS1 = @(x) -2960.8*x + 382.375*x^2 - 15.1327*x^3; %Break 1
s= PS1(7.056) - PS1(6.026); %Energy 6-7

PS2 = @(x) -835.55*x + 143.035*x^2 - 6.776*x^3; %Break 2
q = PS2(9.072)-PS2(7.056); %Energy consumed between 7-9

u=(10*93.613); %Energy from 9-19

PS3= @(x) 6972.9*x - 311.285*x^2 + 4.57133*x^3; %Break 3
a = PS3(20.112)-PS3(19.008); %Energy from 19-20

t=(4.144*4); %Energy from 20-24

squat = s+q+u+a+t;
```

1.4.2.2 Summer – Gas cooler output

```
clc
clear all

GS1 = @(x) -9358.5*x + 1156.95*x^2 - 42.1133*x^3; %Break 1
s = GS1(7.056)-GS1(6.026); %Energy from 6-7
```

```
GS2 = @(x) -3228.6*x + 550.75*x^2 - 26.031*x^3; %Break 2
q = GS2(9.072)-GS2(7.056); %Energy 7-9

u=(10*362.61); %Energy 9-19

GS3 = @(x) 25285*x - 1117.4*x^2 + 16.2007*x^3; %Break 3
a = GS3(20.112)-GS3(19.008); %Energy 19-20

t=(4*16.263); %Energy from 20-24

squat = s+q+u+a+t;
```

1.4.2.3 Summer – Hot water produced.

```
clc

clear all

M1 = @(x) -137.09*x + 0.0053*x^2 - x^3/15000000; %Break 1
s = M1(25401.6)-M1(22712.18); %Energy from 6-7

M2 = @(x) -17.816*x + 0.0008*x^2 - x^3/100000000; %Break 2
q = M2(32659.2)-M2(25401.6); %Energy 7-9

u=(10*1.735625*3600); %Energy 9-19

M3 = @(x) 93.312*x - 0.0011*x^2 + x^3/300000000; %Break 3
a = M3(72403.2)-M3(68428.8); %Energy 19-20

t=(4*0.080397*3600); %Energy from 20-24

squat = s+q+u+a+t;
```

1.4.2.4 Winter – Electricity consumed.

```
clc
clear all

P1 = @(x) -662.44*x + 125.91*x^2 - 7.26967*x^3; %Break 1 from 4-6
s= P1(6.048) - P1(4.047);
P2 = @(x) 150.66*x - 8.4655*x^2 + 0.1661*x^3; %Break 2 from 6-7
q = P2(7.008)-P2(6.096); %Energy consumed between 6-7

u=(11*56.47); %Energy from 7-18

P3= @(x) 1500.9*x - 52.995*x^2 + 0.477033*x^3; %Break 3
a = P3(19.008)-P3(18.048); %Energy from 18-19

t=(3.41*5); %Energy from 19-24

squat = s+q+u+a+t;
```

1.4.2.5 Winter – Gas cooler heat output

```
clc
clear all

G1 = @(x) -2422.1*x + 457.29*x^2 - 26.0743*x^3; %Break 1
s = G1(6)-G1(4.047); %Energy from 4-6

G2 = @(x) 587.97*x - 33.2665*x^2 + 0.671267*x^3; %Break 2
q = G2(7.008)-G2(6.048); %Energy 6-7
```

```
u=(11*220.47); %Energy 7-18

G3 = @(x) 5021.4*x - 161.63*x^2 + 1.04773*x^3; %Break 3
a = G3(19.008)-G3(18.048); %Energy 18-19

t=(5*13.45); %Energy from 19-24

squat = s+q+u+a+t
```

1.4.2.6 Winter – Hot water produced.

```
clc
clear all

M1 = @(x) -10.589*x + 0.00055*x^2 - x^3/100000000; %Break 1
s = M1(21772)-M1(16416); %Energy from 4-6

M2 = @(x) 2.0973*x - (3*x^2)/200000 - x^3/7500000000; %Break 2
q = M2(25228)-M2(21945); %Energy 6-7

u=(11*1.05492*3600); %Energy 7-18

a = (0.537604*3600); %Energy 18-19

t=(5*0.06575*3600); %Energy from 19-24

squat = s+q+u+a+t;
```

1.4.2.7 70-90HW amount of water produced

```
clc
clear all

M1 = @(x) -1.0825*x + 0.0001*x^2 - x^3/750000000; %Break 1
s = M1(29376)-M1(17798.4);

M2 = @(x) 0.9135*x - x^2/5000000 + x^3/600000000000; %Break 2
q = M2(57888)-M2(29548.8);

M3 = @(x) 2.6568*x - x^2/40000 + x^3/7500000000; %Break 3
u = M3(65664)-M3(58060.8);

M4 = @(x) 0.0718*x - x^2/4000000 + x^3/1000000000000; %Break 3
a = M4(85536)-M4(68428.8);

M5 = @(x) -1.0676*x + 0.0001*x^2 - x^3/1000000000; %Break 3
t = M5(68256)-M5(65836.8);

ua=u+a;
```

```
uat=u+a+t;
squat = s+q+uat;
```

1.4.2.8 70-90HW power breakup

```
clc

clear all

M1 = @(x) -66.007*x + 21.1555*x^2 - 1.10257*x^3; %Break 1
s = M1(8.16)-M1(4.944);

M2 = @(x) 36.735*x + 3.14295*x^2 - 0.1195*x^3; %Break 2
q = M2(9.984)-M2(8.208);
u = (63.91855*6);

M4 = @(x) -5050.9*x + 299.93*x^2 - 5.853*x^3; %Break 3
a = M4(18.96)-M4(16.128);
t = (4.07034*5);

qu=q+u;
at=a+t;
squat = s+q+u+a+t;
```

Appendix C

SPP data as received from PTG

Døgnvariasjoner sommer	Maks.	T	Vasking								Produksjon fase 2								Produksjon fase 3								kWh	
Varmebehov Sommer			00:00	01:00	02:00	03:00	04:00	05:00	06:00	07:00	08:00	09:00	10:00	11:00	12:00	13:00	14:00	15:00	16:00	17:00	18:00	19:00	20:00	21:00	22:00	23:00		kW snitt
Avfuktin/oppv.																												
Avliving	88	70 °C	-	-	-	-	-	88	88	88	88	88	88	88	88	88	88	88	88	88	88	88	88	88	88	88	1,672	70
Grading	148	70 °C	-	-	-	-	-	148	148	148	148	148	148	148	148	148	148	148	148	148	148	148	148	148	148	148	2,806	117
Filetering	70	70 °C	-	-	-	-	-	70	70	70	70	70	70	70	70	70	70	70	70	70	70	70	70	70	70	70	1,321	55
Pallelager	148	70 °C	-	-	-	-	-	148	148	148	148	148	148	148	148	148	148	148	148	148	148	148	148	148	148	148	2,806	117
Rom for støttesystemer	0	70 °C	0	0	0	0	0	0	0	0	0	0	0	0	0	0	0	0	0	0	0	0	0	0	0	0	0	-
Kontoravd.																												
Ventilasjon bygg																												
Avliving	242	45 °C	40	40	20	20	20	20	20	20	20	20	20	20	20	20	20	20	20	20	20	20	20	20	20	20	521.3	22
Grading	242	45 °C	20	40	40	20	20	20	20	20	20	20	20	20	20	20	20	20	20	20	20	20	20	20	20	20	521.3	22
Filetering	97	45 °C	8	16	16	8	8	8	8	8	8	8	8	8	8	8	8	8	8	8	8	8	8	8	8	8	208.52	9
Pallelager	29	45 °C	10	10	20	20	10	10	10	10	10	10	10	10	10	10	10	10	10	10	10	10	10	10	10	10	260.65	11
Rom for støttesystemer	25	45 °C	8	8	8	8	8	8	8	8	8	8	8	8	8	8	8	8	8	8	8	8	8	8	8	8	192.48	8
Kontoravd.	25	45 °C																										
Fan-coils	150	70 °C																										
Avliving	50	70 °C																									0	-
Grading	30	70 °C																									0	-
Filetering	30	70 °C																									0	-
Pallelager	0	70 °C																									0	-
Rom for støttesystemer	10	70 °C																									0	-
Kontoravd.	30	70 °C																									0	-
Vasking																											-	-
Cip	1,155	70 °C		1,155	578	578																					2,310	770
Spyling	289	70 °C	289	289	289	289	289																				1,446	289
Varmtvann 35 °C																											-	-
Gulvvarme	12.5	35 °C	12.5	12.5	12.5	12.5	12.5	12.5	12.5	12.5	12.5	12.5	12.5	12.5	12.5	12.5	12.5	12.5	12.5	12.5	12.5	12.5	12.5	12.5	12.5	12.5	300	13
Snøsmelteanlegg	40	35 °C																									0	
Tilgjengelig varmekilder																												
Tilgjengelig varme Vakuumpark	180	60 °C								180	180	180	180	180	180	180	180	180	180	180	180	180	180	180	180	180	3060	

Døgnvariasjoner sommer	Maks.	T	Vasking								Produksjon fase 2								Produksjon fase 3								kWh	
Kjølebehov sommer			00:00	01:00	02:00	03:00	04:00	05:00	06:00	07:00	08:00	09:00	10:00	11:00	12:00	13:00	14:00	15:00	16:00	17:00	18:00	19:00	20:00	21:00	22:00	23:00		kW snitt
Fan-coils																												
Avliving	50	10 °C									50	50	50	50	50	50	50	50	50	50	50	50	50	50	50	50	800	50
Grading	30	10 °C									30	30	30	30	30	30	30	30	30	30	30	30	30	30	30	30	480	30
Filetering	30	10 °C									30	30	30	30	30	30	30	30	30	30	30	30	30	30	30	30	480	30
Pallelager	0	10 °C									-	-	-	-	-	-	-	-	-	-	-	-	-	-	-	-	-	-
Rom for støttesystemer	10	10 °C	10	10	10	10	10	10	10	10	10	10	10	10	10	10	10	10	10	10	10	10	10	10	10	10	240	10
Kontoravd.	30	10 °C	30	30	30		30	30	30	30	30	30	30	30	30	30	30	30	30	30	30	30	30	30	30	30	690	30
Ventilasjon bygg																												
Avliving	72	10 °C	72	72	72	72	72	72	72	72	72	72	72	72	72	72	72	72	72	72	72	36	36	36	36	36	1,548	65
Grading	90	10 °C	90	90	90	90	90	90	90	90	90	90	90	90	90	90	90	90	90	90	90	45	45	45	45	45	1,935	81
Filetering	45	10 °C	45	45	45	45	45	45	45	45	45	45	45	45	45	45	45	45	45	45	45	23	23	23	23	23	968	40
Pallelager	90	10 °C	90	90	90	90	90	90	90	90	90	90	90	90	90	90	90	90	90	90	90	45	45	45	45	45	1,935	81
Rom for støttesystemer	0	5 °C	-	-	-	-	-	-	-	-	-	-	-	-	-	-	-	-	-	-	-	-	-	-	-	-	-	-
Kontoravd.	10	20 °C								10	10	10	10	10	10	10	10	10	10	10	10	5	5				130	9
Avfuktin/nedkj.																												
Avliving	35	10 °C	-	-	-	-	-	-	-	-	107	107	107	107	107	107	107	107	107	107	107	107	107	107	107	107	1,712	71
Grading	75	10 °C	-	-	-	-	-	-	-	-	165	165	165	165	165	165	165	165	165	165	165	165	165	165	165	165	2,640	110
Filetering	25	10 °C	-	-	-	-	-	-	-	-	70	70	70	70	70	70	70	70	70	70	70	70	70	70	70	70	1,120	47
Pallelager	62	10 °C	-	-	-	-	-	-	-	-	152	152	152	152	152	152	152	152	152	152	152	152	152	152	152	152	2,432	101
Rom for støttesystemer	0	10 °C	-	-	-	-	-	-	-	-	-	-	-	-	-	-	-	-	-	-	-	-	-	-	-	-	-	-
Kontoravd.																												
Produktkjøling																												
RSW	435	0 °C								435	435	257	257	257	257	257	257	257	257	257	257	257					3,703	285
RSW filét	57	0 °C								57	12	12	12	12	12	12	12	12	12	12	12	12	12	12	12	12	249	15
Isproduksjon	392	-10 °C	392	392	392	392	392	392	392	392	392	392	392	392	392	392	392	392	392	392	392	392	392	392	392	392	9,408	392
Kjølelager	41	0 °C	-	-	-	-	-	-	41	41	8	8	8	8	8	8	8	8	8	8	8	8	8	8	8	8	212	9
Innfrysning tunell 1	75	-42 °C	75	75	75	56	56	56	56	56	56	56	38	38	38	38	38	38	38	38	38	19	19	19	19	-	1,031	43
Innfrysning tunell 2	75	-42 °C	56	38	38	38	38	38	38	38	38	38	19	19	19	19	-	75	75	75	56	56	56	56	56	56	1,031	43
Fryselager	14	-20 °C	14	14	14	14	14	14	14	14	14	14	14	14	14	14	14	14	14	14	14	14	14	14	14	14	326	14

Figure: *Summer demands of the SPP*

Tilgjengelig varmekilder																												-
Tilgjengelig varme Vakuumpark	180	60 °C								180	180	180	180	180	180	180	180	180	180	180	180	180	180	180	180	180	3060	180

Døgnvariasjoner vinter	Maks.	T	Vasking								Produksjon fase 2								Produksjon fase 3									kW snitt
Kjølebehov vinter			00:00	01:00	02:00	03:00	04:00	05:00	06:00	07:00	08:00	09:00	10:00	11:00	12:00	13:00	14:00	15:00	16:00	17:00	18:00	19:00	20:00	21:00	22:00	23:00	snitt/døgn	
Fan-coils																												
Avliving	50	10 °C																									-	
Grading	30	10 °C																									-	
Filetering	30	10 °C																									-	
Pallelager	0	10 °C																									-	
Rom for støttesystemer	10	10 °C																									-	
Kontoravd.	30	10 °C																									-	
Ventilasjon bygg		10 °C																									-	
Avliving	72	10 °C	72	72	50	18	18	18	18	18	18	18	18	18	18	18	18	18	18	18	18	18	18	18	18	18	572	24
Grading	90	10 °C	23	90	90	63	23	23	23	23	23	23	23	23	23	23	23	23	23	23	23	23	23	23	23	23	716	30
Filetering	45	10 °C	11	11	45	45	32	11	11	11	11	11	11	11	11	11	11	11	11	11	11	11	11	11	11	11	358	15
Pallelager	90	10 °C	23	23	23	90	90	63	23	23	23	23	23	23	23	23	23	23	23	23	23	23	23	23	23	23	716	30
Rom for støttesystemer	0	5 °C	0	0	0	0	0	0	0	0	0	0	0	0	0	0	0	0	0	0	0	0	0	0	0	0	-	-
Kontoravd.	10	20 °C	7	7	7	7	7	7	7	3	3	3	3	3	3	3	3	3	3	3	3	3	3	3	3	3	92	4
Avfuktin/nedkj.																											-	
Avliving	35	10 °C	0	0	0	0	0	0	0	0	0	0	0	0	0	0	0	0	0	0	0	0	0	0	0	0	-	-
Grading	75	10 °C	0	0	0	0	0	0	0	0	0	0	0	0	0	0	0	0	0	0	0	0	0	0	0	0	-	-
Filetering	25	10 °C	0	0	0	0	0	0	0	0	0	0	0	0	0	0	0	0	0	0	0	0	0	0	0	0	-	-
Pallelager	62	10 °C	0	0	0	0	0	0	0	0	0	0	0	0	0	0	0	0	0	0	0	0	0	0	0	0	-	-
Rom for støttesystemer	0	10 °C	0	0	0	0	0	0	0	0	0	0	0	0	0	0	0	0	0	0	0	0	0	0	0	0	-	-
Kontoravd.																											-	
Produktkjøling																											-	
RSW sløying	435	0 °C						154	154	154	154	154	154	154	154	154	154	154	154	154	154						2,162	154
RSW Filét									40	10	10	10	10	10	10	10	10	10	10	10	10	10	10	10	10	10	210	12
Isproduksjon	392	-10 °C	392	392	392	392	392	392	392	392	392	392	392	392	392	392	392	392	392	392	392	392	392	392	392	392	9,408	392
Kjølelager	41	0 °C	0	0	0	0	0	0	41	41	8	8	8	8	8	8	8	8	8	8	8	8	8	8	8	8	212	9
Innfrysning tunell 1	75	-42 °C	75	75	75	56	56	56	56	56	56	56	38	38	38	38	38	38	38	38	38	19	19	19	19	0	1,031	43
Innfrysning tunell 1	75	-42 °C	56	38	38	38	38	38	38	38	38	38	19	19	19	19	0	75	75	75	56	56	56	56	56	56	1,031	43
Fryselager	14	-20 °C	14	14	14	14	14	14	14	14	14	14	14	14	14	14	14	14	14	14	14	14	14	14	14	14	326	14

Døgnvariasjoner vinter	Maks.	T	Vasking								Produksjon fase 2								Produksjon fase 3								kWh		
Varmebehov vinter			00:00	01:00	02:00	03:00	04:00	05:00	06:00	07:00	08:00	09:00	10:00	11:00	12:00	13:00	14:00	15:00	16:00	17:00	18:00	19:00	20:00	21:00	22:00	23:00		kW snitt	faktor vinter
Avfuktin/oppv.																													
Avliving	242	70 °C	242	242	242	242	88	88	88	66	66	66	66	66	66	66	66	66	66	66	66	66	66	66	66	66	2,354	98	
Grading	242	70 °C	242	242	242	242	148	148	148	111	111	111	111	111	111	111	111	111	111	111	111	111	111	111	111	111	3,294	137	
Filetering	97	70 °C	97	97	97	97	70	70	70	52	52	52	52	52	52	52	52	52	52	52	52	52	52	52	52	52	1,483	62	
Pallelager	148	70 °C	29	29	29	29	148	148	148	111	111	111	111	111	111	111	111	111	111	111	111	111	111	111	111	111	2,442	102	
Rom for støttesystemer	0	70 °C	0	0	0	0	0	0	0	0	0	0	0	0	0	0	0	0	0	0	0	0	0	0	0	0	0	-	
Kontoravd.																											0		
Ventilasjon bygg																													
Avliving	242	45 °C	242	242	182	182	182	182	182	182	182	182	182	182	182	182	182	182	182	182	182	182	182	182	182	182	4477	187	
Grading	242	45 °C	182	242	242	182	182	182	182	182	182	182	182	182	182	182	182	182	182	182	182	182	182	182	182	182	4477	187	
Filetering	97	45 °C	73	73	97	97	73	73	73	73	73	73	73	73	73	73	73	73	73	73	73	73	73	73	73	73	1794.5	75	
Pallelager	29	45 °C	22	22	22	29	29	22	22	22	22	22	22	22	22	22	22	22	22	22	22	22	22	22	22	22	536.5	22	
Rom for støttesystemer	25	45 °C	19	19	19	19	25	25	19	19	19	19	19	19	19	19	19	19	19	19	19	19	19	19	19	19	462.5		
Kontoravd.	25	45 °C	25	25	25	25	25	25	25	19	19	19	19	19	19	19	19	19	19	19	19	19	19	19	19	19	493.75		
Fan-coils																												-	
Avliving	50	70 °C	50	50	50	50	50	50	50	50	50	50	50	50	50	50	50	50	50	50	50	50	50	50	50	50	1200	50	
Grading	30	70 °C	30	30	30	30	30	30	30	30	30	30	30	30	30	30	30	30	30	30	30	30	30	30	30	30	720	30	
Filetering	30	70 °C	30	30	30	30	30	30	30	30	30	30	30	30	30	30	30	30	30	30	30	30	30	30	30	30	720	30	
Pallelager	0	70 °C	0	0	0	0	0	0	0	0	0	0	0	0	0	0	0	0	0	0	0	0	0	0	0	0	0	-	
Rom for støttesystemer	10	70 °C	10	10	10	10	10	10	10	10	10	10	10	10	10	10	10	10	10	10	10	10	10	10	10	10	240	10	
Kontoravd.	30	70 °C	30	30	30	30	30	30	30	30	30	30	30	30	30	30	30	30	30	30	30	30	30	30	30	30	720	30	
Vasking																													
Cip	1,365	70 °C		1,365	683	683																							
Spyling	332	70 °C	332	332	332	332	332																						
Varmtvann 35 °C																													
Gulvvarme	150	35 °C	150	150	150	150	150	150	150	150	150	150	150	150	150	150	150	150	150	150	150	150	150	150	150	150	3600	150	
Snøsmelteanlegg	40	35 °C	40	0	40	0	40	0	40	0	40	0	40	0	40	0	40	0	40	0	40	0	40	0	40	0	480	20	

Tilgjengelig varmekilder																												-
Tilgjengelig varme Vakuumpark	180	60 °C								180	180	180	180	180	180	180	180	180	180	180	180	180	180	180	180	180	3060	180

Figure: *Winter demands of the SPP*

Vinter					
Isproduksjon					
T_{fu}	T_{fi}	m	C_p	q	P_{ford}
-10	-3	7	4.2	13.33 l/s	392
T_{ci}	T_{CU}	m	Cp		P_{cond}
4	21	17	4.2	5.49 l/s	392
RSW					
T_{fu}	T_{fi}	m	C_p	q	P_{ford}
0	14	14	4.2	2.63 l/s	154
4	28	24	4.2	1.53 l/s	154
Kjølelager					
T_{fu}	T_{fi}	m	C_p	q	P_{ford}
0	7	7	4.2	1.39 l/s	40.8
T_{ci}	T_{CU}	m	Cp		P_{cond}
4	21	17	4.2	0.57 l/s	40.8
Innfrysning					
T_{fu}	T_{fi}	m	C_p	q	P_{ford}
-42	-13	29	4.2	1.23 l/s	150
T_{ci}	T_{CU}	m	Cp		P_{cond}
4	21	17	4.2	2.10 l/s	150
Fryselager					
T_{fu}	T_{fi}	m	C_p	q	P_{ford}
-42	-13	29	4.2	0.11 l/s	13.6
T_{ci}	T_{CU}	m	Cp		P_{cond}
4	21	17	4.2	0.19 l/s	13.6

Figure: *Evaporator and condenser capacity of different systems inside the SPP*

Appendix D

Modelica code to export R717 refrigerant for system simulations

```
record TILMedia_NH3 "TILMedia AMMONIA"
  extends TILMedia.VLEFluidTypes.BaseVLEFluid(
    final fixedMixingRatio=true,
    final nc_propertyCalculation=1,
    final vleFluidNames={"TILMedia.AMMONIA"},
    final mixingRatio_propertyCalculation={1});
end TILMedia_NH3;
```

R744 Heat pump simulation using simple tubes instead of an IHX

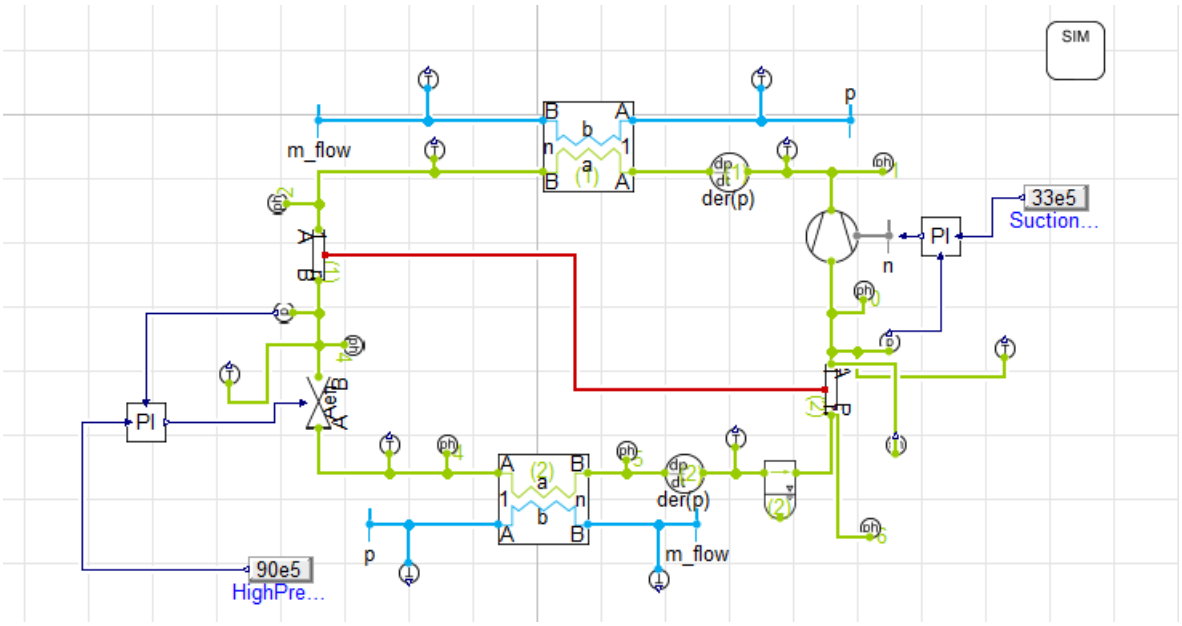

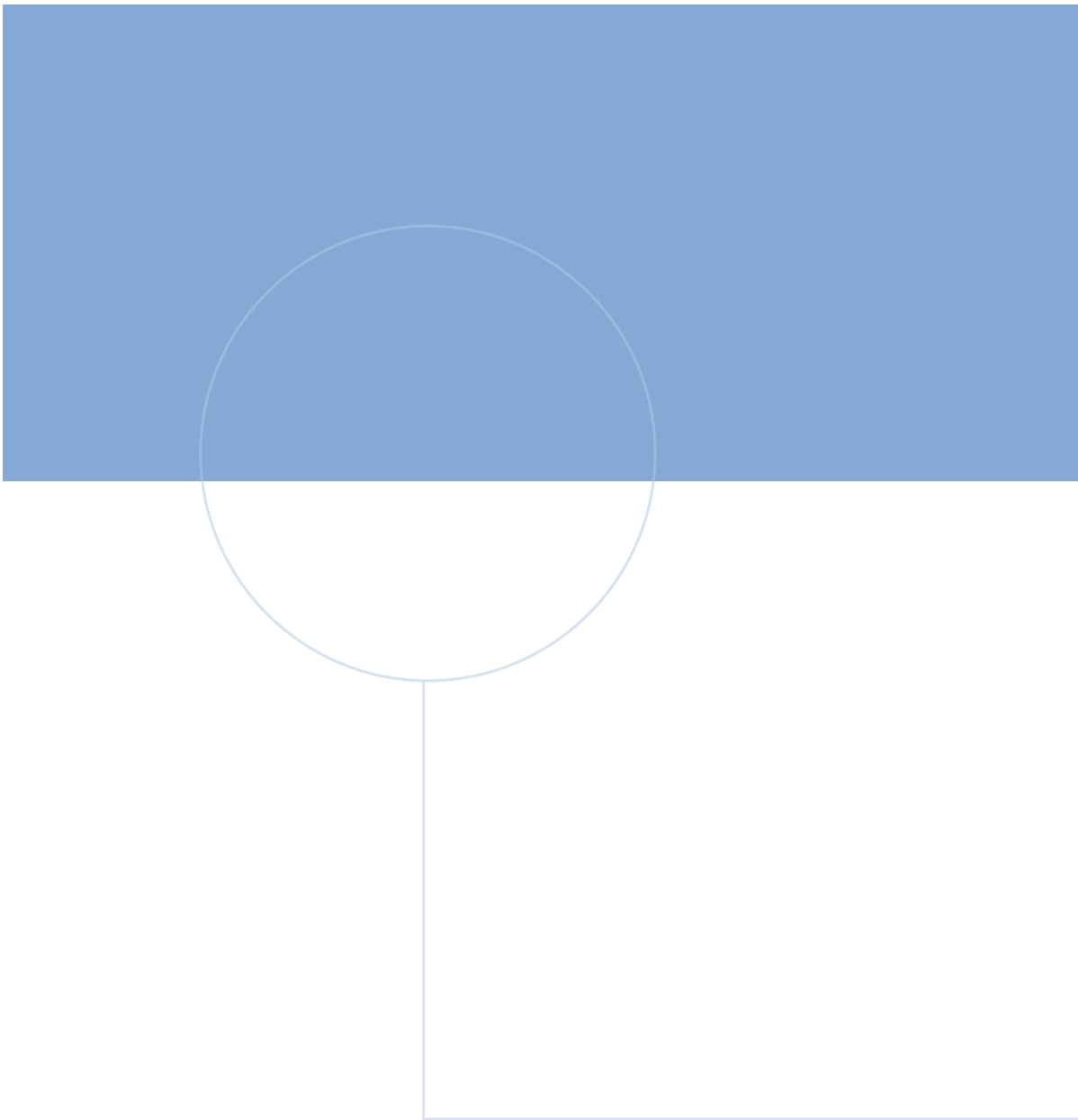

NTNU

Norwegian University of
Science and Technology